Dipl.-Ing. Bettina Gamper

Hyperfine Structure Analysis of Praseodymium and Lanthanum

DOCTORAL THESIS

For obtaining the academic degree of

Doktorin der technischen Wissenschaften

Doctoral Program of Technical Sciences
Technical Physics

Graz University of Technology

Supervisor:
Univ.-Prof. Dipl.-Ing. Dr.techn. Laurentius Windholz
Institute of Experimental Physics

Graz, November 2013

TU
Graz
Graz University of Technology
Senat

Deutsche Fassung:
Beschluss der Curricula-Kommission für Bachelor-, Master- und Diplomstudien vom 10.11.2008
Genehmigung des Senates am 1.12.2008

EIDESSTATTLICHE ERKLÄRUNG

Ich erkläre an Eides statt, dass ich die vorliegende Arbeit selbstständig verfasst, andere als die angegebenen Quellen/Hilfsmittel nicht benutzt, und die den benutzten Quellen wörtlich und inhaltlich entnommenen Stellen als solche kenntlich gemacht habe.

Graz, am 17-09-2013 ……………………

(Unterschrift)

Englische Fassung:

STATUTORY DECLARATION

I declare that I have authored this thesis independently, that I have not used other than the declared sources / resources, and that I have explicitly marked all material which has been quoted either literally or by content from the used sources.

17-09.2013
date

(signature)

Abstract

This work is about hyperfine structure analysis of Praseodymium and Lanthanum by laser spectroscopic investigations. The spectra, and thus the hyperfine structure, including energy levels and spectral lines, of Praseodymium and Lanthanum has gained a new interest since Praseodymium and Lanthanum lines are visible in the spectra of several stars and the abundance of Praseodymium and of Lanthanum provides insight in the star formation process. Atomic data, including hyperfine constants, are necessary to identify lines in highly resolved star spectra.

The experimental part of this work is done with the techniques of optogalvanic, laser-induced fluorescence and saturation spectroscopy. A hollow cathode lamp is used as a source for Praseodymium or Lanthanum atoms or ions and an excitation of different transition is done with tunable dye laser operating with different dyes and being pumped with high power lasers.

When investigating the spectra of Praseodymium or Lanthanum low pressure plasma, which is generated in the hollow cathode lamp, it turned out that a huge number of spectral lines could not be classified as a transition between known energy levels. Thus we are searching up to know unknown energy levels.

In the emission spectrum of Praseodymium there are a lot of blended spectral lines, which have nearly the same center of gravity wavelength. Such lines can only be separated by the technique of laser-induced fluorescence spectroscopy. Furthermore, via laser-induced fluorescence spectroscopy new spectral lines are identified and new energy levels are introduced and the magnetic interaction constant A of these levels are determined. A further goal is to model the emission spectrum of Praseodymium by a sum of the hyperfine profiles of all spectral lines in a certain region.

It will be shown that our Lanthanum discharge is quite sensitive to optogalvanic detection. In order to find new transitions we tune our laser light source until we find an optogalvanic signal and record the hyperfine structure of the excited transition. Then we set the laser frequency in resonance with the recorded spectral line and look for laser-induced fluorescence signals. The combination of this two methods allows us to identify so far unknown energy levels and their magnetic interaction constant A and to classify spectral lines.

Kurzfassung

Die vorliegende Arbeit beschäftigt sich mit Hyperfeinstruktur Untersuchungen von Praseodym und Lanthan mittels laserspektroskopischen Untersuchungen. Die Spektren, und damit die Hyperfeinstruktur, mitsamt den Energieniveaus und den Spektrallinien, von Praseodym und Lanthan erringen neues Interesse, da Spektrallinien von Praseodym und Lanthan in Spektren von verschiedenen Sternen vorkommen und dieses Vorkommen von Praseodym und Lanthan gibt Einblick in den Prozess der Entstehung von Sternen. Daten von Atomen, mitsamt Hyperfeinstrukturkonstanten, sind unabkömmlich, um Spektrallinien in hochaufgelösten Sternspektren zu identifizieren.

Der experimentelle Teil dieser Arbeit wird mit den Methoden der optogalvanischen Spektroskopie, der laserinduzierten Fluoreszenzspektroskopie und der Sättigungsspektroskopie durchgeführt. Als Quelle für Praseodym- bzw. Lanthanatome und Moleküle wird eine Hohlkathodenlampe verwendet, wobei eine Anregung von verschiedenen Übergängen mit durchstimmbaren Farbstofflasern erfolgt, welche mit verschiedenen Farbstoffen betrieben werden und von leistungsstarken Lasern gepumpt werden.

Beim Untersuchen der Spektren vom Praseodym- bzw. Lanthan-Niederdruckplasma, welches in der Hohlkathodenlampe erzeugt wird, stellte sich heraus, dass eine sehr große Anzahl von Spektrallinien nicht als ein Übergang zwischen bekannten Energieniveaus klassifizierbar ist. Aus diesem Grund suchen wir nach bislang unbekannten Energieniveaus.

Im Emissionsspektrum von Praseodym gibt es viele sich überlappende Spektrallinien, welche eine ähnliche Schwerpunktswellenlänge besitzen. Solche Linien können mithilfe von laserinduzierter Fluoreszenzspektroskopie voneinander getrennt bzw. unterschieden werden. Weiter können mit laserinduzierter

Fluoreszenzspektroskopie neue Spektrallinien identifiziert und neue Energieniveaus eingeführt werden sowie die magnetische Hyperfeinstrukturkonstante A bestimmt werden. Ein weiteres Ziel ist es, ein Emissionsspektrum von Praseodym als eine Summe von Hyperfeinstrukturprofilen von allen Spektrallinien in einer bestimmten Region zu modellieren.

Es wird gezeigt, dass unsere Lanthan-Entladung ziemlich sensibel auf optogalvanische Detektion reagiert. Um neue, bislang unbekannte, Übergange zu finden, wird die Wellenlänge des anregenden Lasers so lange durchgestimmt bis ein optogalvanisches Signal gefunden wird und die Hyperfeinstruktur des angeregten Überganges wird aufgenommen. Anschließend wird die Laserfrequenz mit der aufgenommenen Linie in Resonanz gestellt und nach laserinduzierten Signalen gesucht. Die Kombination dieser zwei verschiedenen Methoden erlaubt uns neue, bislang unbekannte. Energieniveaus mitsamt ihrer magnetischen Hyperfeinstrukturkonstanten A zu finden und neue Spektrallinien zu identifizieren.

Für David und Ella

Danke

Ich bedanke mich bei den Mitgliedern des Instituts für Experimentalphysik für die kollegiale Zusammenarbeit und die Hilfsbereitschaft in jeder Situation.

Insbesondere gilt mein Dank meinem Betreuer Prof. Lorenz Windholz für die vielen erfolgreichen Stunden, die wir zusammen im Labor verbrachten und für seine Loyalität, die er mir in jeder Situation entgegenbrachte. Ich konnte unter seiner Betreuung sehr viel lernen, auch weit über fachspezifische Themen hinaus.

Ein großes Danke an meine Eltern, meine Geschwister, meine Großfamilie, ... so weit entfernt, jedoch immer nah.

Ein herzliches Danke an meine Kinder David und Ella, die jede Veränderung mit Optimismus hinnehmen. Der Forschergeist meiner Kinder lässt mich die Wissenschaft jeden Tag neu erleben.

Ich danke meinem Mann Michael von Herzen für das Emotionale, das Sachliche, das Fachliche und für die Selbstverständlichkeit.

Contents

List of Figures

List of Tables

1

Introduction

It is widely believed that investigations on the optical spectra of atoms have been completed several years, even decades, ago. But, when having a closer look, it can be seen that this is not true at all. The spectra of most elements with a lot of electrons are not fully investigated.

Investigations of the hyperfine structure of several elements started the Institute of Experimental Physics at the Graz University of Technology a few years ago. Beside us there work a few other European groups, like a group in Poznan, Poland, a group in Hamburg, Germany and a group in Belfast, Turkey and some groups in Pakistan on this topic, with whom we have a lot of cooperations.

In my work I treat the two elements Praseodymium and Lanthanum. The fine structure level lists and the spectral line lists are not complete at all and their hyperfine structure is not very well known. In the second chapter of my PhD thesis, I treat basic atomic theory like the fine structure and the hyperfine structure. The third chapter is about the investigated and used materials. In the fourth chapter the setup of the experiments and the different investigation methods like optogalvanic spectroscopy, laser-induced fluorescence spectroscopy and saturation spectroscopy are treated. Furthermore the different broadening effects, which influence the line shape of spectral lines are described in this chapter. The fifth chapter is mainly an accumulation of two different publication, where results of measurements and modelling of spectral lines of Praseodymium are treated. Results on investigations of Lanthanum are given in the sixth chapter. I describe different examples of given and solved problems. Examples of investigating spectral lines with low intensity, improving center of gravity wavelengths of spectral lines, introducing so far unknown energy levels, investigating unclassified spectral lines and improving hyperfine structure constants are discussed.

During this work a lot of very useful classification work was done. All the results, all investigated spectral lines and all newly introduced spectral lines and new energy levels of both of the investigated chemical elements are given in the Appendix. This work should be very useful and important for further investigations on atomic spectra of these elements, for ab-initio calculations and also for investigations of stellar spectra, as both elements are part of the emission solar spectrum.

2

Basics

2.1 Background

2.1.1 The gross structure and the spectral lines

The gross structure is predicted when in an atomic system non-relativistic electrons with no spin are considered, only the quantum numbers n (principle quantum number) and l (orbital angular momentum number) are taken into account. For example in the hydrogen atom the gross structure depends only on the principle quantum number n. Nevertheless if a more accurate model should be considered, relativistic effects and the spin should be taken into account.

Spectral lines can be seen as an atomic fingerprint and they are the result of an interaction between a quantum system (atoms in this work, but it can also be molecules) and a single photon. If a photon is absorbed, it will result in a change of the energy state of the system and the photon will then be re-emitted. The energies of the stationary states cannot be measured, but only the transitions between them and thus only the energy differences $h\nu = E_2 - E_1$ can be measured [1].

One of the first to observe absorption lines of the spectrum of the sun was Fraunhofer in 1817 [2]. He called them ”lines”, because he used a line shaped blind and therefore the observed different wavelengths appeared to him as lines.

2.1.2 Energy levels

In a quantum mechanical system an electron which is bound to a nucleus can only have discrete energy values, which are called energy levels. Energy levels are the eigen-values of the Hamiltonian and therefore they do not depend on time. If we have a system which is not disturbed, it wants to be in its ground state.

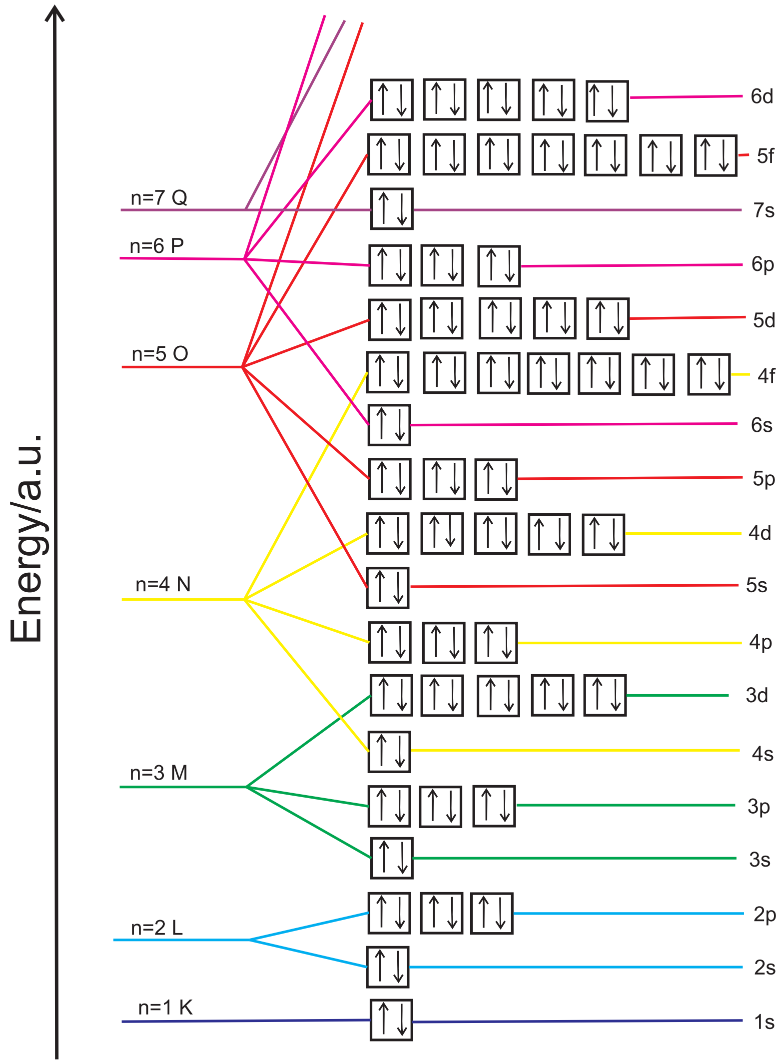

Figure 2.1: Energy level diagram - A schematic energy level diagram.

Every two electrons of a system stay in a so called orbital, which is the probable staying area of the two electrons. The orbitals (boxes in figure 2.1) are given by their level energy. The electrons (arrows in figure 2.1) in the orbitals are arranged according to the Pauli principle (two electrons with a different spin quantum number in every orbital). Figure 2.1 shows a schematic energy level diagram. All orbitals which are at the same horizontal height, have the same energy. Three orbitals at the same energy level are called p-orbitals, five orbitals at the same energy level are called d-orbitals, seven orbitals with same energy level are called f-orbitals and so on. If there is only one orbital at a certain energy level, than it is called s-orbital. According to the Aufbau principle, electrons fill the orbitals by starting at the lowest possible energy level before filling higher energy levels and the number of electrons in one orbital is limited according to the Pauli principle. The electrons (having different spins) of one orbital are occupied according to the Hund's rule[1]. One orbital can have two electrons at maximum. If the energy level of different orbitals are nearby, than they can be occupied atypically.

All the orbitals and therefore the electrons of an atom are distributed in so called shells, which are arranged from the inside to the outside according to the principle quantum number n. The first shell is the K-shell, there are two electrons at maximum (1s), in the second one, in the L-shell, there are eight electrons at maximum (2s and 2p), the third shell is called M-shell and there are at maximum 18 electrons (3s, 3p and 3d) and so on. Also the shells are shown in figure 2.1; different shells have different colors.

2.2 The fine structure

The fine structure (FS) is caused by the interaction between the orbital angular momentum l and the spin s of the electrons. This interaction describes the splitting of the gross structure energy levels due to the first order of relativistic corrections. It has to be emphasized that we talk here only about the interaction between the electrons, the electric and magnetic field of the nucleus and its components is not yet taken into account apart from the central-symmetric Coulomb interaction.

The Hamiltonian of the FS is given by the sum of the undisturbed Hamiltonian and the three correction terms: the kinetic energy term, the spin-orbit term and the Darwinian term:

$$H = H_0 + H_{kin} + H_{so} + H_{Dar}. \tag{2.1}$$

As we want to know about the state of an electron, we should know about its quantum numbers n, l, m_s and m_l. n is the main quantum number and it describes

---

[1] Tendency to the maximum multiplicity-if two or more orbitals at the same energy are available, electrons will occupy them single before filling them in pairs.

the shell where the electron is localized and can have any natural number bigger than zero. The orbital angular momentum number l gives the classification into the s-, p-, d-, f-, ...shell. The values of l are limited by the main quantum number n: $l = 0, 1, 2, 3, \ldots n - 1$. The absolute value $|\vec{l}|$ of of the orbital angular momentum is determined by l in the following manner:

$$|\vec{l}| = \sqrt{l(l+1)} \cdot \hbar, \tag{2.2}$$

where $\hbar$ is the the reduced Planck constant.

The magnetic quantum number m_l gives the place of the electron trajectory in the space. Its values are characterized by l: $m_l = -l \ldots + l$. This says that there can only be $2l + 1$ different values for m_l.

The length of the electron's spinvector $\vec{s}$ is estimated by:

$$|\vec{s}| = \sqrt{s(s+1)} \cdot \hbar. \tag{2.3}$$

The magnetic quantum number m_s can only have two values: $m_s = +1/2$ or $m_s = -1/2$ and it describes the orientation relative to a direction in space of $\vec{s}$.

Of course, but never to forget, the Pauli exclusion principle is valid: no two identical fermions (particles with half-integer spin) can occupy the same quantum state simultaneously.

Finally the total angular momentum vector $\vec{j}$ of one electron is:

$$|\vec{j}| = \sqrt{j(j+1)} \cdot \hbar. \tag{2.4}$$

For a one electron system the equation

$$\vec{j} = \vec{l} + \vec{s} \tag{2.5}$$

is valid.

In general the interaction between the electrons, which are caused by the Coulomb repulsion and by the magnetic dipole-dipole interaction, can be described with two limit cases: the jj- and the LS coupling. The true coupling situation is somewhere in between of those two cases [3].

2.2.1 The jj-coupling

Concerning heavy atoms, one sees that the Coulomb interaction between the single electrons is not dominant, but the interaction between their orbital angular momenta and their spins. Therefore we talk about a jj-coupling when the orbital angular momentum of every single electron couples first with its spin to the angular momentum $\vec{j_i}$:

$$\vec{j_i} = \vec{l_i} + \vec{s_i}. \tag{2.6}$$

After that one has to sum up vectorally over all electrons deriving to the total angular momentum $\vec{J}$:

$$\vec{J} = \sum \vec{j_i}. \tag{2.7}$$

2.2.2 The LS-coupling

If one has atoms with a small atomic number the LS-coupling (also called Russel-Saunders-coupling) is dominant. The electrostatic interaction is large compared to spin orbit interaction of single electrons. Therefore the total angular momentum is calculated differently compared to the jj-coupling. First the the total orbital momenta $\vec{L}$ and the total spins $\vec{S}$ are calculated:

$$\vec{L} = \sum \vec{l_i} \tag{2.8}$$

and

$$\vec{S} = \sum \vec{s_i}. \tag{2.9}$$

The total angular momentum is than the sum of $\vec{L}$ and $\vec{S}$:

$$\vec{J} = \vec{L} + \vec{S}, \tag{2.10}$$

where J can have the following values:

$$|L - S| \leq J \leq L + S. \tag{2.11}$$

2.3 The hyperfine structure

As described above the interaction between the electrons of an atom leads to a formation of fine structure levels (n, l, m_l, m_s). Those spectral lines are interpreted as transition between energy levels. But there exist also, apart from the central symmetric coulomb interaction, a further interaction between the electrons and the nucleus of an atom. In order of that the atomic states of the fine structure split into the hyperfine (hf) structure states, which is approximately 1000 times smaller than the fine structure splitting.

The nucleus of an atom has a nuclear spin $\vec{I}$:

$$|\vec{I}| = \sqrt{I(I+1)} \cdot \hbar, \tag{2.12}$$

where I can be a half-integer or integer number, depending on the number of nucleons.

The magnetic moment of the nucleus and the magnetic moment due to the orbital angular momentum of the electrons orientate to each other, which is only possible in discrete directions. Different orientations cause different additional energy to the fine structure energy of an electron state [4]. This effect is called magnetic interaction. The vector which results of this coupling is the total angular momentum F:

$$\vec{L_F} = \vec{L_J} + \vec{L_I}, \tag{2.13}$$

where

$$|J - I| \leq F \leq |J + I|. \tag{2.14}$$

The quantum number F can be half integer or integer and the number of possible components of the hf structure is caused by:

$$n = 2I + 1 \; for \; I \leq J, \tag{2.15}$$

$$n = 2J + 1 \; for \; I \geq I. \tag{2.16}$$

The characteristic constants of the hf structure are the so called hyperfine structure constants. To estimate the magnetic coupling constant A first the hf structure energy has to estimated. According to [5] this energy is:

$$W_{magn} = \vec{\mu_I} \cdot \overline{\vec{B}_j(0)}. \tag{2.17}$$

In this equation $\vec{\mu_I}$ is the magnetic moment of the nucleus:

$$\mu_I = g_I \cdot \vec{I} \cdot \mu_k, \tag{2.18}$$

where g_I is the gyro-magnetic ratio and μ_k the nucleus magneton. Further $\overline{\vec{B}_j(0)}$ corresponds to the time-averaged magnetic field of the atomic shell at the nucleus place. Thus the additional magnetic energy can be calculated quantum-mechanically:

$$W_{magn} = \frac{F(F+1) - I(I+1) - J(J+1) \cdot (\vec{\mu_I} \cdot \overline{\vec{B}_j(0)})}{2I \cdot J}, \tag{2.19}$$

where the shortcut

$$\alpha(F) = \frac{F(F+1) - I(I+1) - J(J+1)}{2} \tag{2.20}$$

is called the Casimir-factor and

$$A = \frac{\vec{\mu_I} \cdot \overline{\vec{B}_j(0)}}{h \cdot I \cdot J} \tag{2.21}$$

is called the A-value of the hf structure. It has the unit s^{-1} and it is usually given in MHz and is also called interval-factor. It results from the interaction energy of the mean magnetic field $\overline{\vec{B}_j(0)}$ of the atomic shell at the nucleus place and the magnetic moment of the nucleus:

$$A \propto \overline{\vec{B}_j(0)} \cdot \mu_I. \tag{2.22}$$

The A-value can be positive as well as negative, where a positive A-value means that the hf structure levels with large F-values are lying at higher energies in the energy level diagram. Correspondingly a negative A-value means that those with small F-values are lying at higher energies.

Altogether the magnetic energy can be written as:

$$W_{magn} = h \cdot \alpha(F) \cdot A. \tag{2.23}$$

Besides the magnetic interaction there exists also an additional electrostatic interaction. If the charge distribution of an atomic nucleus is not spherical, there exists a quadrupole field besides the Coulomb-field, which is very weak compared with it. Caused by the quadrupole moment of the nucleus and the gradient of the electric field of the atomic shell at the nucleus place an additional energy exists. Therefore, there is a further energy shift of the hf structure term:

$$W_{electr} = e \cdot Q \cdot \overline{\vec{\Phi}_{jj(0)}} \cdot \frac{3\alpha(F) \cdot (2\alpha(F)+1) - 2I(I+1) \cdot J(J+1)}{4I(2I-1) \cdot J(2J-1)}. \tag{2.24}$$

Here e is the elementary electric charge, Q is the electric quadrupole moment of the nucleus and $\vec{\Phi}_{jj(0)}$ is the time-averaged mean value of the gradient of the electric field of the atomic shell at the nucleus position. Again, this formula can be shorten with the following short cuts in the Casimir-factor:

$$\beta(F) = \frac{3\alpha(F) \cdot (2\alpha(F)+1) - 2I(I+1) \cdot J(J+1)}{4I(2I-1) \cdot J(2J-1)} \tag{2.25}$$

and in a hf structure constant, the quadrupole constant B:

$$B = \frac{e \cdot Q \cdot \overline{\vec{\Phi}_{jj(0)}}}{h}. \tag{2.26}$$

Also the quadrupole constant B has the unit s^{-1}, which once more is usually given in MHz, but it has less influence to the hf structure compared to the A-value. The B-value is only unequally to 0 if the atomic nucleus is not spherically ($Q \neq 0$) at all:

$$B \propto \overline{\frac{\delta E}{\overline{\delta_{z_0}}}} \cdot Q. \tag{2.27}$$

The energy which results of the electrostatic interaction can now be written as

$$W_{electr} = h \cdot \beta(F) \cdot B. \tag{2.28}$$

If the total energy of the hf structure should be estimated, the magnetic and the electric energy have to be added to the center of gravity (cg) energy of the fine structure term. This results in the so called Casimir-equation:

$$W_{tot}(F) = W_J + h\alpha(F)A + h\beta(F)B. \tag{2.29}$$

If this equation is divided by h it results, because of $W = h\nu$, in a not measurable frequency ν:

$$\nu_F = \nu_J + \alpha A + \beta B, \tag{2.30}$$

or fully written:

$$\nu_F = \nu_J + A_J \frac{C}{2} + B_J \frac{3/4C(C+1) - I(I+1)J(J+1)}{2I(2I-1)J(2J-1)}, \tag{2.31}$$

where

$$C = F(F+1) - I(I+1) - J(J+1). \tag{2.32}$$

If we want to calculate the hf splitting of a transition, the energy of the lower level has to be subtracted from the energy of the upper level and this difference of energies can be measured:

$$\Delta W_{F_{up}-F_{low}} = W_{F_{up}} - W_{F_{low}}, \tag{2.33}$$

or

$$\nu_{F_{up}-F_{low}} = \nu_{F_{up}} - \nu_{F_{low}}. \tag{2.34}$$

$\nu_{F_{up}-F_{low}}$ is now a measurable frequency which is emitted from or absorbed by the atom and which can be measured. As a result of that a hf structure component $F_{up} - F_{low}$ has a position which is shifted relative to the cg frequency ν_c:

$$\nu_{F_{up}-F_{low}} = \nu c + (\alpha_{up} A_{up} - \alpha_{low} A_{low} + \alpha_{up} B_{up} - \alpha_{low} B_{low}). \tag{2.35}$$

α and β can be calculated via the corresponding quantum numbers:

$$\alpha_{up} = \frac{1}{2}[F_{up}(F_{up}+1) - I(I+1) - J_{up}(J_{up}+1)] \tag{2.36}$$

$$\alpha_{low} = \frac{1}{2}[F_{low}(F_{low}+1) - I(I+1) - J_{low}(J_{low}+1)] \tag{2.37}$$

$$\beta_{up} = \frac{\frac{3}{4}C_{up}(C_{up}+1) - I(I+1)J_{up}(J_{up}+1)}{2I(2I-1)J_{up}(2J_{up}-1)} \tag{2.38}$$

$$\beta_{low} = \frac{\frac{3}{4}C_{low}(C_{low}+1) - I(I+1)J_{low}(J_{low}+1)}{2I(2I-1)J_{low}(2J_{low}-1)}. \tag{2.39}$$

To determine the constants of interest $A_{up}, A_{low}, B_{up}, B_{low}$ and ν_c the position of five components and the corresponding quantum numbers have to be known [6].

If $B = 0$ the interval rule for the distance between the hf levels can be applied: the distances behave as the relation of the quantum numbers: $F : (F-1) : (F-2) \ldots$

2.3.1 The selection rules for an atomic transition

The transitions for hf structure levels are limited with the following rule:

$$\Delta F = 0, \pm 1, \tag{2.40}$$

where the rule for transitions between fine structure levels are still valid:

$$\Delta J = 0, \pm 1. \tag{2.41}$$

Another important part is the parity of the energy levels involved in a transition. The two levels involved in a dipole transition have to have according to the Laporte rule [7] different parities:

$$\Delta P = 1. \tag{2.42}$$

The parity is the symmetry of the wavefunction [8, 9] and can be calculated by summing up the orbital angular momentum quantum numbers of the electrons and it is either even (e) or odd (o).

All of the said rules have to be applied all the time. The only exception is a transition between two levels with the quantum number $F = 0$ which is a forbidden transition.

In a hf pattern most of the times there can be seen high intensive components as well as low intensive components. Each component is a transition between two hf structure levels. As, according to 2.40 there are transition rules of ΔF, there usually are three groups of components in a hf pattern: $\Delta F = 0$, $\Delta F = -1$ and $\Delta F = 1$, which depend, according to 2.14 and 2.41, on J and ΔJ. The transition probability and the corresponding intensity of the spectral lines of a hf transition is larger for the group of F-values with $\Delta F = \Delta J$ than for the group of F-values with $\Delta F \neq \Delta J$. So the group of F-values with $\Delta F = \Delta J$ corresponds to the group of large components of a hf pattern, which decline from the large to the small F-values.

3

Materials

3.1 The chemical element Praseodymium

Praseodymium (Pr) is a metal and belongs to the group of lanthanides. Its name comes from the Greek words *prasinos* (green) and *didymos* (twin). The metal is silver-white colored, in air it gets yellowish. In air, it oxidizes very quickly, a centimeter-sized sample of Pr completely oxidizes within a year. Because of that it is usually stored in oil. In contrast to the other rare earth metals, which show antiferromagnetic or/and ferromagnetic ordering at low temperatures, Pr is paramagnetic at any temperature above 1 K.

In 1841 Didymium was extracted from Lanthanum-oxid by Carl Gustav Mosander. In the year 1874 Per Teodor Cleve discovered that the element Didymium consists of two elements in reality. Finally in 1885 the Austrian Carl Auer von Welsbach was able to split Didymium in Praseodymium and Neodymium.

In nature Pr has just one stable isotope: ^{141}Pr. The two radioactive isotopes ^{142}Pr and ^{143}Pr have short half-lives of 19.12 h and 13.57 d [10], respectively. The half lives of all the other known 38 radioactive isotopes are even shorter, in the range of a few seconds to less than six hours [10].

Pr has an atomic number of $Z = 59$ and its electronic ground state configuration is $[Xe]4f^3 6s^2$. Like all lanthanides also Pr has an open 4f shell. Due to its odd number of protons the Pr atom (Pr I) has a non-zero nuclear spin $I = 5/2$ and therefore shows a hf splitting. Its ground state is $4I^o_{9/2}$ and its magnetic dipole moment is $\mu_I = 4.2754(5)\mu_N$ [11] and the electric quadrupole moment is $Q = -0.0024b$ [12]. The electric quadrupole moment of Pr is very small because Pr has an almost spherically charge distribution in his nucleus. Pr has a huge number of spectral lines, most of them in green spectral range.

The rare earth element is mostly used in alloys, like Pr-Mg or Pr-Co-Fe. Since several years Pr alloys are used in lightning engineering for example in fluorescence tubes, energy-saving lamps, catalysts and glasses. Spectral lines of Pr are also part of the stellar spectrum [13]. Figure 3.1 shows a sample of Pr chippings which is stored under oil in order to prevent oxidation.

Figure 3.1: Pr sample - Praseodymium chippings stored in oil.

The hf structure of Pr has been investigated quite for a while [14, 15, 16, 17, 18, 19, 20]. Since some years new Fourier Transform spectra are available [21] and therefore it could be done a lot of useful classification work at our institute [22, 23]. But still the spectral line list and the level list of Pr is far from being complete.

3.2 The chemical element Lanthanum

Lanthanum (La) is the first element in the lanthanide series. The metal is silvery white and oxidizes rapidly when it is exposed to air. It can be found in rare earth minerals, usually in combination with other rare earth elements, mostly with Cerium.

The word lanthanum comes from the Greek word *lanthano* which means "to lie hidden". La was discovered by Carl Gustav Mosander 1839.

Natural La is composed of two isotopes, the long living radioactive ^{138}La with a natural abundance of 0.09 % and a half-life of $1.05 \cdot 10^{11}$ years and a stable isotope ^{139}La with a natural abundance of 99.91 % [10]. The two isotopes have nuclear spin quantum numbers of 5 and 7/2, respectively. Further 37 isotopes could be characterized with half-lives of less than 24 h.

La has an atomic number of $Z = 57$ the ground state $[Xe]5d^1 6s^2$, $2D^o_{3/2}$ and it has one valence electron in its ground state in the 5d shell. The isotope ^{139}La, on which all measurements were done, has a magnetic dipole moment of $\mu_I = 2.7830455(9)\mu_N$ [24] and, caused by its spherically charge distribution in his nucleus, a rather small electric quadrupole moment of $Q = -0.20(1)b$ [25].

Compounds of La have several applications such as catalysts, additives in glass, carbon lighting for studio lighting and projection, ignition elements in lighters and torches, electron cathodes or scintillators. Lanthanum carbonate ($La_2(CO_3)_3$) was approved as a medication against renal failure.

Figure 3.2 shows a copper cathode whose inner part is made of La.

A lot of people already investigated the hf structure splitting of La with a lot of different techniques. Those techniques were Fabry-Perot interferometry [26, 27], atomic beam magnetic resonance [28, 29] and different techniques of laser spectroscopy, such as Doppler-free laser atomic beam spectroscopy [30, 31], laser atomic beam magnetic resonance [32, 33], Doppler-reduced intermodulated optogalvanic and laser induced fluorescence spectroscopy [34, 35, 36]. The discovery of previously unknown energy levels is reported in [37, 38, 39, 40, 41, 42, 43]. Nevertheless the hf structure investigations of La is far from being complete.

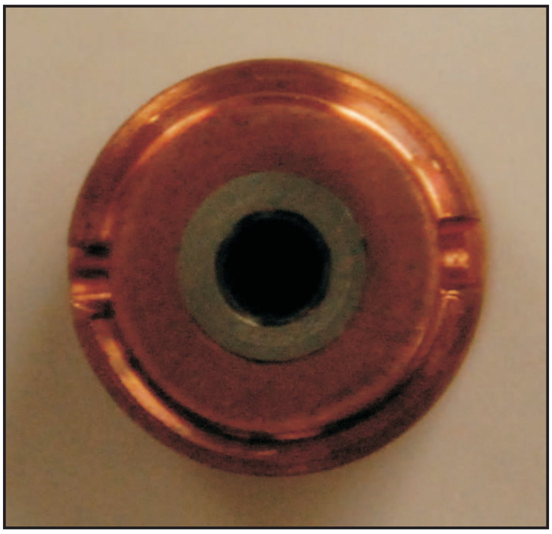

Figure 3.2: La sample - Lanthanum in the inner part of a copper cathode.

3.3 Laser

The first laser, a Rubin laser, was invented by Theodore Maiman in 1960 [44]. The word laser is an acronym from the words Light Amplification by Stimulated Emission Radiation. Those words already describe how a laser works: Light is amplified by stimulated emission. In a three or four level scheme the population of an upper level is increased by optical pumping and therefore also the fluorescence from this level, which can be observed as laser light. How different laser types work in detail is described in several literature, such as in [45].

In the present work dye lasers are used. A dye lasers is the optimal laser to perform spectroscopy because they are tunable over a certain wide spectral range according to the dye they are operating with. Our dye lasers are operating in single mode, that means, they emit only one single frequency. The active medium of a dye laser is the dye jet which is formed by a nozzle at a pressure of about 4 bar of the liquid dye solvent. If the light of a high power fixed frequency laser is focused on this jet, the laser dye is absorbing this pumping laser light and is emitting radiation in the way described above. In order to enhance induced emission processes, the active medium must be placed inside an optical resonator. By induced emission the fluorescence light of the dye is amplified and a laser beam is formed.

As we want a dye laser which is operating in single mode which can be tuned continuously, a few additional wavelength selecting elements have to be used. Such lasers demand a synchronous control of the cavity length and of the transmission maxima of the selected elements. Figure 3.3 shows a schematic diagram of a single mode continuous wave (cw) ring laser.

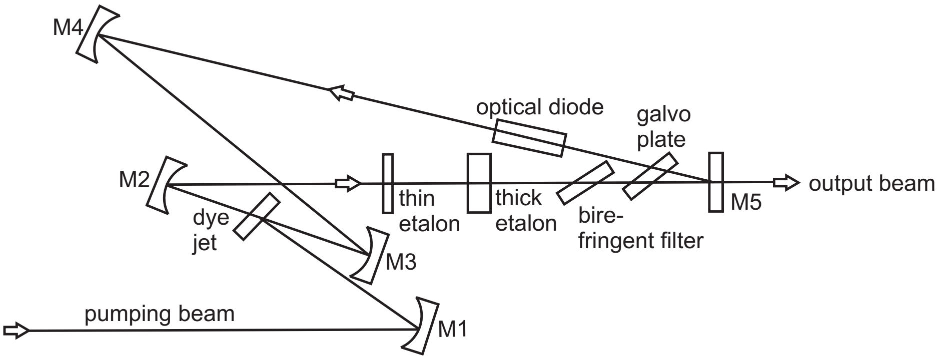

Figure 3.3: Laser - A schematic diagram of a single mode cw ring laser.

Figure 3.4 is a photograph of a dye laser in our lab operating with DCM and being pumped by an Ar-ion laser.

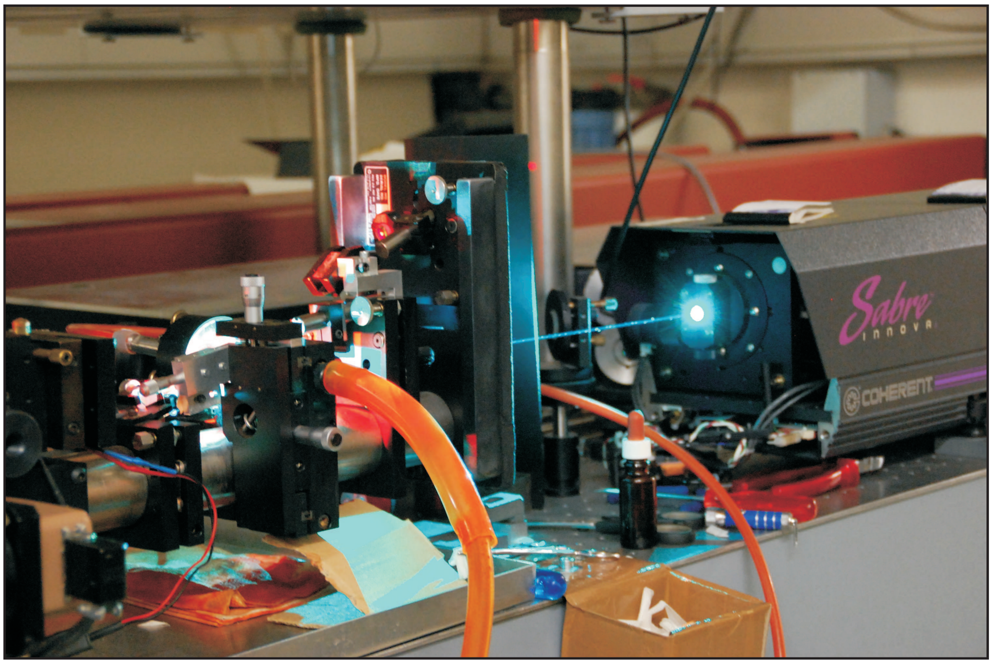

Figure 3.4: Laser-photograph - A photograph of a dye laser in our lab.

4

Setup & Methods

4.1 Experimental Setup

For both investigated chemical elements the same experimental setup is used.

4.1.1 The hollow cathode lamp

We use a home made Schüler's type hollow cathode lamp [46, 47], which consists of a copper cathode whose inner part is made from the investigated metal and two aluminum anodes. The anodes are spaced with ceramics insulators. The inner diameter of the cathode is 3 mm and its length is 20 mm. Also the anodes have bores, which have as well a diameter of 3 mm. The ceramic insulators are enlarged with glass tubes on both sides in order to force the discharge to burn inside. Photographs of the cathode as well as from the cathode, the anodes and the ceramic insulators are shown in figure 4.1 and in figure 4.2.

All of the parts described above are in a brass tube, which is closed with quartz glasses at both sides. As a working gas we usually use Argon (Ar) with a pressure of about 0.5 mbar. The gas discharge lamp is cooled down with liquid nitrogen, which is stored in a basin around and above the brass tube. Cooling down the discharge has the effect that the Doppler width is reduced and also the sputtering rate is better. When turning on the discharge current, the Ar ions start to sputter metal atoms from the cathode in order to generate a metal-Ar plasma. Figure 4.3 shows a photograph of the emitted discharge light of a La cathode.

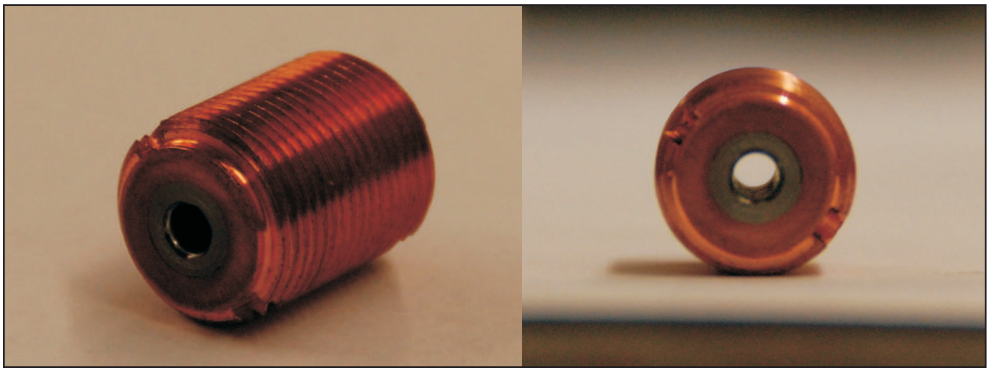

Figure 4.1: The cathode - Photograph of the cathode

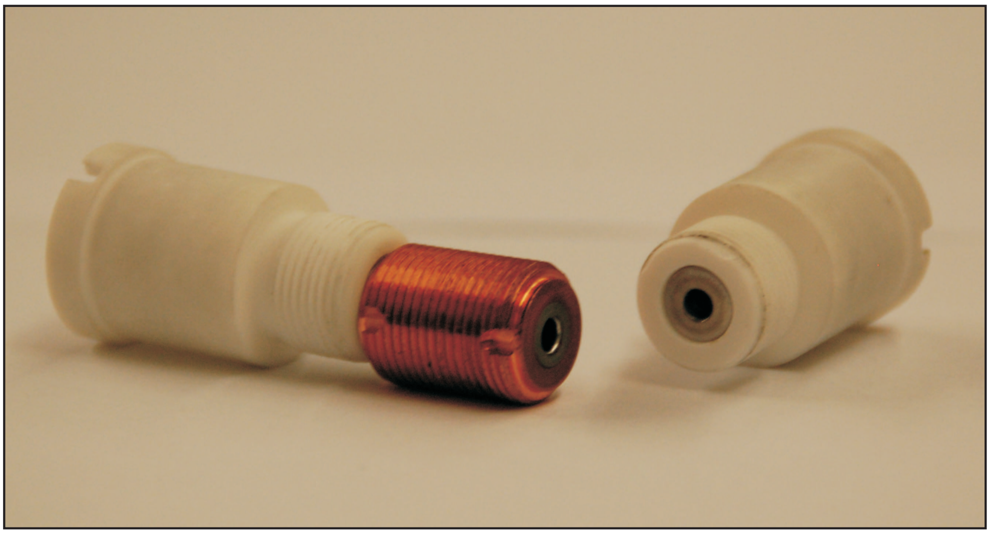

Figure 4.2: The cathode and the anodes - Photograph of the cathode and the anodes as well as the ceramic insulators.

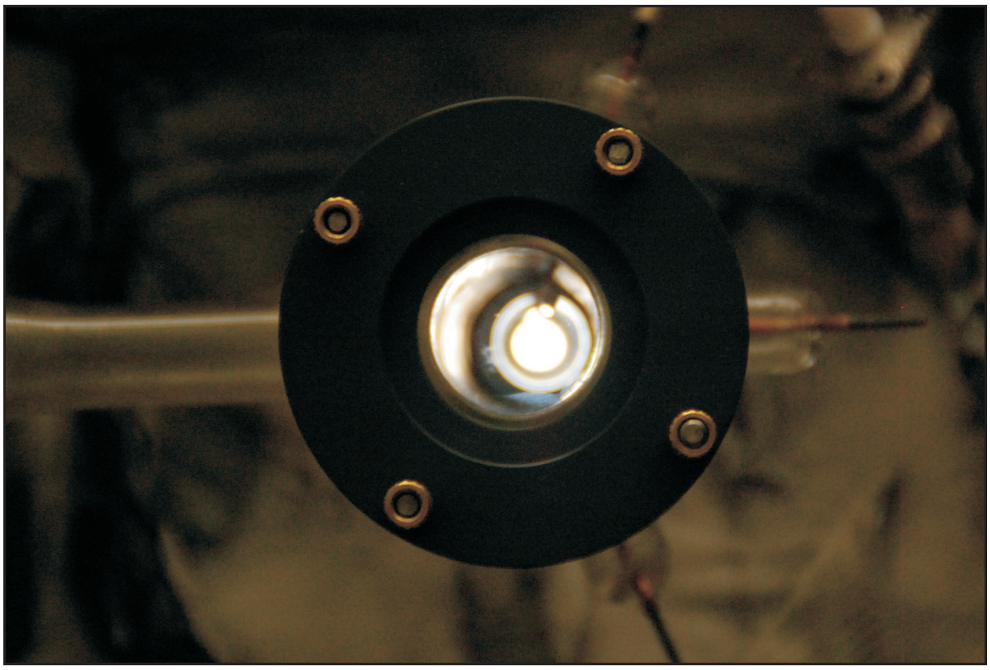

Figure 4.3: Discharge light - The emitted discharge light of a La cathode.

The advantage of this kind of setup is that the investigated metal atoms are not only in the ground state but also in higher excited states. The discharge current is about 90 mA. A drawing of the hollow cathode lamp is shown in figure 4.4

4.1.2 The optical setup

The optical setup of the experiment is represented in figure 4.5. Laser light, which is coming from an Ar-ion pumped dye laser, is focused by a set of lenses (L1, L2) and mirrors (M4, M5) into the hollow cathode lamp (HCL) and somewhere outside the lamp it has to pass a chopper, which cuts the laser beam periodically, before entering the lamp. The chopping frequency is the reference frequency for a Lock-in amplifier. Right in front of the entrance into the hollow cathode lamp, there is a mirror with a hole in it (M6). The laser light should pass through the hole into to lamp. The function of the mirror is to collect the fluorescence light which is coming out the discharge. This light is then focused with lenses (L3, L4) into the entrance slit of a grating monochromator. At the exit of the monochromator there is a photomultiplier who detects the outcoming fluorescence light and sends a photo current to the Lock-in amplifier. As the Lock-in

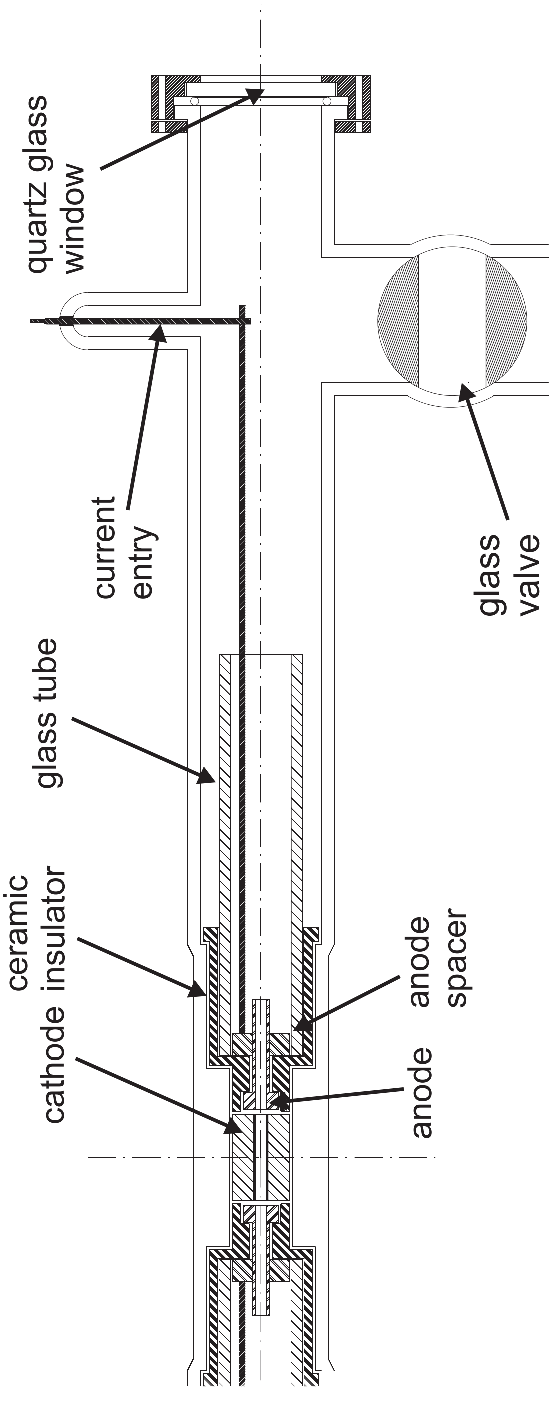

Figure 4.4: HKL - The hollow cathode lamp.

amplifier has the chopping frequency as a reference, it detects just those signals which are modulated with the reference frequency. The signal is recorded electronically but also by an analog plotter. Figure 4.5 shows a sketch of the optical setup and figure 4.6 is a photograph of the optical setup. Part of the laser light is sent to a λ-meter to measure the wavelength of it.

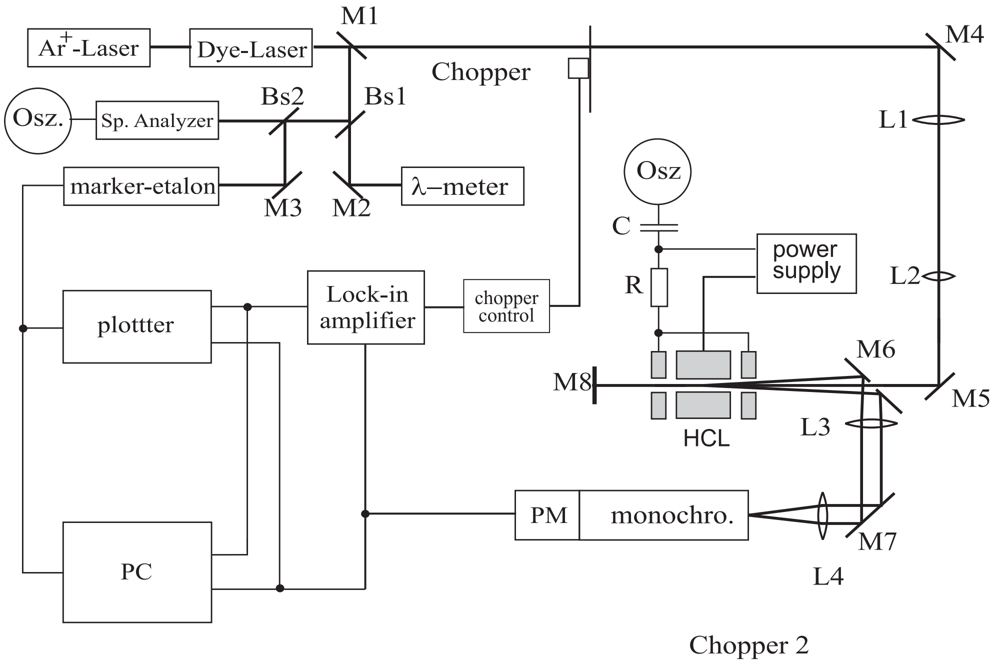

Figure 4.5: Setup-sketch - The optical setup.

The scanning of the laser frequency is not completely linear with time. It has to be made a comparison between the line profile and the wavelength of the laser by a so-called marker-etalon. Some part of the laser light passes through the marker-etalon, which is a temperature stabilized Fabry-Perot interferometer, which lets pass the laser light in calibrated, equidistant frequency intervals. In order of that, every registered line profile has also some frequency comb, with the help of which the line profile can be linearized then. The distance between the transmission maxima is very well known: $\Delta f = 367.33\,\mathrm{MHz}$ for the yellow region, $\Delta f = 150.2976\,\mathrm{MHz}$ for the blue region and $\Delta f = 197.6009\,\mathrm{MHz}$ for the red region.

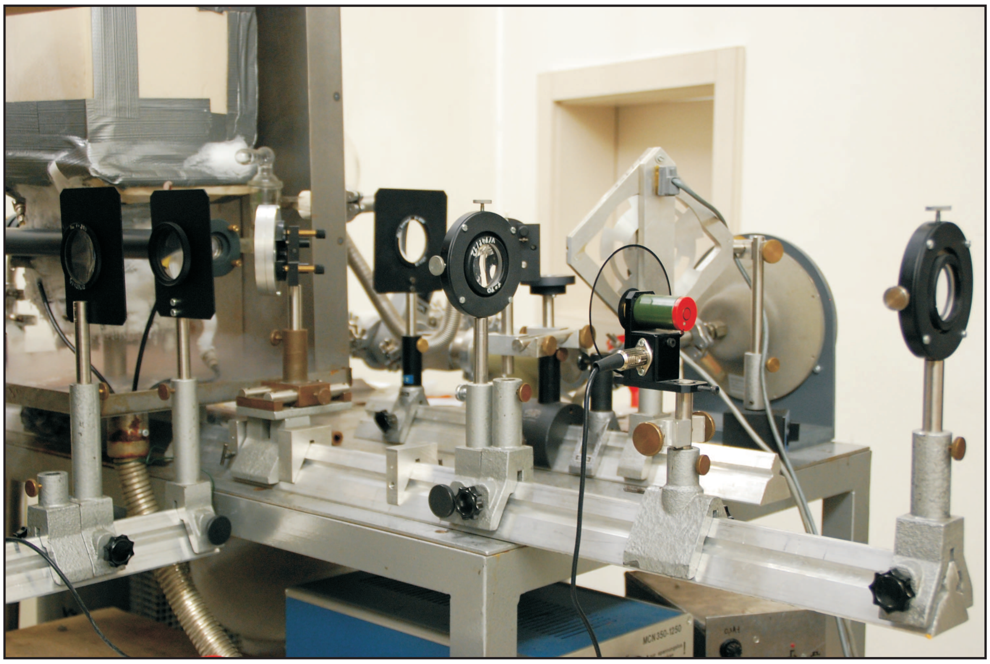

Figure 4.6: Setup-photograph - Photograph of the optical setup.

4.1.3 The vacuum setup

Figure 4.7 shows the vacuum setup. The whole apparatus is pumped by a rotary pump (P) to 10^{-3} mbar. A few hours before an experiment can be started, liquid nitrogen is filled into the cooling trap (CT1) in order to trap the oil which might come upwards from the pump and some water which might be in the system condensates in the cooling trap.

To start the discharge Ar gas has to be filled into the system (pressure about 0.5 mbar). To do that, first the valve (V1) and the gate (G2) have to be closed. When the discharge is running, liquid nitrogen has to filled into the second cooling trap (CT2) in order to trap impurities so that they condensate in the cooling trap rather than at the cold electrodes. At the end also the discharge itself has to be cooled down with liquid nitrogen in order to reduce the Doppler with and to increase the sputtering rate.

The glass valves (H1 and H2) can be closed when the electrodes have to be changed so that the hollow cathode lamp is splitted from the rest of the vacuum system. The hole system is pumped if all valves and gates are open. Figure 4.7 shows the vacuum setup.

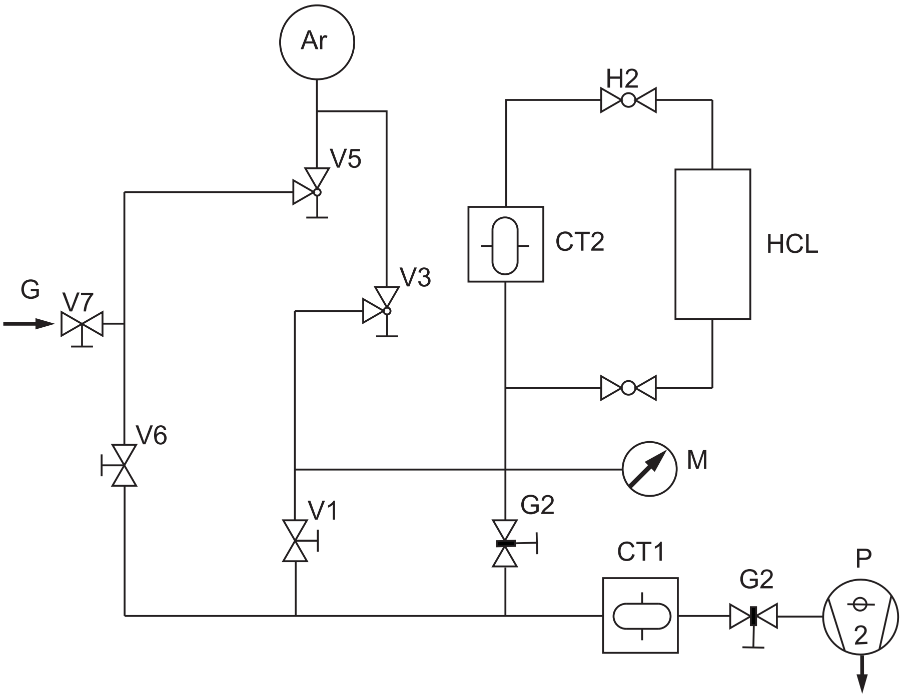

Figure 4.7: The vacuum setup. - The vacuum setup.

4.2 Absorption spectroscopy

If atoms are exposed into radiation they can absorb energy as a photon and every photon can stimulate an atom in such a way that one of his electrons jumps from a lower lying energy level into an upper lying one. The energy difference between to levels can be measured and is:

$$\Delta E = h \cdot \nu. \tag{4.1}$$

This effect is called induced absorption. The probability for absorption is

$$P_{12} = B_{12} \cdot \rho(\nu), \tag{4.2}$$

where B_{12} is the Einstein coefficient and $\rho(\nu)$ the spectral density of the radiation field.

When performing absorption spectroscopy, an absorbing medium is irradiated by light of a certain frequency range. All atoms in this medium are in the ground state because generally the thermal energy is low compared to the excitation energy. The atoms can absorb certain frequencies of the irradiating light and emit them in every direction. The emitted light is analyzed by a spectrograph and shows dark absorption lines. The first one to observe absorption lines was Frauenhofer, who saw absorption lines in the spectrum of the sun.

4.3 Emission spectroscopy

Besides the said absorption also the emitted radiation can be analyzed. This is possible because in gasses at high temperature a small part of the atoms are already in higher excited states. The atoms can pass by spontaneous emission to lower lying energy levels. The probability of such a transition is:

$$P_{21(spon.)} = A_{21}, \tag{4.3}$$

where A_{21} is the Einstein coefficient for spontaneous emission.

The atoms only stay for a short time in the excited state; they decay spontaneously to lower lying states while emitting light.

The atoms can undergo transitions also induced by electro magnetic fields (photons). The probability of induced emission is:

$$P_{21} = B_{21} \cdot \rho(\nu), \tag{4.4}$$

where B_{21} is the Einstein coefficient for induced emission and $\rho(\nu)$ the spectral density of the radiation field.

In a gas discharge the induced emission probability is very low compared to the probability for spontaneous emission and can usually be neglected. In contrary to that, in lasers the spectral energy density $\rho(\nu)$ is so high that the induced emission is dominating.

When performing emission spectroscopy the atoms get the energy for occupying higher lying states from collisions, usually from collisions between the atoms and the electrons in a gas discharge. In order of that all energy levels are occupied and therefore all spectral lines are emitted, because the level population is non-selective. Again a spectrograph can analyze the emitted light.

4.4 The line broadening

4.4.1 The natural line width

If an atom is excited, it has an energy excess, which is emitted as an electromagnetic wave. As this emittance of energy cannot last forever, it can be described with the classical model of a damped oscillation. The oscillation equations can be Fourier transformed and solved and so the intensity profile can be calculated. When the intensity profile is standardized it correlates to a Lorentz-profile $g(\omega)$:

$$g(\omega-\omega_0)=\frac{\gamma/2\pi}{(\omega-\omega_0)^2+(\gamma/2)^2}, \tag{4.5}$$

where γ is the attenuation coefficient. The half width $\Delta\omega$ of this profile corresponds to the natural half width and is equal to the attenuation coefficient $\Delta\omega=\gamma$.

If we go beyond the classical model and start to think about quantum mechanics, the energy of an excited state is only determinable to $\Delta E=\hbar/\tau_i$ anymore caused by the Heisenberg uncertainty principle. Therefore the FWHM of the natural half width now is

$$\Delta\nu=\frac{\Delta E}{h}=\frac{1/2\pi}{\tau_i}. \tag{4.6}$$

If there is a transition between two excited energy states, both half-lives influence the natural linewidth, because both energy uncertainties sum up:

$$\Delta\nu_n=\frac{1}{2\pi}(\frac{1}{\tau_i}+\frac{1}{\tau_k}). \tag{4.7}$$

The natural linewidth corresponds to the smallest frequency uncertainty, which could be reached theoretically if all other effects could be neglected and if the light could be emitted from stationary atoms and its FWHM is about a few MHz.

4.4.2 The Doppler broadening

Most of the times the effects which cause the observable line width of a spectral line are larger than the natural line width. The most important effect causing the appearance of spectral lines of gases under low pressure is the Doppler broadening. The reason for the Doppler broadening is the movement of the particles in every direction. Due to the Doppler effect the absorption does not take place at a single frequency but over a certain frequency interval which dependents on the velocity of the atoms.

The half width $\Delta\nu$ of the Doppler broadened line is:

$$\Delta\nu = \frac{2\nu_0}{c}\sqrt{2 \cdot ln2 \frac{k_b T}{m}}, \tag{4.8}$$

where T is the temperature in K, k_b the Boltzmann constant, m the atomic mass and c the velocity of light in vacuum.

The Doppler width increases linearly with the frequency and decreases for heavy atoms and molecules when the temperature is constant. When keeping the temperature of a light emitting source as low as possible the Doppler broadening can be kept small.

The FWHM of a Doppler profile is 100 times bigger than the FWHW of the natural line broadened profile. In contrast of that the line profile of a laser is much smaller than the Doppler profile, it is even smaller than the natural line broadening.

The half width $\Delta\nu$ of the Doppler broadened line depends on the energy of the excited level:

$$\Delta\nu = f(E_{exc.}). \tag{4.9}$$

The higher the energy of an excited level, the higher is the Doppler half width. Figure 4.8 shows two recorded spectral lines, where two different energy levels have been excited. In the figure it can be seen that the spectral line on the left handside which has the higher energy ($E' = 43344.94$ cm^{-1}) of the excited level has a high Doppler width. The single hf components of the spectral line on the right hand side ($E' = 40599.36$ cm^{-1}) are resolved better caused by the lower Doppler width

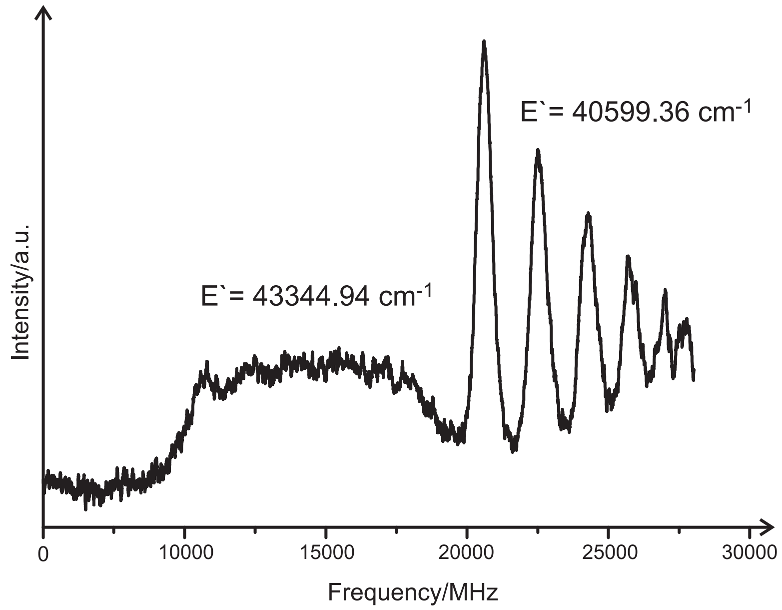

Figure 4.8: Doppler width of recorded lines - Two recorded spectral lines with different Doppler widths. The higher level energy of the left line is 43344.94 cm^{-1} and the energy of higher level the right line is 40599.36 cm^{-1}.

4.4.3 The collisional broadening

If two atoms with different energy levels near each other collide, it can occur that their energy levels are shifted because of the interaction of the two atoms. We talk about a collision when two particles near each other up to a distance R, where they disturb each other.

The level's energy shift depends on the structure of the levels and on their distance to each other, which is distributed over the mean value of the distance $\overline{R}$. $\overline{R}$ depends on the pressure and on the temperature of the gas. Also the atom's emitted frequency ν_{if} is distributed over a mean value which is displaced compared with the emitted frequency ν_0 of an undisturbed atom.

Elastic collisions as well as inelastic collisions are responsible for the collision broadening. The elastic collision do not only have influence on the broadening but they also lead to a displacement of the spectral lines which results in a Lorentz profile of the lines.

The energy shift is positive when there is a repulsive potential between the atoms and it is negative when the interaction is attractive. Further the energy shift differs for the different energy levels.

4.4.4 The saturation broadening

If the laser power is high enough there are more atoms in the upper than in the lower level of a transition, caused by optical pumping. The optical pumping rate of a transition is greater than the relaxation time.

The saturation broadening depends on the saturation rate, which gives the pumping rate per mean relaxation rate ($S_0 = P\overline{R}I$), and can be written as:

$$\Delta\omega_S = \Delta\omega_0\sqrt{1 + S(\omega_0)}. \tag{4.10}$$

It can be seen that the line profile gets broadened by a factor of $\sqrt{2}$ if the pumping rate is equal to the whole decay rate.

If we have inhomogeneous broadened transitions so called hole burning can be seen. It is caused by selective spectral saturation, which is the dependence of the absorption probability on the velocity of the atoms.

As a result of the saturation broadening the small components of a hf profile can be enlarged compared to the big components when recording a hf structure.

4.4.5 The complete line profile

The said four causes of the broadening of the line profile of an atomic transition give, by a convolution of them, the complete line profile of a spectral line:

$$I(\omega) = I_N(\omega) * I_D(\omega) * I_I(\omega) * I_S(\omega), \tag{4.11}$$

where $I_N(\omega)$ is the natural line profile, $I_D(\omega)$ the Doppler broadened line profile, $I_I(\omega)$ is the collision broadened line profile and $I_S(\omega)$ gives the saturation broadened line profile.

$I_N(\omega)$, $I_I(\omega)$ and $I_S(\omega)$ appear to have a Lorentzian line profile, therefore also the convolution of them is a Lorentzian line profile, which has a FWHM which is the sum of the single FWHM. In contrary to that $I_D(\omega)$ is a Gaußian profile. Both, a Lorentzian and a Gaußian profile, have the same FWHM and the same area beneath their curve, but above the intersection the Gaußian profile is broader, while the wing of the Lorentzian profile dominates when comparing both curves. If the Lorentzian profile and the Gaußian profile are convoluted, the resulting profile is a Voigt profile. Figure 4.9 shows the three different profiles, where all three profiles have the same area beneath them.

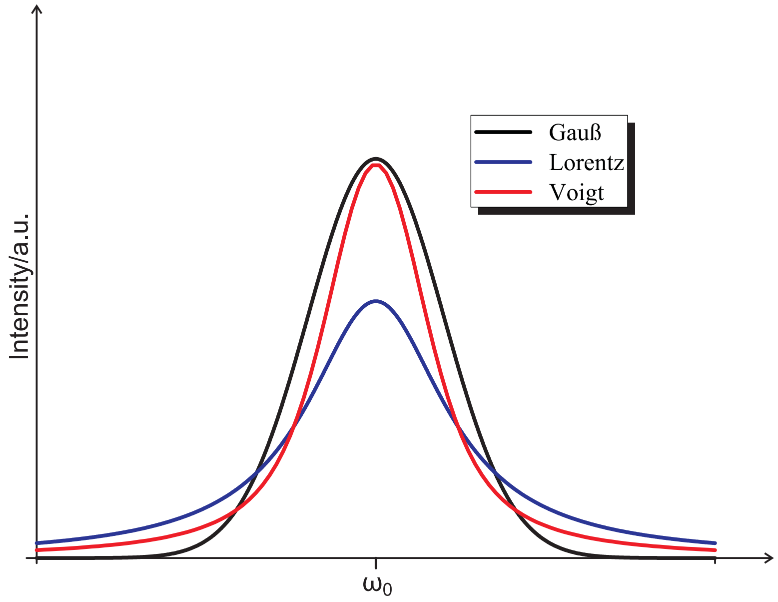

Figure 4.9: Line profiles - The three line profiles of the same area: Gauß, Lorentz and Voigt.

4.5 Optogalvanic spectroscopy

When the frequency of laser light is tuned over a certain frequency range while passing through a hollow cathode lamp, the population densities of energy levels (n'(E') and n(E)) are changing if the laser frequency is in resonance with an optical transition (E' - E). This population change is visible as a change of ΔI of the discharge current. It can be detected as a voltage change $\Delta U = R\Delta I$ with a lock-in amplifier, which reference frequency is the frequency of a chopper wheel who chops the laser light.

This is called the optogalvanic (OG) effect and when it is used as a spectroscopic tool it is called OG spectroscopy [48], respectively. The OG effect was discovered several decades ago [49], but it was not used as a spectroscopic tool until the invention of tunable lasers. It turned out that it is a simple, but excellent technique to perform laser spectroscopy. Moreover it is very sensitive to detect also very weak spectral lines and even with moderate laser powers large signals can be achieved [43]. To perform OG spectroscopy a very stable and silent (not oscillating, as less noise as possible) discharge is required [50]. If the laser frequency is scanned over a spectral region, a signal can be detected whenever the laser frequency is in resonance with an optical transition between energy levels. Therefore, if two or even more lines, have the same cg wavelength, both lines will be detected at the same time, which is called a blend situation. Those blended spectral lines are not distinguishable by OG spectroscopy. This is a disadvantage of the technique of OG spectroscopy: it is only useful if there are spectral lines which are standing as single lines. Furthermore one cannot tell which energy levels are involved in the investigated transition and by OG spectroscopy detected spectral line. In figure 4.10 an OG signal on an oscilloscope is illustrated.

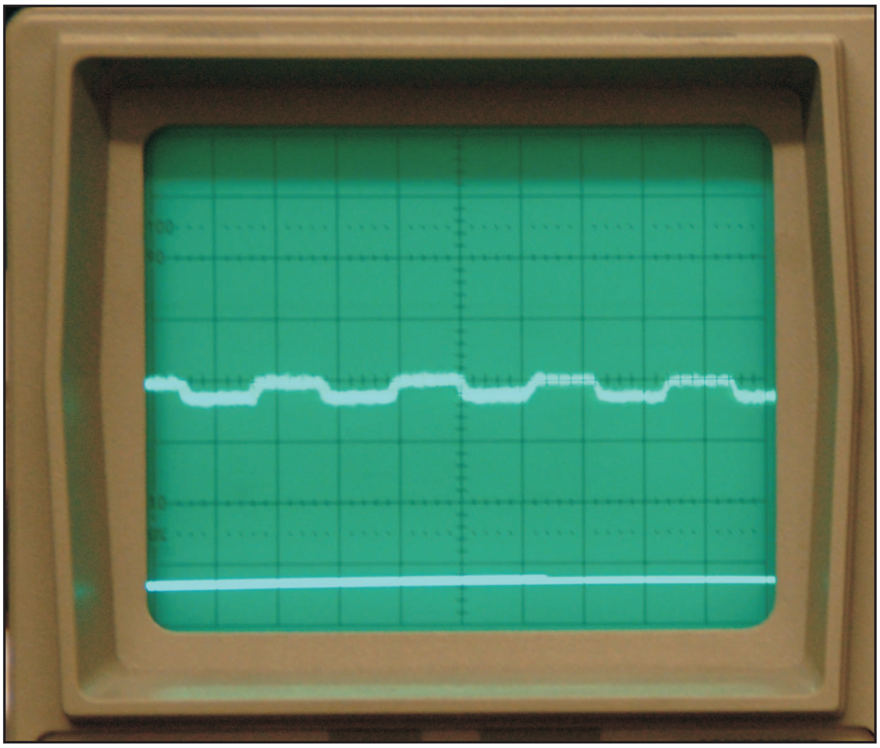

Figure 4.10: OG signal - An OG signal on an oscilloscope.

To summarize, OG spectroscopy is an optimal tool find out the position of spectral lines, but it cannot be used to assign a transition to certain energy levels.

4.6 Laser-induced fluorescence spectroscopy

If a spectral line should be assigned to a transition between energy levels the technique of laser-induced fluorescence (LIF) spectroscopy can be used.

When the laser frequency is in resonance with an optical transition, the population of the upper level of the investigated transition is increased and therefore also the fluorescence transitions from the upper level to other lower lying levels are increased. The laser light passes through the discharge and when the discharge light from the hollow cathode lamp is focused into a spectrometer such as a monochromator, fluorescence channels can be chosen and the increase of a LIF transition can be observed via a lock-in amplifier, whose reference frequency is, once more, the chopper frequency.

Simultaneously the population of the lower level of the investigated and excited transition is decreased. If the lower level has a high enough energy, it has fluorescence decays to even lower lying energy levels. The intensity of those decays decreases the same way as the fluorescence lines from the upper level increase. The decrease can also be observed at the lock-in amplifier with a signal which has the opposite phase as the fluorescence lines from the upper level. Therefore we call them negative fluorescence lines.

A third effect, which can be observed via LIF spectroscopy is the collisional coupling. If two energy levels (high or low) have an energy within a certain range it can occur that energy is transferred by inelastic collision to this near lying level. The fluorescence lines which decay from this level can than be observed. Those lines have nothing to do with the actually excited transition and are therefore quite difficult to assign. Collision coupling can occur to the upper level as well as to the lower level of an optical transition.

All effects described above are illustrated as a level scheme in figure 4.11

With the technique of LIF spectroscopy spectral lines can clearly be assigned to a transition between energy levels. Each fluorescence line (either from the upper or from the lower level) belonging to the same transition show the same hf pattern, the one from the excited line. If two or more spectral lines have mostly the same cg wavelength, they have an overlapping hf structure. As described in chapter 4.5, such blended lines are not distinguishable by OG spectroscopy. If the laser frequency is in resonance with such a blend situation, the laser excites more than one transition and, when scanning the monochromator usually a lot of fluorescence lines are observable. If the hf pattern

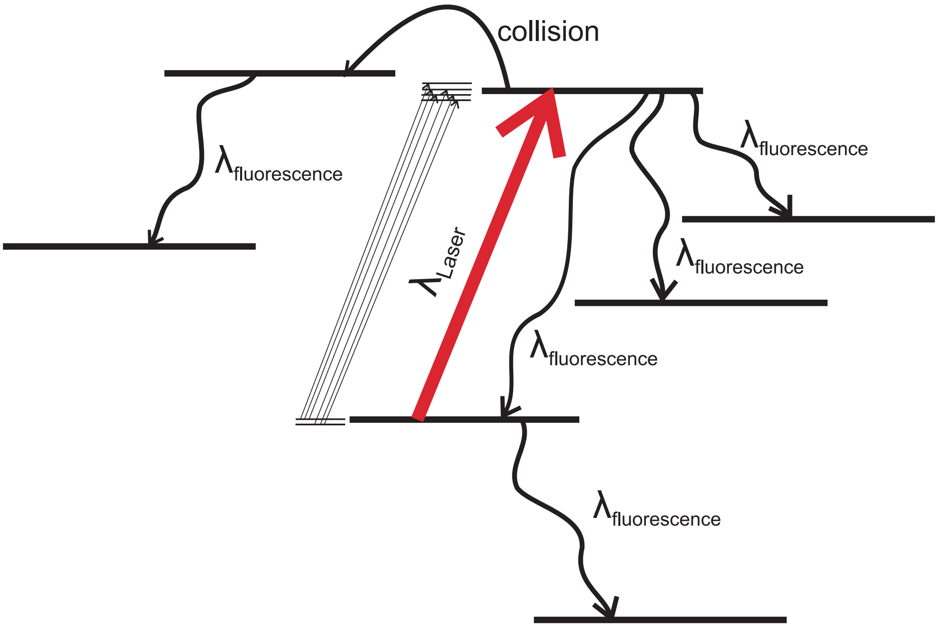

Figure 4.11: LIF - The level scheme of Laser induced fluorescence spectroscopy.

is recorded for every fluorescence channel, the different fluorescence wavelengths can be combined. Every wavelengths that show the same pattern belong to the same spectral transition.

4.7 Saturation spectroscopy

When saturation spectroscopy is performed experimentally, the laser beam has to be splitted in two equally distributed parts by a beam splitter before entering the hollow cathode lamp. One beam goes through the discharge as before and the second one passes outside of it; they meet at the end of the discharge tube, where there is a mirror. This mirror reflects the laser light and it can be used twice.

The atoms in a hollow cathode lamp move with different velocity distributions, according to the Maxwell distribution, in every direction in space. If a laser scan is running, every velocity group is excited one by another because of the Doppler effect. That is the reason for the Doppler broadening of the components of a spectral line. If the laser light strikes the atoms from two opposite directions, the light in one direction excites another velocity groups than the light of the other direction. Therefore two velocity classes of the atoms are excited simultaneously. If it is now the case, that the laser light has a frequency which excites those atoms which move orthogonal to the light propagation, than both laser beams excite the same velocity class and saturation can occur. In the line pattern there is a small dip visible which is called Lamp-dip. Those Lamp-dips give a very accurate position of every hf component of a transition. Doppler-free measurements in a hollow cathode lamp where performed for example by Hänsch et al. [51].

When a chopper disk with two differently divided circles (different frequencies) is used, one for each part of the splitted laser beam, it is possible to suppress the Doppler broadened background. This is only possible if the different frequencies of the chopper disk have a fixed phase relation with the lock-in amplifier. It has to be monitored the sum frequency of both slits of the beam splitter, than the lock-in amplifier shows the frequency sum of both chopped laser beams. As a result only the non linear parts are shown when making a frequency scan.

An example of a recorded hf pattern recorded via LIF spectroscopy in combination with saturation spectroscopy is shown in figure 4.12. The FWHM of one component is now about 300 MHz.

If one has a closer look at figure 4.12, it can be seen that there are more components than there should be. Those components are called cross over resonances and they are caused by an overlap of two hf transitions with a common upper or common lower level. Each two or three hf components in the figure 4.12 have the same lower level. The frequency position of such a cross over resonance is just in the middle of the between the transition 1 and 2 or between 2 or 3, respectively.

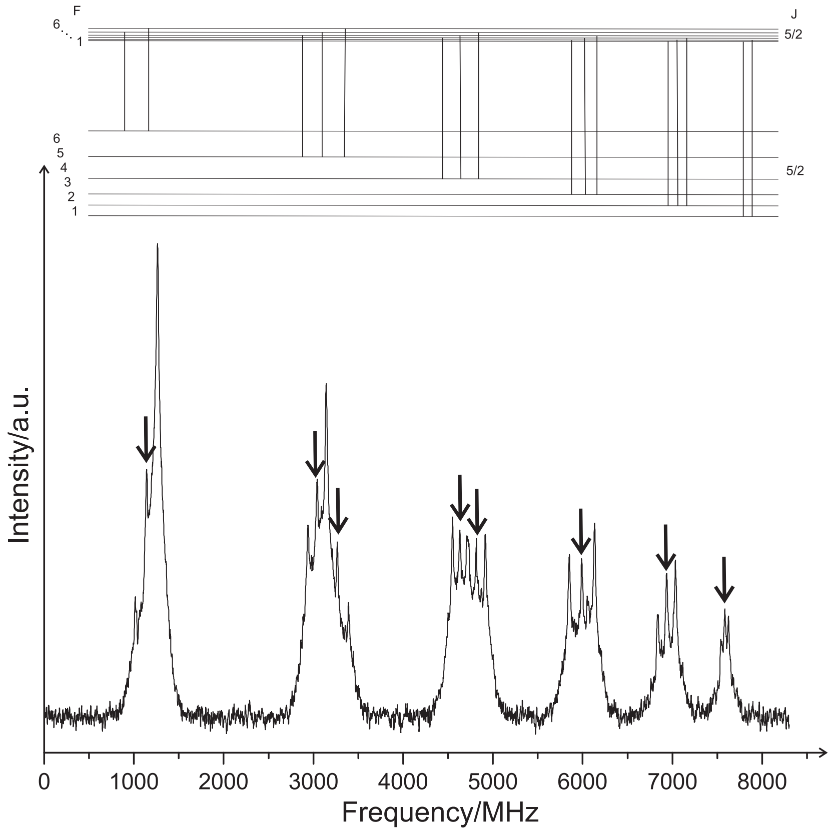

Figure 4.12: Saturation spectroscopy - An example of a spectral line investigated via LIF saturation spectroscopy. Cross over resonances are visible and marked with arrows.

5

Results-Praseodymium

5.1 Analysis of the FT spectrum

In the years 2006 and 2007 we went to the institute of quantum optics of the Leibniz University of Hannover to record new FT spectra of Pr over a spectral range of 2500 Å to 16500 Å. We used our discharge lamp as a light emitting Pr source. This work was done during my diploma thesis: [52].

The following part is taken from "B GAMPER, Z UDDIN, M JAHANGIR, O ALLARD, H KNÖCKEL, E TIEMANN and L WINDHOLZ: **Investigation of the hyperfine structure of Pr I and Pr II lines based on highly resolved Fourier transform spectra** *Journal of Physics B*, 44, 045003, 2011" [21]. I eliminated all the spectral lines and energy levels, which were not completely investigated from me, they were investigated by one of the other authors. All the rest, which is written here, was done by me.

> The recorded FT spectra of the different spectral regions were combined to form one spectrum which can be used by the existing classification program [53]. The amount of spectral lines in Pr is enormous. An example of the FT spectrum in the visible region is shown in figure 5.1. This figure shows a very small extract of 2.5 Å of the whole FT spectrum. In this region there are noticeable at least 13 lines, which are marked by an arrow. Some of the lines in this figure appear to be overlapping, and sometimes an overlap of several lines with prac-

tically the same center of gravity (cg) wavelength can be found. This fact is due to the very big number of electronic energy levels of the Pr atom: Transition energies between certain different pairs of levels are nearly or exactly the same. For such blend situations the assignment of the correct level pair is not possible using only the wave number difference of the levels in comparison with the cg wave number from the FT hf pattern. Moreover, the shape of the hf pattern has to be considered. For a huge number of lines the classification is possible since the hf pattern predicted from already known hf constants of the involved levels coincides with the hf pattern observed in the FT spectrum. Of course, this procedure provides that the hf constants of the combining levels are already known from earlier measurements.

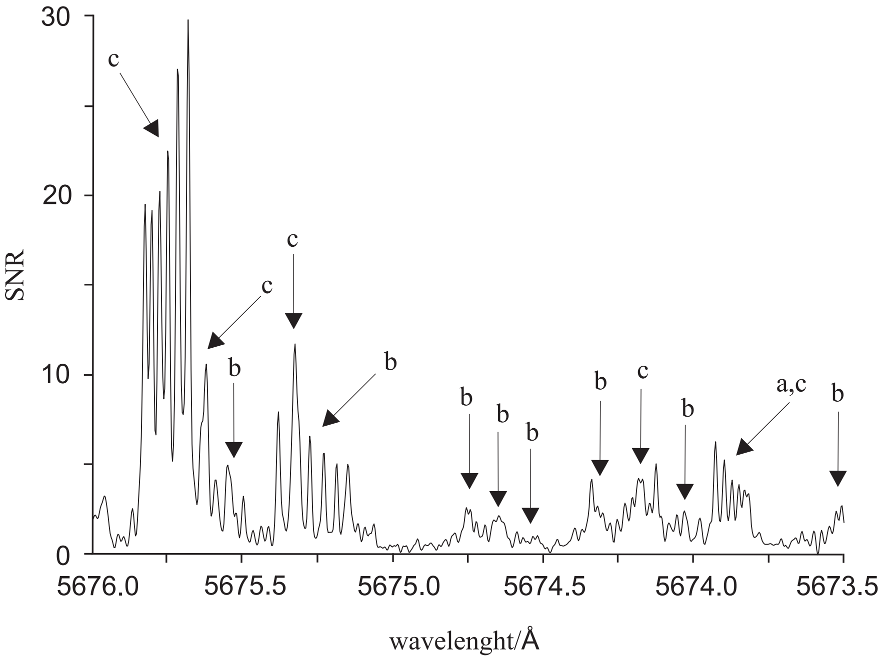

Figure 5.1: Part of the FT spectrum - Part of the FT spectrum in the visible region.
a . . . line classified before having the FT spectrum by laser spectroscopy [54]
b . . . line which is seen for the first time with help of this spectrum (new line)
c . . . line which is classified already in [55]

Otherwise, hf constants can be determined using the FT pattern, if the transition is known but the hf constants not. The proof, if the hf constants are correct is to compare the hf patterns of other lines combining with the level under investigation in the FT spectra. For this purpose it is necessary to extend the FT spectrum over a range as wide as possible.

If the situation in the FT spectrum is very complex, so that the observed spectral structures can not be clearly distinguished, laser spectroscopic experiments are necessary to divide the excited levels by their characteristic fluorescence lines. In this case the FT spectrum can be used conveniently to set the desired laser excitation wavelength.

All line components in figure 5.1 which one can see are also possible excitation wavelengths for laser-induced fluorescence (LIF) spectroscopy. The excitation wavelengths can be determined from FT spectra with a uncertainty of few 0.001 Å. The index ”a” describes those lines which have already been excited and classified in reference [54]. Those lines which were seen additionally for the first time are marked with ”b”. Only 5 lines were mentioned in the list of Ginibre [55]; they are marked with ”c”.

Originally, our database contained approximately 17000 lines of Pr I and Pr II. Up to now we could enlarge this list to about 26000 lines. Many of the 26000 lines are not yet classified, meaning that not every line listed in Ginibre’s tables [55] or discovered in the present FT spectra is related to a transition between two already known energy levels.

In table 5.1 new atomic and ionic lines with an signal to noise ratio (SNR) larger than 50, classified without doubt via the highly resolved FT spectra are listed. In table A.1 all new spectral lines of the praseodymium atom which clearly could be assigned to a transition between two energy levels, are given. This table, containing more than 1200 lines, is available in its full length [. . .] in A.1.

Table 5.1: Spectral lines of Pr I and Pr II with an intensity larger than 50 which clearly could be assigned to a transition between two energy levels

		Even		Odd	
λ/Å	SNR	J-value	Level Energy/cm^{-1}	J-value	Level Energy/cm^{-1}
5391.580	58	15/2	9745.391	15/2	28287.674
5394.051	91	9/2	8643.839	9/2	27177.628
5424.089	64	11/2	9268.741	11/2	27699.892
5435.134	55	5/2	9710.615	7/2	28104.309
5445.407	89	19/2	11151.448	19/2	29510.445
5453.232	118	11/2	27066.095	13/2	8733.450
5456.397	69	9/2	8029.290	9/2	26351.314
5456.876	56	17/2	12736.636	19/2	31057.048
5462.883	61	9/2	18300.341	9/2	0.000
5471.965	79	15/2	8765.556	15/2	27035.451
5530.631	53	15/2	8765.556	15/2	26841.658
5534.181	55	7/2	8013.104	7/2	26077.608
5538.374	nl 240	11/2	26784.270	13/2	8733.450
5567.521	nl 2	8	13021.330	7	30977.671
5617.656	54	17/2	11714.367	19/2	29510.445
5624.964	213	7/2	6535.587	9/2	24308.545
5645.683	64	15/2	22088.820	15/2	4381.100
5649.278	56	11/2	9268.741	13/2	26965.207
5748.007	75	13/2	6603.606	15/2	23996.130
5753.327	61	11/2	9268.741	13/2	26645.170
5756.391	nl 81	11/2	8829.078	13/2	26196.253
5843.479	53	9/2	8320.255	11/2	25428.607
5893.492	234	11/2	6714.199	13/2	23677.365
5907.249	112	9/2	18300.341	11/2	1376.605
5936.246	nl 58	9/2	8029.290	11/2	24870.318
5949.765	nl 171	17/2	27523.120	17/2	10720.400
5987.819	nl 94	9/2	8320.255	11/2	25016.201
5994.418	nl 82	9/2	18054.202	11/2	1376.605
6023.642	68	15/2	27265.622	15/2	10668.960
6030.234	54	15/2	28342.772	17/2	11764.250
6061.992	70	9/2	27145.754	7/2	10654.110
6074.993	134	9/2	24706.499	9/2	8250.170
6083.735	78	11/2	6714.199	13/2	23146.917
6085.810	142	9/2	24677.280	9/2	8250.170
6107.014	90	9/2	25205.463	11/2	8835.380
6280.999	54	11/2	27662.982	13/2	11746.340
6440.364	53	13/2	13146.599	11/2	28669.174
6441.818	56	15/2	27265.622	13/2	11746.340

[a] Previously unknown energy level

Table 5.1 – Continued

		Even		Odd	
λ/Å	SNR	J-value	Level Energy/cm^{-1}	J-value	Level Energy/cm^{-1}
6486.560	650	17/2	25059.089	15/2	9646.850
6616.025	196	7/2	15110.661	9/2	0.000
6617.336	51	15/2	24759/250	15/2	9646.850
6725.360	85	5/2	6451.823	7/2	21316.810
6995.508	52	7/2	6535.587	5/2	20826.530^{a}
7255.175	380	13/2	15156.070	11/2	1376.605
7889.311	60	17/2	9770.330	15/2	22442.185^{a}
8993.509	67	9/2	19196.472	11/2	8080.440
9144.025	53	5/2	9710.615	3/2	20643.800
9293.861	50	5/2	9710.640	5/2	20467.450^{a}
9319.006	50	17/2	11714.367	15/2	22442.185^{a}

^{a} Previously unknown energy level

[. . .]

The two [. . .] tables have the same structure: Column 1 contains the cg wavelength in air in Å. Information about the SNR is given in column 2 (per definition, noise is treated to have SNR = 1). If there is written ”nl” in front of the SNR it means that this line is a new one, not known before these investigations. All the other lines are mentioned in the list of Ginibre [55] but they are not classified, either because the energy levels involved in the transition were found after she did her work or because the hf patterns were not sufficiently resolved in her spectra. In columns 3 and 5 the J-values of the involved levels are listed. The corresponding energies in cm^{-1} are given in columns 4 and 6. The energy levels are listed according to their parities, in the column 4 the even ones and in the column 6 the odd ones. If a new level is involved, it is marked with an upper index ’a’.

For some well resolved lines, which could not be classified as transitions between known levels, it was possible to determine the hf constants and to identify one of the involved levels by its hf constants. Then a new level could be introduced combining the wave number of the identified level and the wave number of the transition. The proof that such a level exists is done by calculating all possible decay wavelengths and comparing the corresponding regions of the FT spectrum with the predicted pattern. If appearing structures coincide with the expected pattern and the expected cg wavelength, the level is assumed to be really existing. This method of finding new levels is especially important for spectral regions where laser excitation is difficult, e.g. in the IR or UV.

Table 5.2: New levels found by analysis of FTS hf patterns.

energy/cm^{-1}	J-value	A [1]/MHz	parity	lines which can be explained (Å)
20467.450(10)	5/2	792(16)	o	9293.861, 9241.771, 8027.119
20942.933(5)	11/2	363(3)	o	9958.534, 9503.761, 8724.067, 8709.564, 7509.564, 7115.484, 7026.094
22442.185(5)	15/2	959(9)	o	9612.268, 9319.006, 9189.156, 8393.847, 8210.847, 7889.311, 7873.840, 7309.733, 7101.187, 6311.952
22516.49(5)	1/2	-994(5)	o	9945.496, 9751.939, 9553.105, 9426.870, 9385.756, 8926.403
24183.415(10)	11/2	969(3)	o	9058.096, 8233.786, 7265.574, 6630.181
24289.760(10)	19/2	990(3)	o	8653,316, 7609.254[2], 6885.420
24751.780(10)	19/2	1012(2)	o	8986.241, 8320.561, 7668.138
26692.000(5)	17/2	837(5)	o	9956.092, 9216.883[2], 8069.405[2], 7651.767, 7163,745

[1] The value of the hyperfine constant B could not be determined with significance therefore it is not taken into account in this work. B was set to zero when determining A.

[2] The line was already classified in reference [55], but this classification is wrong.

In this way, we could determine several new energy levels. The hf constants were determined by fitting the hf pattern of the line under investigation, using the program ”Fitter” ([56]). These levels are marked in table A.1 and table 5.1 with subscript ”a”. The results are shown in table 5.2. Column 1 of this table gives the energies in cm^{-1} of the newly discovered levels, determined under the assumption that the energy of the lowest even state, 4432.24 cm^{-1}, is correct. Their J-values are listed in column 2; in the next column the hyperfine constants A (in MHz) are given. Due to the limited resolution of the FT spectrum the value of B was assumed to be zero. The 5th column tells us which lines (wavelengths in air in Å) can be explained with the new levels. The corresponding transitions can be found in table A.1.

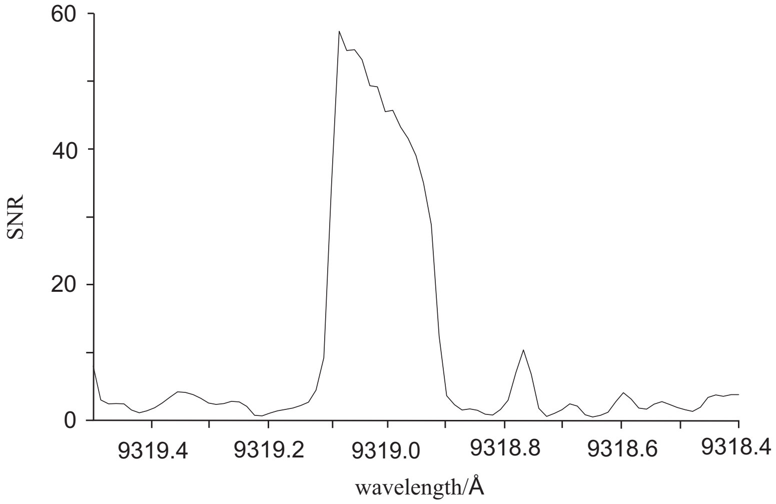

Figure 5.2: Line 9319.006 Å - FT spectrum - Appearance of the line 9319.006 Å in the FT spectrum

As an example we discuss the line with the cg wavelength 9319.006 Å. The relative intensities and distribution of the components (figure 5.2) suggest a transition with $\Delta J = -1$ with almost equal values of the hyperfine constants A of both levels. The small sharp peak at the high frequency side of this hfs pattern is generated under this hypothesis by the coincidence of the five off diagonal ($\Delta F = 0$) hyperfine components within the Doppler width. We fitted the structure assuming $J = 17/2$ and $J' = 15/2$ (the prime marks the upper level of the transition). As a result we got $A = 970$ MHz and $A' = 961$ MHz. Then we looked in our level data base for a level having J and A as determined in the fitting process. We found an even level with the energy 11714.367 cm^{-1}, with $A = 970.2(3)$ MHz, $B = -16(4)$ MHz and $J = 17/2$. Believing that this level is the lower level involved in this transition, we fitted the structure again with fixed hyperfine constants of the lower level and added the cg wave number of the investigated line to the wave number of the lower level. Finally we determined the new level to have 22442.185(5) cm^{-1}, $J' = 15/2$,

$A' = 959(9)$ MHz with odd parity (best fit is shown in figure 5.3). The new level explains 5 other lines in the IR region and 3 lines in the visible region (see Table 5.2).

We have to emphasize that such a fit is only possible if some of the small components (or a convolution of them) are clearly resolved in the FT spectra. Otherwise, the splitting of the diagonal components is sensitive more to the difference $(A - A')$ than to the absolute values of A, A', and one cannot identify one of the involved levels by its A-value.

Altogether [...] 8 new levels could be found by the analysis of FT patterns, mainly in the IR region; each explains other previously unclassified lines, mostly in the IR region.

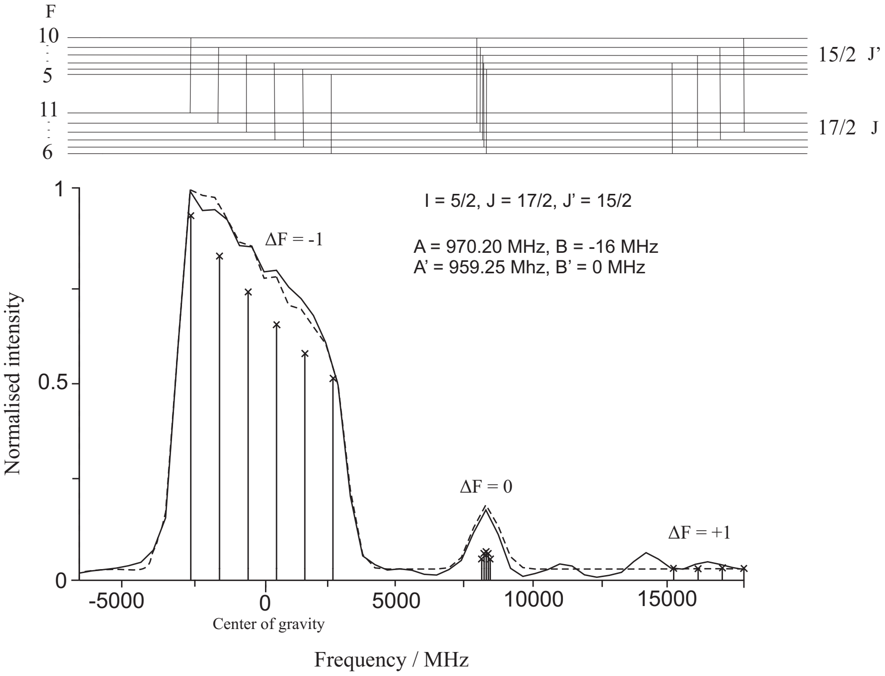

Figure 5.3: Line 9319.006 Å - best fit - Best fit of the FT spectrum of the line 9319.006 Å assuming a transition $J = 17/2$ to $J' = 15/2$. The hf constants of the lower level were fixed, the B factor of the upper level was assumed to be zero. The appearance of the line in the FT spectra (solid line) is compared to fitted line profile (dashed line). All spectral lines appear in the FT spectrum with relative intensity ratios which are very close to the theoretical ones. The upper part of the figure shows the hf level scheme and all transitions.

5.2 The region between 5810.5 Å and 5812.0 Å

The following part is cited from [57]. Everything which was not done by myself is removed.

> We treat here a very narrow part of the Pr spectrum of just 1.5 Å the region between 5810.5 Å and 5812.0 Å. This part of the FT spectrum is shown in figure 5.4, the y-axes represents the signal to noise ratio (SNR). In this figure one can see that there are a lot of overlapping spectral lines, because there barely are lines with a regular distribution of the hf components, moreover, most of the components are not resolved in the FT spectrum. In this part there are at least 14 different overlapping spectral lines which are marked with brackets in figure 5.4. The designation of the brackets mean the following: (a) lines were classified by Ginibre [15], (b) spectral lines which were not in the level list of Ginibre, they have a newly found energy level involved, (c) seem to be spectral lines in the FT spectrum, but could not be assigned to an optical transition up to now and (d) lines which could be introduced as new lines (nl), but the energy levels involved in the transitions were already known.
>
> As an example of the method of LIF spectroscopy we discuss the line with the cg wavelength 5810.940 Å, marked with an asterisk in figure 5.4. We set the laser wavelength in resonance with the transition and could observe two fluorescence lines with the wavelength 5095 Å and 4913 Å. In figure 5.5 the recorded LIF signal (dashed line) as well as the fitted structure (solid line) are shown.
>
> The signal shows a regular flag pattern, where 4 of the 6 main components ($\Delta F = +1$) are resolved, which starts with the highest component on the left side; but at the right side it is not quite possible to distinguish them from the weaker components ($\Delta F = 0$). This fact indicates a $\Delta J = +1$ transition from J' to J (the prime marks the upper level of the transition) with medium J-values. We fitted (our fit program is from Guthöhrlein [56]) the structure assuming $J' = 5/2$

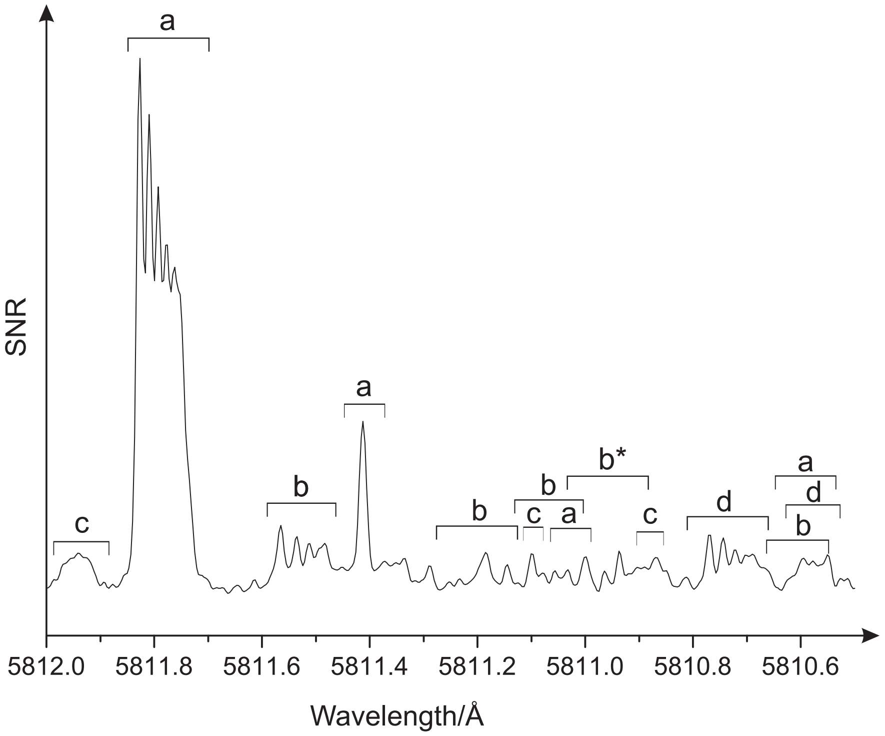

Figure 5.4: Part of the FT around 5811 Å - Part of the FT spectrum between 5810.5 Å and 5812.0 Å.
a . . . refers to lines classified by Ginibre [15];
b . . . refers to spectral lines which were not in the level list of Ginibre, they have a newly found energy level involved; * . . . refers to the line discussed in section 5.1;
c . . . refers to lines which seem to be spectral lines in the FT spectrum, but could not be assigned to an optical transition up to now;
d . . . refers to lines which could be introduced as new lines (nl) , but the energy levels involved in the transitions were already known.

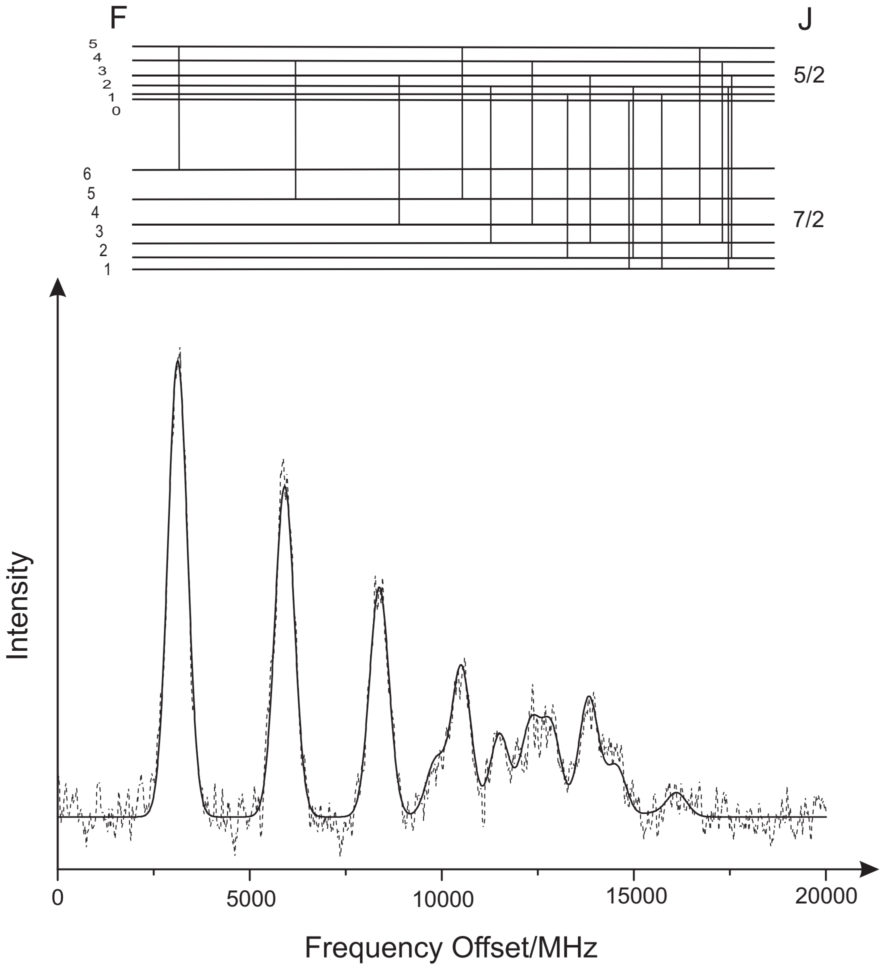

Figure 5.5: Line 5810.940 Å - Hf pattern of the line with cg wavelength 5810.940 Å recorded via LIF spectroscopy. The fluorescence channel is 5095 Å.

and $J = 7/2$ and got $A' = 802$ MHz and $A = 1140$ MHz. In our level database we found an energy level with $J = 7/2$, $A = 1142$ MHz and an energy of 18597.913 cm^{-1}. Now we fitted the structure again with a fixed A-value for the lower level and got $A' = 800$ MHz. Assuming that this is the lower level involved in our transition, we added the cg wavenumber to this energy and got the energy of our new upper level: $E' = 35802.062$ cm^{-1}. As a confirmation that the newly introduced energy level really exists we searched in our spectral line list for other unclassified lines and we found a line with the cg wavelength of 5007.245 Å which could clearly be assigned to a transition involving the new level as the upper level because of its appearance in the FT spectrum. This also proofs that the assumption that the lower level energy 18597.913 cm^{-1} of the actually investigated transition is right, because the newly introduced upper level would not exist if the lower level was wrong.

Altogether we could identify and classify seven of the spectral lines in this region as new lines involving five new energy levels. Before our investigations there were just four lines classified; we confirmed these classifications either by LIF spectroscopy or with the help of the FT spectrum. We investigated eight lines by LIF spectroscopy and classified them. Three of the spectral lines are clearly resolved in the FT spectrum, therefore we could assign them to a transition between already known energy levels just by analyzing their shape in the FT spectrum. All the investigated lines are listed in table 5.3. The first column gives the cg wavelength. The signal to noise ration (SNR) of the lines in the FT spectrum is written in the second column. If there is written ”nl” in front of the SNR it means that this line is a new one. The columns three to five give the J-value, energy and parity of the upper level involved in the transition; the corresponding values of the lower level are listed in the columns six to eight. The previously unknown energy levels are marked with subscript ”a”and explained in table 5.4. The accuracy of the energies depends mainly on the SNR of the investigated hf patterns and uncertainty of the

Table 5.3: Spectral lines of Pr in the treated range which clearly could be assigned to a transition between energy levels (uncertainty of the energies is ± 0.001 cm^{-1}).

		Upper Level			Lower Level		
λ/Å	SNR	J-value	Energy/cm^{-1}	Parity	J-value	Energy/cm^{-1}	Parity
5811.791[b]	70	9/2	18578.232	e	11/2	1376.602	o
5811.530	nl 8	9/2	28605.413[1a]	e	7/2	11403.011	o
5811.414[b,c]	6	11/2	27634.464	e	11/2	10431.716	o
5811.220	nl 2	9/2	32343.286[1a]	o	9/2	15139.967	e
5811.050	nl 2	11/2	32221.911[1a]	e	13/2	15018.088	o
5811.018[c]	1	5/2	30123.235	e	7/2	12919.316	o
5810.940	nl 5	5/2	35802.062[a]	o	7/2	18597.913	e
5810.730[b]	nl 7	13/2	28487.636	o	7/2	11282.865	e
5810.599	nl 2	9/2	30932.614[1a]	o	11/2	13727.482	e
5810.581	2	9	28816.267	e	8	11611.084	o
5810.571	nl 2	11/2	30856.797	o	13/2	13654.555	e

[a] Previously unknown energy level.

[1a] [Previously unknown energy level, which was estimated for the first time by one of the co-authors.]

[b] Spectral lines classified by analyzing the FT spectrum.

[c] Spectral lines which have already been classified and assigned to a transition between energy levels before our investigations; we confirmed the classification.

upper and lower energies is ±0.001 cm^{-1}. The spectral lines which have a subscript ”b” are classified by analyzing the FT spectrum. This is possible because those lines appear as single lines in the FT spectrum and they are pretty well resolved.

Table 5.4 lists the five newly found energy levels in the investigated region from 5810.5 Å to 5812.0 Å. In the first column the level energy is listed, the J-value is mentioned in the second one. The columns three and four give the A-value and the parity of the level. The hyperfine constant B could not be determined accurate enough and was therefore set to zero when determining the hyperfine constant A. The last column gives the cg wavelength of the spectral lines in the FT spectrum which clearly could be assigned to a transition involving the newly introduced level. On the lines which are marked with an asterisk LIF spectroscopy was performed and the newly found level was confirmed by a second or even third excitation.

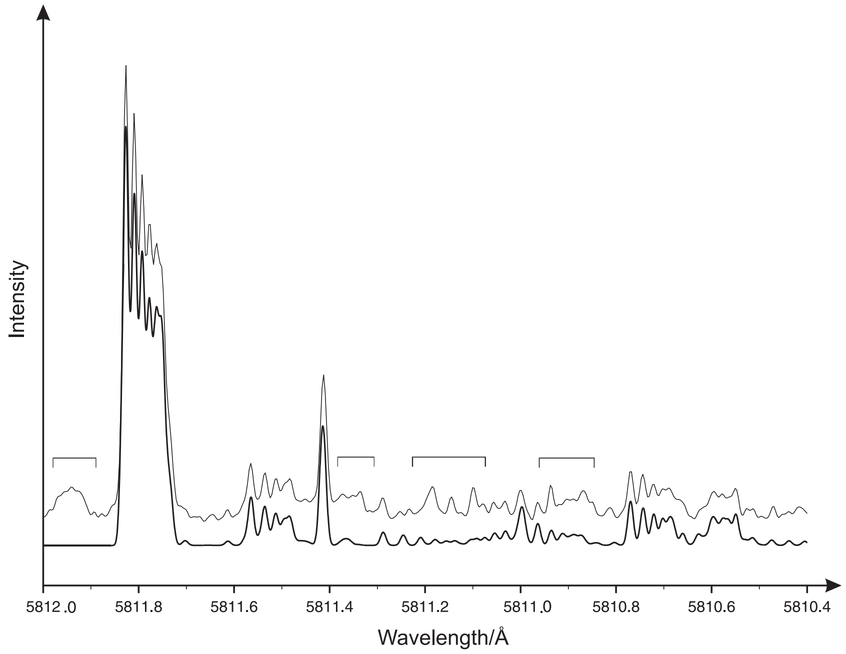

Figure 5.6: FT spectrum - sum hf profiles - The FT spectrum compared with the sum of the hf profiles. The upper one is the FT spectrum and the lower one the sum of the hf patterns. The spectral lines which are marked with brackets could not be explained yet.

Finally we summarized all the classified hf profiles of the investigated region taking relative intensities from the FT spectrum and compared it to the emission spectrum recorded via FT spectroscopy. The result is shown in figure 5.6. The upper line is the FT emission spectrum and the lower one is the modelling of this spectrum by summarizing the hf patterns of all the overlapping lines from 5810.5 Å to 5812.0 Å. The figure shows that the two different patterns fit pretty well. The result is the expected one: both traces have the same shape, which is one more proof that the classifications done were right. The figure shows also that there still are some lines, marked with brackets

Table 5.4: New energy levels of Pr I found by LIF spectroscopy in the region of 5810.5 Å to 5812 Å.

Level energy/cm^{-1}	J	A [1]/MHz	parity	Lines explained with new level/Å
28605.413 [1a]	9/2	615.6(9)	e	5658.160*, 5784.493*
30932.614 [1a]	9/2	676.0(8)	o	4702.878
32221.911 [1a]	11/2	422(1)	e	6377.793*, 4785.134
32343.286 [1a]	9/2	654.2(1)	o	5908.737*, 5698.840*, 4410.220
35802.062	5/2	800.2(1)	o	5007.245

[1] The value of the hyperfine constant B could not be determined with significance therefore it is not taken into account in this work. B was set to zero when determining A.

* On these spectral lines a second laser excitation was performed and the newly introduced energy level was confirmed.

[1a] [Energy level, which was estimated for the first time by one of the co-authors.]

in figure 5.6, which are not yet explained. Some peaks which appear in the FT spectrum are missed in the modeled one, they have to be investigated further by LIF spectroscopy.

6

Results-Lanthanum

6.1 Spectral lines with a very low intensity

We use a Fourier transform (FT) spectrum which was provided to us from Riga to look for possible spectral lines and the position of them in order to find out laser wavelengths of possible excitations. In the FT spectrum of La the density of strong lines is rather low. Most of the strong lines were already classified several years ago. When we started to investigate La, we were looking for spectral lines with low intensity which could not be interpreted as transitions between known energy levels, that means, up to now unknown levels are involved. An example of a line with low intensity is the line with the cg wavelength 6239.539 Å. The appearance of this line in the FT spectrum is illustrated in the upper part of the figure 6.1. At the right side of this line, toward lower wavelengths, a line with high intensity appears.

Nevertheless the intensity of this line is rather low, when making an OG frequency scan over it, a very well resolved signal with high intensity could be observed. The registered pattern is presented in the lower part of the figure 6.1.

As this spectral line could not be assigned to a transition between known levels, we assumed that a new level is involved. Therefore we set the laser frequency in resonance with the observed transition and scanned the monochromator in order to search for fluorescence lines. A strong negative fluorescence channel at 4280 Å could be seen. As this fluorescence should derive from the lower level of the transition of interest, we were looking for a strong spectral line with this wavelength in the FT spectrum, which is really there. Supposing the upper energy level (24409.684 cm^{-1} 7/2 o) of this

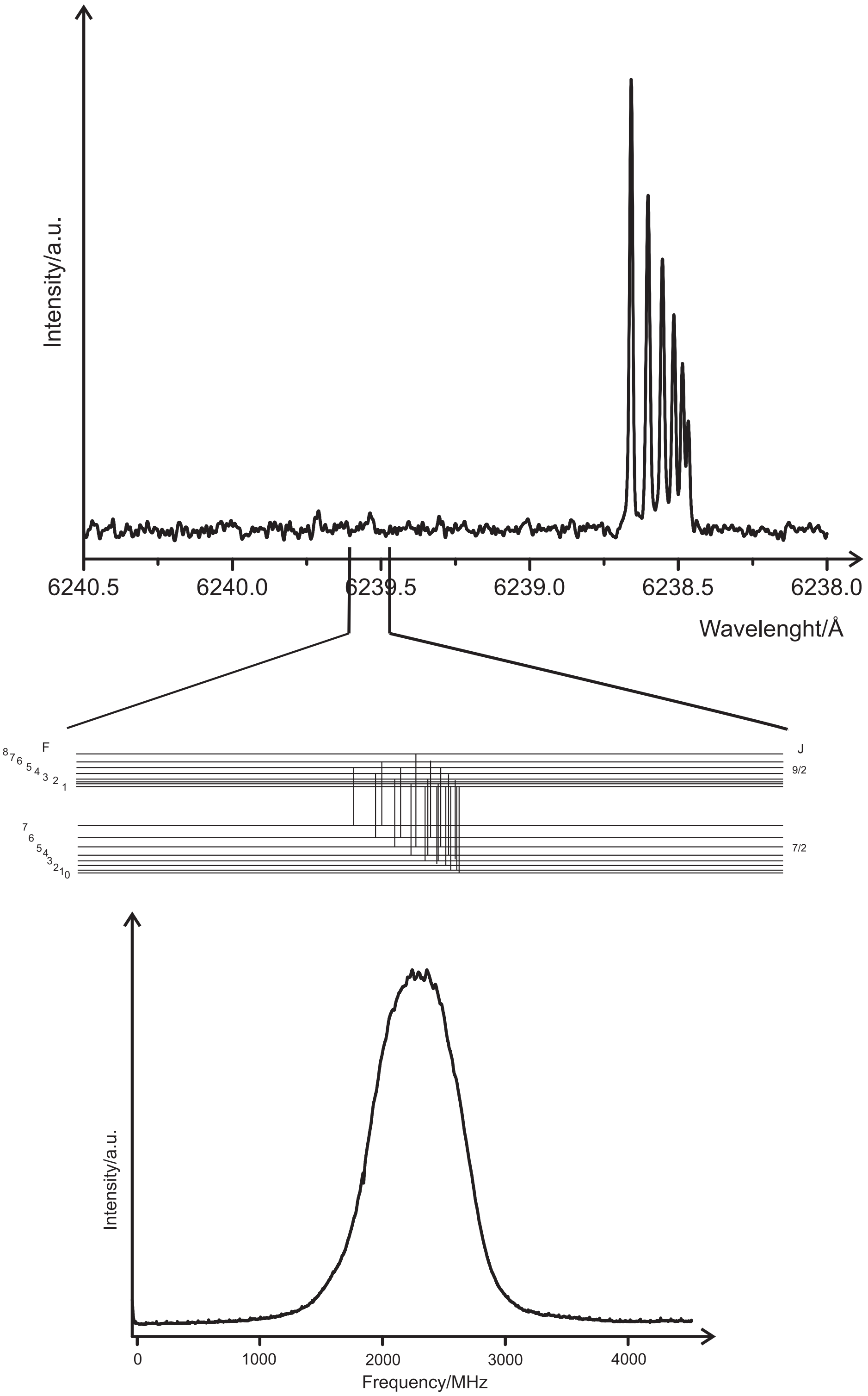

Figure 6.1: Low intensity line - A spectral line which has a very low intensity, it is not visible in the FT spectrum. In the lower part the recorded OG signal is shown.

line was the lower energy level of the investigated line, we add the cg wavenumber of the excited transition to the lower level and calculated a new upper energy level: $E' = 40432.076$ cm^{-1} with even parity. When simulating the pattern a J-value of $J' = 9/2$ was assumed, which was still not sure because the small components are not resolved in the registered pattern. As shown in the middle part of the figure 6.1, they are lying beneath the strong components. To confirm the newly introduced energy level, we tried to excite it from other lower levels. The first excitation was a spectral line with the cg wavelength 6513.40 Å having a lower energy of 25083.356 cm^{-1} and $J = 7/2$. The observed pattern showed the expected shape, it is a confirmation that the newly introduced level exists. Also an excitation of the line with the cg wavelength 6412.32 Å was a confirmation of the new level. The lower level energy of this transition is 24841.410 cm^{-1} and it has a J-value of 11/2. Now the J-value of the new level $J = 9/2$ is sure, as $\Delta J = 1, \pm 1$, no other J-value is possible, because we excited the newly introduced upper level from lower levels with $J = 7/2$ and $J = 11/2$. As a next step we fitted the first recorded structure with $J = 9/2$ and estimated the A-value of the new energy level to $A = 118(2)$ MHz.

Also the two excited lines for the confirmation of the new level are spectral lines with a very low intensity, they are not visible in the FT spectrum. When looking through the FT spectrum, we found an unclassified line at 4692.912 Å with middle high intensity. When analyzing the pattern of the line in the FT spectrum, we were able to classify it as a transition involving the newly introduced level as a upper level. The lower level energy of this transition is 19129.307 cm^{-1}.

6.2 Improving the cg wavelength of the spectral line 6402.4 Å with the help of a spectral line visible in the FT spectrum

The newly introduced level with the energy 40525.20 cm^{-1} was excited for the first time at 6531.18 Å. For a second excitation we tried to excite the spectral line with a cg wavelength 6402.4 Å, as this spectral is the energy difference between the newly introduced level and a lower level ($E = 24910.375$ cm^{-1}) which has a different parity and $\Delta J = -1$ compared to the newly introduced energy level. The spectral line 6402.4 Å, is not visible in the FT spectrum, but there is a strong, well resolved one in the

FT spectrum nearby, which is a well known transition between the known energy levels $E' = 31119.020\,\mathrm{cm}^{-1}$ and $E = 15503.630\,\mathrm{cm}^{-1}$. As the FT spectrum gives us an accuracy of the cg wavelength of spectral lines in the range of ± 0.001 Å we know that the cg wavelength of this visible line is 6402.169 Å. Therefore we wanted to make an OG laser scan where both spectral lines are recorded in order to make a two line fit to and to determine more accurately the cg wavelength of the new spectral line.

When recording the region of interest, we saw that there is one more line at 6402.3 Å between the spectral line involving the newly introduced energy level and the spectral line visible in the FT spectrum. By its recorded hf pattern it could be assigned to a transition between two well known energy levels ($E' = 40599.34\,\mathrm{cm}^{-1}$ and $E = 24984.294\,\mathrm{cm}^{-1}$). So, when fitting the recorded three spectral lines nearby, a three line fit was performed, which as a results gives the center of gravities of the three lines as an offset frequency MHz. The first line (highest wavelength) has a cg of 9264.17 MHz, the middle one 16223.42 MHz and the last one (lowest wavelength) 25835.55 MHz. As we know the cg wavelength of the last line (highest frequency) with high accuracy (6402.169 Å), we were able to calculate the cg wavelengths of the two other lines with the same accuracy. As a result we got two new spectral lines at 6402.396 Å and at 6402.301 Å.

Figure 6.2 shows the recorded region with the appearance of the three spectral lines (black line) as well as the fitted structure (red line). The three cg frequency are marked with crosses in blue, green and violet. The structure with the highest frequency is not recorded completely because the scan region is not large enough. Nevertheless the quality of the fit is good enough to determine the cg frequency with high accuracy.

If now the cg wavelengths of the two spectral lines are improved, also the level energies involved in the transition can be improved. The lower level energy ($E = 24984.294\,\mathrm{cm}^{-1}$ of the transition of the line with the cg wavelength of 6402.301 Å is very well known and has an accuracy of ± 0.003 cm^{-1}, therefore by adding the now well known cg wavenumber, also the level energy of the upper level can be improved. This improved level energy of the upper level is $E' = 40599.361\,\mathrm{cm}^{-1}$ and has an uncertainty of ± 0.003 cm^{-1}. Before our measurements the uncertainty[1] was ± 0.03 cm^{-1}.

---

[1] The uncertainty is always given without any systematic error.

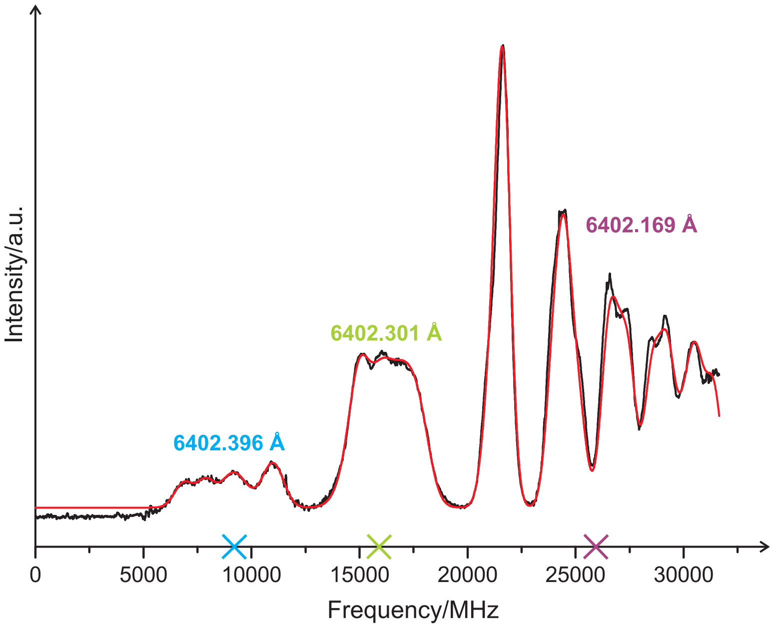

Figure 6.2: Improving cg wavelength - Improving the cg wavelength of the spectral lines with the help of the spectral line with a cg wavelength 6402.169 Å which is visible in the FT spectrum.

In the same way also the level energy of the newly introduced upper level involved in the transition of the spectral line with the cg wavelength 6402.396 Å could be improved: $E' = 40525.211\,\mathrm{cm}^{-1}$, with an uncertainty of ± 0.003 cm^{-1}.

6.3 The level with the energy 40129.64 cm^{-1}

We set the laser wavelength to 6704.55 Å and an OG signal could be observed. In this region there is no spectral line visible in the FT spectrum. To record the hf pattern of the observed line, a laser frequency scan was performed. The recorded structure is shown in figure 6.3. In our database no transition between known energy levels with the wavenumber difference of interest and the observed hf pattern exists. So, it can be supposed that at least one energy level involved in the transition is a so far unknown level. To identify at least one of the levels involved in the transition of interest, we scanned the monochromator manually over a region of 2500 Å to 7500 Å and looked for fluorescence channels. Three relatively strong negative fluorescence lines could be observed: 5958 Å , 5822 Å and 5637 Å. As the wavelength of the negative fluorescence lines should belong to a very strong spectral line in the FT spectrum, we looked for the observed lines. In fact, all three of them are strong spectral lines and also all three of them have the same upper energy level: 25218.265 cm^{-1}. This fact leads to the assumption that this might be the energy of the lower level involved in the investigated hf structure when exciting with a laser wavelength of 6704.55 Å. Supposing to have identified the lower lying energy level, we just add the cg wavenumber of the investigated line to the energy of the lower level. The energy of the new upper level is calculated: 40129.647 cm^{-1}. The lower level has odd parity, a J-value of 5/2 and a A-value of 101 MHz. As in an optical transition the parity of the two involved levels always has to change, we immediately know that the parity of the newly introduced energy level is even. For the J-value and A-value it is not so easy: the structure of interest can be fitted with a J-value of 5/2 as well as with a J-value of 3/2. For those two values the hf constant A changes, respectively. Our first guess was that the newly introduced energy level has $J' = 5/2$ and $A' = 90$ MHz.

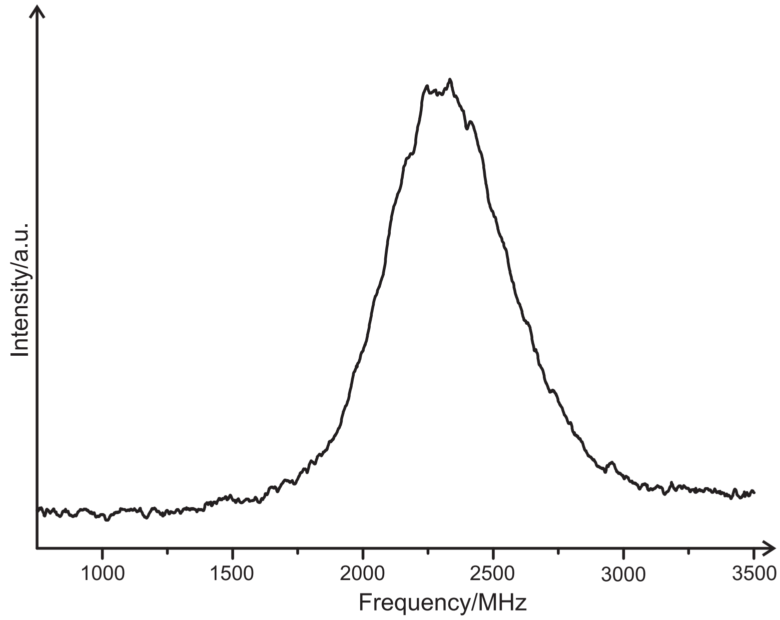

Figure 6.3: Line 6704.55 Å - The recorded OG signal of the spectral line with a cg wavelength 6704.55 Å.

Every newly introduced energy level has to be confirmed by at least one other laser excitation. Possible further excitation wavelengths can be calculated in the following manner: we look in our level database for energy levels whose parameters fulfill the selection rules between fine structure levels ($\Delta P = 1$, $\Delta J = 0, \pm 1$), when one of the levels involved in a possible transition is the newly introduced one. After that the energy difference between of each pair of energy levels is calculated by subtracting the energy of the lower level from the energy of the upper level. The inverse of it is than the wavelength of a possible spectral line involving the new level. For the newly introduced level with the energy 40129.647 cm^{-1}, we tried to excite a spectral line at 6505.66 Å, which is not visible in the FT spectrum though. When making an OG scan over the region of interest a hf pattern could be observed, which had the same appearance as the predicted one, using $J' = 5/2$ and $A' = 90$ MHz for the upper level and the already known values for the lower level. The recorded hf pattern is presented in figure 6.4. Also a strong negative signal was visible at the lock-in amplifier, when setting the monochromator at the wavelength 4037 Å. This is a proof that the newly introduced level has the right energy, because we excited it from another lower level. This lower level has a J-value of 3/2. So, we still cannot be sure about the J-value of the newly introduced level, the angular momentum quantum number can still be 5/2 or 3/2, as $\Delta J = 0, \pm 1$.

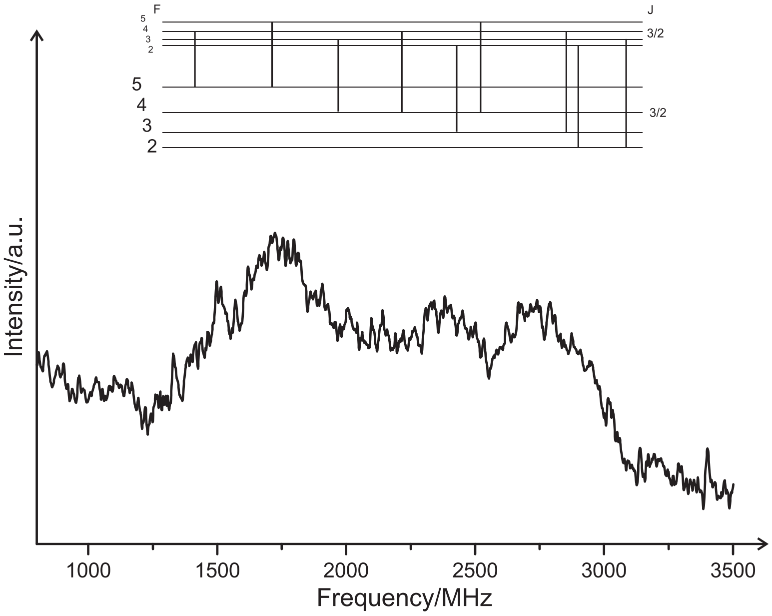

Figure 6.4: Line 6505.66 Å - The recorded OG signal of the spectral line with a cg wavelength 6505.66 Å.

As a next step, we tried two excitations from levels with $J = 7/2$, but at both wavelengths no OG signal could be observed, meaning that there is no transition (eighter due to the transition rule $\Delta J = 0. \pm 1$ or since the transition probability is too low). Therefore we now assumed that the newly introduced level with the energy of $E' = 40129.647$ cm^{-1}, might have $J' = 3/2$. To confirm this assumption we searched for possible excitation wavelengths of transitions whose lower levels have $J = 1/2$. As a transition between an energy level with $J = 5/2$ and an energy level with $J = 1/2$ is forbidden, this would be a proof that the J-value of the new level is right. When setting the laser wavelength to 6812.11 Å an OG signal could be observed. We started a laser frequency scan to record the structure and could observe two spectral lines (in the FT spectrum no line(s) are seen). The spectral line with the higher cg wavelength (lower frequency) could be assigned to a transition between two known energy levels by its pattern and the observed fluorescence wavelength (nf 5253). The spectral line with lower wavelength (higher frequency) of the two observed lines had the expected pattern when assuming it is a transition to the newly introduced level.

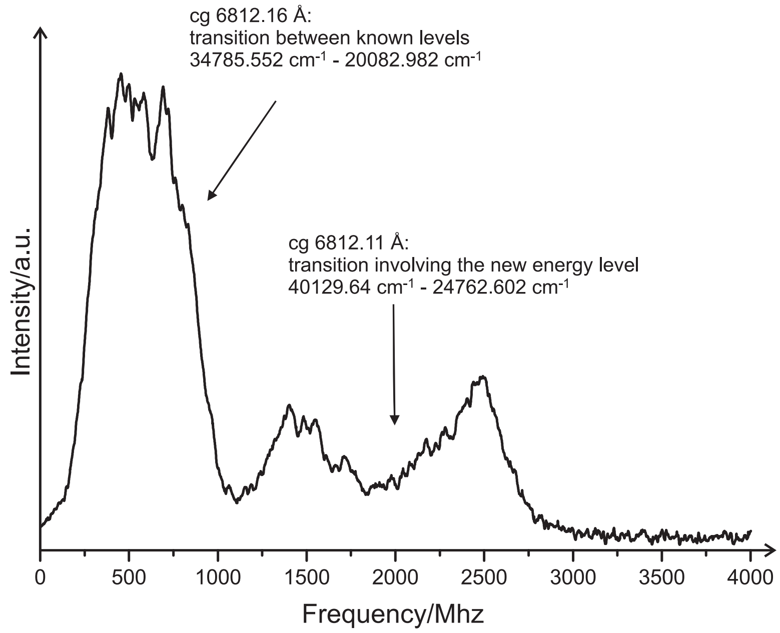

Figure 6.5: Line 6812.11 Å - Recorded OG signal of the spectral line with a cg wavelength 6812.11 Å.

In figure 6.5 the recorded pattern is shown. Also a negative fluorescence line at 3928 Å could be observed. This is the undoubtedly proof that the new level has a

J-value of 3/2. Now this structure was fitted with $J = 3/2$ for the newly introduced upper level and $J' = 1/2$ for the combining lower level. As we know the hf constants for the lower level, we fix those in the fitting process and leave the A-value of the upper level as a free fit parameter. The fitted A-value of the newly introduced energy level turned out to be $A = 163(6)$ MHz.

To summarize all the involved transitions when identifying the new level a level scheme is shown in figure 6.6. It should be pointed out, that there is no doubt that the assumed lower level of the first observed transition is right because the newly introduced energy level would not have the assumed energy when the lower level was not right. Furthermore it is very important to understand that the so called negative fluorescence lines are only observable if the right transition is excited, the one whose lower level is the upper level of the observed (negative) fluorescence lines.

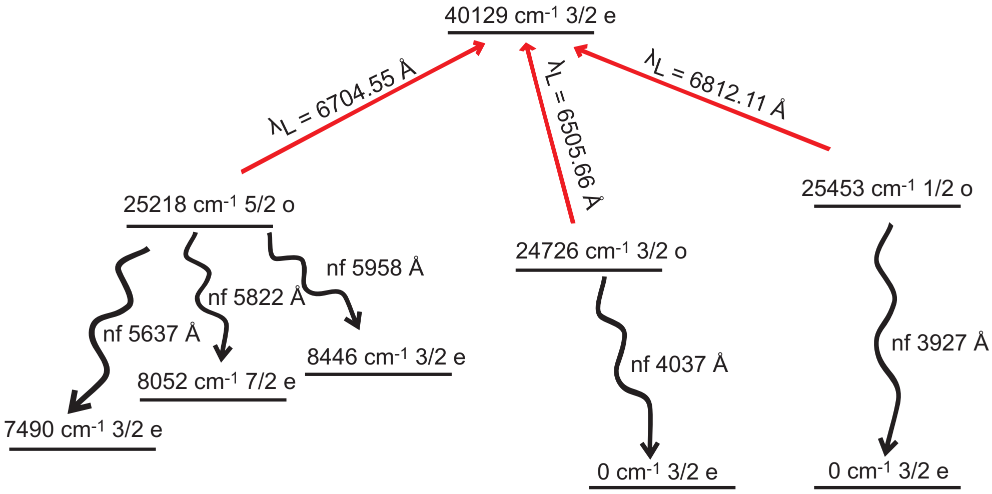

Figure 6.6: Level scheme - The level scheme of all investigated transition when finding the new level with the energy 40129.647 cm^{-1}. All level energies are given without decimal point to make it easy to read; after the energy the J-value and the parity are given. nf means negative fluorescence, meaning the fluorescence derives, as shown, from the lower level involved in the transition.

6.4 The spectral line with the cg wavelength 6575.50 Å

We discuss the excitation of the spectral line with the cg wavelength 6575.50 Å.

In the FT spectrum there is no line visible in this region. Nevertheless we tried to excite a transition between energy levels, because it turned out that our discharge is quite sensitive to OG detection. For this purpose we scanned the laser frequency over some spectral range, starting at 6575.66 Å. In fact, we registered a good resolved spectral line with a cg wavelength 6575.50 Å via OG spectroscopy. In our data base there was no suggestion for any transition between known spectral lines. So there should be involved at least one new energy level in the observed transition. We set the laser frequency in resonance with the highest hf component of the observed signal and looked for laser-induced fluorescence lines, which show a signal of opposite phase compared to the OG signal. We saw one negative fluorescence signal at 4648 Å and one at 5992 Å. Both of those spectral lines have a very high intensity in the FT spectrum and they both had the same upper level. In this way the lower level of the driven transition was identified: it has the energy $E = 24173.830$ cm^{-1}, $J = 3/2$, $A = -228.9$ MHz , $B = 30$ MHz and an odd parity. Now the energy of the new upper level can be calculated by adding the cg wavenumber of the investigated spectral line to the identified lower level. The new upper level has the energy $E' = 39377.715$ cm^{-1} (the prime marks the upper level). By simulating the recorded OG signal we can guess the J-value of the newly introduced level. The pattern of the observed structure indicates a $\Delta J = 0$ transition, therefore we set $J' = 3/2$. We fitted the recorded structure and, as we already know the parameters of the lower level, we fixed those and got the hf constant of the upper level: $A' = 188$ MHz. We set the B-value equal to zero. In figure 6.7 the recorded OG signal (solid line) as well as the fitted structure (dashed line) are shown.

Every newly introduced fine structure level has to be confirmed by at least one second laser excitation. We looked in our database, where all possible decays of the new upper level are calculated, if there is a spectral line in the range of our dye laser operating with DCM. We found a possible excitation line at 6378.67 Å. Also at this wavelength there is no line visible in the FT spectrum. Nevertheless we were able to see an OG signal and by scanning the laser frequency over the line, we could compare the observed pattern with the predicted one; it fits very well. We set the laser frequency in resonance with the most intense hf component and looked for the theoretically predicted

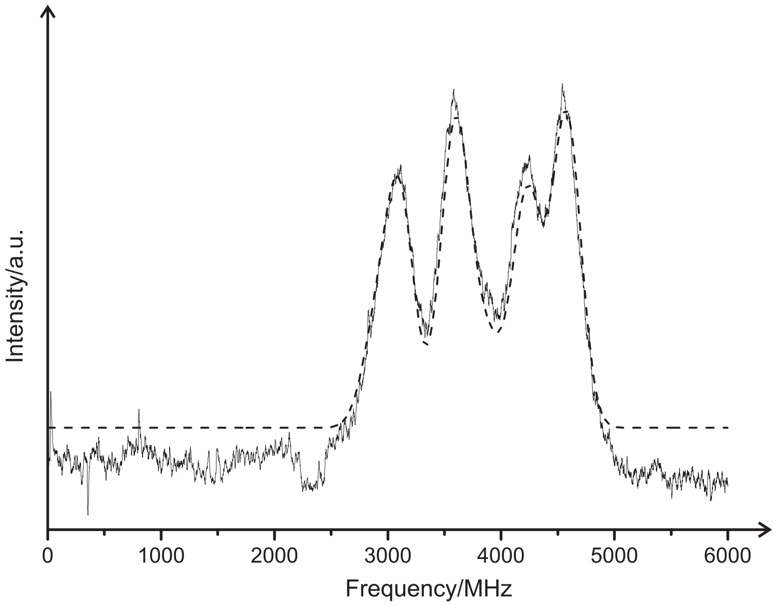

Figure 6.7: Line 6575.2 Å - Recorded OG signal of the line 6575.66 Å assuming a transition $J = 3/2$ to $J' = 3/2$. The hf constants of the lower level were fixed, the B-factor of the upper level was assumed to be zero. The appearance of OG signal (solid line) is compared to fitted line profile (dashed line).

fluorescence channel at 6068 Å, which should be a transition from the lower energy level involved in the transition. In fact, we could also see a negative signal at the theoretical predicted fluorescence channel 6068 Å. This is a proof that the new level really exists. In figure 6.8 the level scheme of all the energy levels, excitation and fluorescence wavelengths involved directly or indirectly in the newly introduced level are illustrated.

When we started the laser scan at a little higher wavelength, it was quite a surprise that, when we made an OG laser frequency scan over that region, we saw three spectral lines close to each other. In figure 6.9 the OG frequency scan is visible. The line with the highest frequency, with the cg wavelength 6378.67 Å is the before seen transition from our newly introduced upper level with the energy $E' = 39377.715$ cm^{-1}. There are still two more spectral lines which are also not visible in the FT spectrum. We started to investigated the line in the middle in figure 6.9 with the cg wavelength 6378.69 Å. As before, we set the laser frequency in resonance with the highest hf peak and searched for fluorescence lines by scanning the monochromator manually. We could see two strong

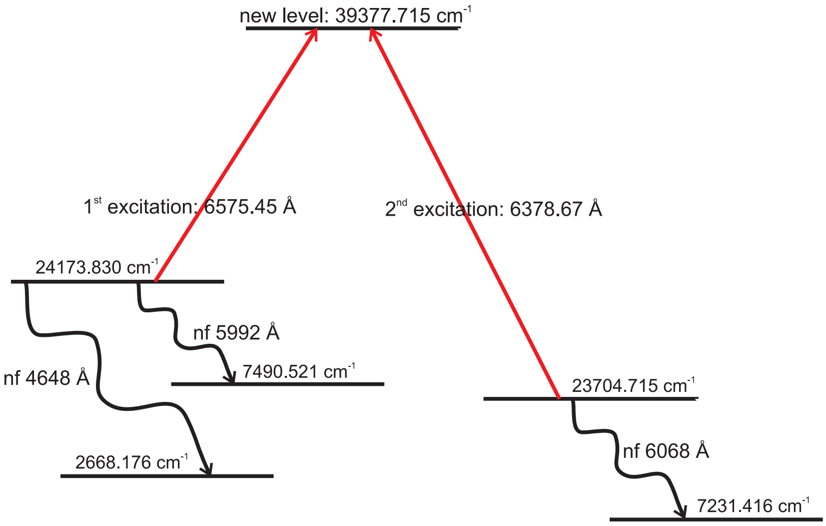

Figure 6.8: LIF scheme - Level scheme which explains the way the new level with the energy 39377.715 cm^{-1} was found and explained. nf means negative fluorescence, the detected fluorescence lines derive from the lower level involved in the transition.

fluorescence signals, positive ones, at 4300 Å and 4192 Å. With the help of those and the appearance of the recorded spectral line, we were able to classify the line as a transition between the two known energy levels $E' = 32390.152$ cm^{-1} and $E = 16617.284$ cm^{-1}.

The first line in figure 6.9 with the cg wavelength 6378.90 Å could not be identified as a transition between two known energy levels. When setting the laser frequency in resonance with it and scanning the monochromator manually, we observed the fluorescence lines 5304 Å , 5358 Å , 5465 Å and 5825 Å with negative phase at the lock-in amplifier. In our database there was no suggestion for a transition between known energy levels. A new level should be involved in the observed transition. Again, we checked in the FT spectrum if there where spectral lines visible in the region of the observed fluorescence wavelengths. All the observed wavelengths where visible and they had the same upper level. The lower level of the transition of interest is found: $E = 26338.932$ cm^{-1}, $J = 5/2$, $A = 103.2(2.2)$ MHz and odd parity. By adding the cg wavelength of the investigated line to the the energy of the identified lower level, the energy of the new upper level is calculated: $E' = 42011.285$ cm^{-1}. As the pattern shows a weak hf splitting, it is assumed that it is eighter a $\Delta J = 0$ or $\Delta J = -1$ transition. Therefore the newly introduced level could have a J-value $J = 5/2$ or $J = 7/2$. A way to find out which one is the right J-value is to fit the structure. As the hf pattern of

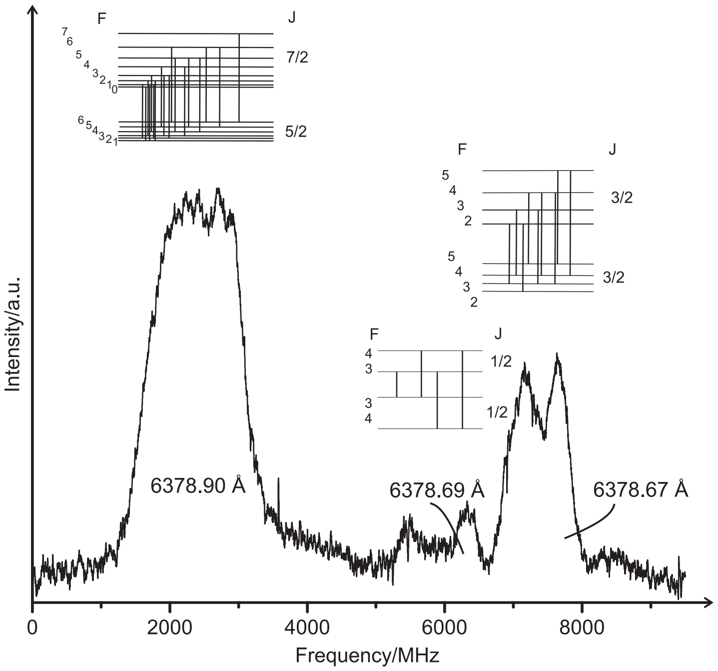

Figure 6.9: Region 6378.67 Å - Recorded OG signal over the region around 6378.67 Å. three spectral lines are visible.

this recorded line is not very well resolved, it is not very constructive in this case. It is possible to fit the structure with both considered J-values. Therefore we tried to excite the newly introduced level from at least one other lower level in order to find out the right J-value. As the level was already excited from a lower level with a J-value of 5/2 and we assume that the new level has $J = 7/2$, we were looking for a possible excitation from a lower level with $J = 9/2$. So we tried to excite the new upper level form the lower level $E = 25977.181$ cm^{-1}, $J = 9/2$, $A = 414,3(2)$ MHz and odd parity. As the inverse of the difference of the two energy levels can be given in Å we set the laser frequency in resonance with this difference, whose inverse is 6242.75 Å and we were able to observe an OG signal and to record the structure, which had the expected pattern. Furthermore we observed the following fluorescence line: 4579 Å. This is an undoubtful proof that the newly introduced energy level exists, moreover, now we know that it has a J-value of 7/2. Also the line with the cg wavelength 6719.08 Å has the newly introduced energy level as the upper level. Its lower level is: $E = 27132.434$ cm^{-1}, $J = 7/2$ MHz, $A = 67.11$ MHz and odd parity. The A-value of the newly introduced upper level, $E' = 42011.285$ cm^{-1} and $J = 7/2$, turned out to be 222(16) MHz.

6.5 Improving the hf structure constants of the known level with the energy 18156.960 cm^{-1}

The level with the energy 18156.960 cm^{-1} is a very well known energy level from [58] with the hf structure constants $A = 633(1)$ MHz and $B = 18(10)$ MHz, nevertheless the uncertainty of the hf structure constants is rather high. The energy level is involved in a lot of transitions, most of them present as strong lines in the FT spectrum with a high intensity. One of them is the spectral line with the cg wavelength 6454.501 Å. In this transition the investigated level is the upper one, the lower level energy of the transition is 2668.176 cm^{-1}. The hf structure constants of this lower level are very well known from atomic beam experiments by [29]: $A = -480.312$ MHz and $B = 15.082$ MHz. Not so the hf structure constants from the upper level, though; the uncertainty is rather high for such a strong line and a good resolved hf pattern.

As described in chapter 4.7 the Doppler reduced method of saturation spectroscopy is a very good tool to investigate strong spectral lines. We used this technique on the spectral line with the cg wavelength 6454.501 Å. Saturation spectroscopy can be used together with both, OG spectroscopy as well as LIF spectroscopy. It was possible to observe a very high intensive positive fluorescence line at 5506 Å. Therefore we recorded the spectral line with saturated LIf spectroscopy at this fluorescence channel several times. One component of the recorded pattern has a FWHM of approximately 350 MHz, all the small components are very well resolved. We fitted the structure with fixed hf structure constants of the lower level and let both values of the hf structure constants of the upper energy level as free fit parameters. The fitting function was a sum function of a Gaußian and Lorentzian profile, where the lower part of a single component has a Gaußian profile and the upper part a Lorentzian profile. The recorded pattern and the fitted structure is shown in figure 6.10. The black line represents the recorded signal while the red line is the fitted one.

As expected, when fitting the recorded pattern, it was possible to improve the A-value as well as the B-value of the upper energy level 18156.960 cm^{-1}. The new A-value is 632.26(3) MHz, the error is just in the second position after the decimal point anymore. The accuracy of the improved B-value, of now 54.2(9) MHz, is also better than before.

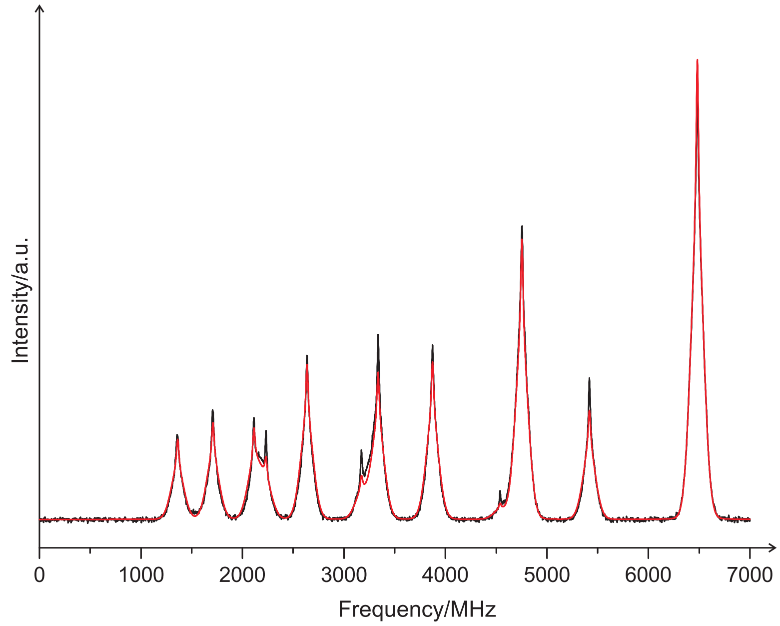

Figure 6.10: Line 6454.501 Å - The recorded pattern of the spectral line with the cg wavelength 6454.501 Å (black) and the fitted one (red). It is recorded via LIF spectroscopy. The fluorescence channel is 5506 Å.

6.6 The blended spectral line with the cg wavelength of 6866.5 Å

In the FT spectrum, there is observable quite a strong line with a cg wavelength of 6866.5 Å. This spectral line and the corresponding energy levels are well known. It is a transition between $E' = 29578.815$ cm^{-1} , $J' = 5/2$, $A' = -42.5$ MHz, even parity and $E = 15019.496$ cm^{-1} , $J = 7/2$, $A = 673$ MHz, odd parity. But when having a closer look at the hf pattern, it should catch someone's eyes, that it shows no regular flag pattern. The intensities of the single components are not regularly distributed. In figure 6.11 the discussed line is represented, the part where there is another line beneath is marked with an arrow.

We set the laser frequency in resonance with said part and looked for fluorescence lines. We were able to identify two fluorescence wavelengths with a negative signal at the lock-in amplifier, one at 4177 Å and one at 4549 Å. Both of those lines appear as lines with a high intensity in the FT spectrum and those lines have the same upper energy level: $E = 24984.294$ cm^{-1} , $J = 5/2$, $A = 284.5$ MHz, odd parity. Assuming that

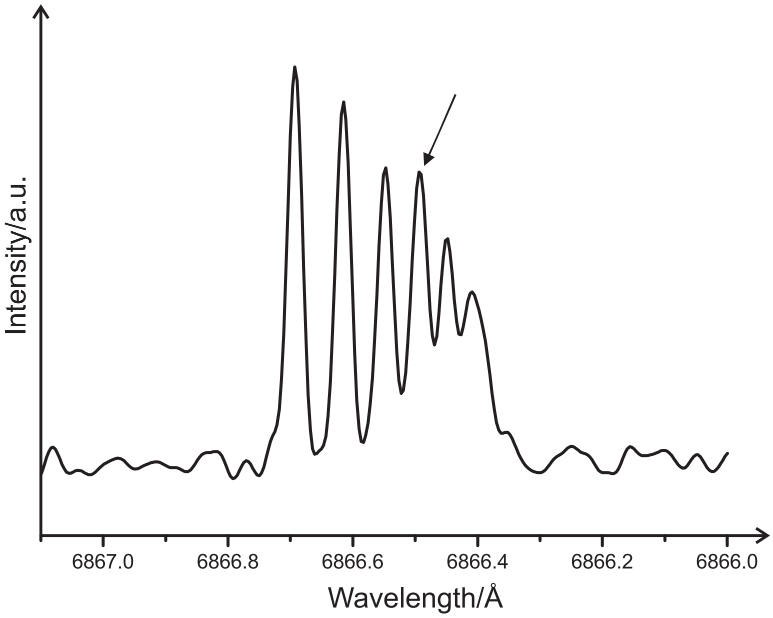

Figure 6.11: Blended line 6866 Å - The blended spectral line at 6866.5 Å as it appears in the FT spectrum.

said level is the lower level of the transition of interest, we added the cg wavenumber of the investigated line and calculated a possible energy of the new upper level: $E' = 39543.751$ cm^{-1}. By simulating the pattern of the recorded line, we assumed that the J-value of the newly introduced level might be 3/2 and when fitting the structure we got $A' = 168.6$ MHz as a result from the fit program.

To confirm the existence of the new energy level a second and a third laser excitation from two other lower level was performed. As a first confirmation the spectral line with a cg wavelength 6831.81 Å was investigated. The recorded pattern clearly matched the expected one. Also the spectral line at 6707.54 Å has the newly introduced level as an upper one; once more redoubtable confirmed by the appearance of its hf pattern.

6.7 The blended spectral region at 5792.99 Å

When recording the spectral region around 5792.99 Å optogalvanically, a blended situation could be observed. Figure 6.12 shows the recorded structure. The recorded pattern cannot be interpreted; the spectral lines cannot be assigned to transition between energy levels. The only way to distinguish overlapping spectral lines is by their fluorescence lines. Therefore LIF spectroscopy was performed. First the laser frequency was set in resonance with the first component (lowest frequency- highest wavelength) and we looked for fluorescence channels. Two strong negative fluorescence signal could be observed at 5506 Å and at 6454 Å. When recording the structure via LIF spectroscopy at the fluorescence channel 5506 Å a wide structure could be observed (compare figure 6.12). By fitting the structure and in combination with the observed fluorescence channels, the spectral line could clearly be assigned to a transition between two known energy levels: $E = 18156.960\mathrm{cm}^{-1}$, $E' = 35414.441\mathrm{cm}^{-1}$. The cg wavelength of this spectral line is 5798.98 Å.

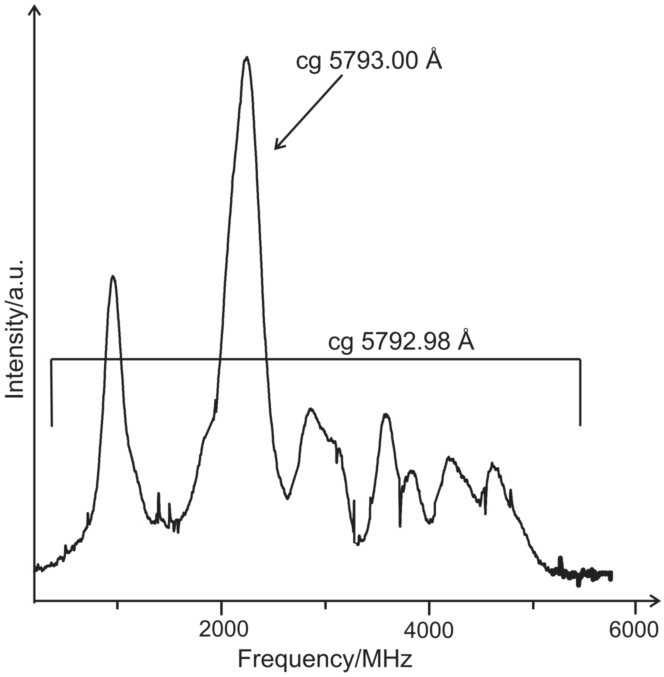

Figure 6.12: Blended region 5792.99 Å - The blended region at 5792.99 Å involving two spectral lines with almost the same cg wavelength.

As a second step, the second component of the structure in figure 6.12 was excited by laser light. This component is clearly enlarged in the OG recorded pattern. We could observe a negative fluorescence channel at 5211 Å and when recording the structure at this channel by LIF spectroscopy, a single peak could be observed. This structure could not be assigned to a transition between two known energy levels, a new level was involved. With the help of the fluorescence line, the lower level involved in the transition could be identified: $E = 23303.275\mathrm{cm}^{-1}$, $J = 7/2$ and odd parity. By adding the cg wavenumber to the lower energy we calculated the energy of the upper level: $E' = 40560.65\text{cm}^{-1}$ and by fitting the structure the J-value ($J' = 5/2$) and the A-value ($A' = -60$) could be identified. The cg wavelength of this spectral line is 5793.00 Å.

It should be emphasized that overlapping spectral lines can only be divided by LIF spectroscopy.

6.8 The uncertainty of the wavelengths of spectral lines and of the level energies

The spectral lines which are visible in the FT spectrum have an uncertainty of ± 0.001 Å. The wavelengths of all the lines visible in the FT spectrum where estimated with also seen Ar lines in the spectrum, whose wavelengths are known with high accuracy. As described with the help of an example in 6.2 also the uncertainty of spectral lines which are nearby spectral lines visible in the FT spectrum is ± 0.001 Å, because their wavelengths can be estimated by performing a two or more line fit.

If a spectral line is investigated, which is not visible in the FT spectrum, than we just know the wavelength which is given by the λ-meter. As the uncertainty of the λ-meter is ± 0.01 Å, also the uncertainty of those spectral lines is ± 0.01 Å. Most of the spectral lines investigated in this work are not visible in the FT spectrum, therefore their wavelengths are only given with two decimal places.

As a spectral line is can be interpreted as the difference of two energy levels, the accuracy of the level energies depend on the accuracy of the wavelength or wavenumber, respectively, of the spectral lines. Furthermore, an energy of a newly introduced energy level depends also on the accuracy of the other level energy involved in the transition. When a spectral line is known with an uncertainty of ± 0.01 Å the uncertainty of a level energy is ± 0.05 cm^{-1}. If the uncertainty of a spectral line is ±0.001 Å and the other level energy of the involved level is known with an uncertainty of ± 0.001 cm^{-1}, the uncertainty of a newly introduced level energy is ± 0.005 cm^{-1}.

it should be pointed out that in all given and discussed uncertainties no systematic error was taken into account.

7

Discussion

We showed that laser spectroscopy of atoms is a fruitful technique to find out a lot of new things about several atoms. Furthermore it could be shown that there are a lot of basic physics we do not know about atoms with many electrons. Even though it is really basic physics, it is very important to know also those things. Without the basics people will never learn everything which seem to be more interesting.

We investigated the two rare earth elements Pr and La. In Pr a few hundred of spectral lines were investigated by laser spectroscopy, over 1000 spectral lines were investigated by analyzing the FT spectrum and 35 new energy levels with odd parity and 12 energy levels with even parity could be discovered. In La over 1000 spectral lines were investigated by laser spectroscopic techniques, most of them are lying between 6100 Å and 6950 Å. Altogether 66 new La energy levels were discovered, all of them with even parity. Despite this enormous new data, there still are spectral lines which have to be investigated and for sure also the energy level list of both elements is far from being complete.

As Pr and La are both part of the emission solar spectrum, the new data can be used to identify so far unknown spectral lines.

Furthermore the line lists as well as the level lists of Pr and La could be enlarged a lot and it is therefore very useful for further studies of those two elements. A group in Poznan, Poland, does ab initio calculation of Pr and La. For them our new knowledge is very interesting and useful, as some of their predicted levels could be confirmed by our measurements.

Although the experimental techniques of my work are quite well known each, I showed that it is still possible to combine those techniques and to find out a lot of previously unknown information of several chemical elements. I am sure that those information can be used by several people in future.

In the Appendix A and the Appendix B the entire work done on Pr and on La is listed.

Appendix A

Praseodymium

A.1 Spectral lines of Pr classified by analyzing the FT spectrum

In table A.1 all new spectral lines of praseodymium which clearly could be assigned to a transition between two energy levels, are given. Column 1 contains the cg wavelength in air in Å. Information about the SNR is given in column 2 (per definition, noise is treated to have SNR = 1). If there is written "nl" in front of the SNR it means that this line is a new one, not known before these investigations. All the other lines are mentioned in the list of Ginibre [55] but they are not classified, either because the energy levels involved in the transition were found after she did her work, or because the hf patterns were not sufficiently resolved in her spectra. In columns 3 and 5 the J-values of the involved levels are listed. The corresponding energies in cm^{-1} are given in columns 4 and 6. The energy levels are listed according to their parities, in the column 4 the even ones and in the column 6 the odd ones. If a new level is involved, it is marked with an upper index 'a'. The table was published in [21]. The uncertainty of the level energies is $\pm\, 0.005\ \mathrm{cm}^{-1}$ and the uncertainty for the spectral lines is $\pm\, 0.001$ Å (no systematic error is taken into account).

Table A.1: Spectral lines of Pr which clearly could be assigned to a transition between two energy levels

		Even		Odd	
λ/Å	SNR	J-value	Level Energy/cm^{-1}	J-value	Level Energy/cm^{-1}
4181.612	nl 11	9/2	4432.240	7/2	28339.724
4962.213	23	5/2	29133.138	3/2	8986.444
5352.117	nl 9	9/2	8643.839	7/2	27322.843
5355.191	nl 4	11/2	6714.199	13/2	25382.476
5357.859	nl 17	15/2	11483.442	13/2	30142.420
5366.731	33	15/2	10466.704	15/2	29094.773
5378.800	nl 9	15/2	8363.916	15/2	26950.256
5379.328	nl 6	13/2	10266.516	13/2	28851.022
5381.780	nl 29	11/2	6714.199	9/2	25290.248
5382.696	nl 31	13/2	10470.344	15/2	29043.236
5386.394	nl 19	11/2	9483.533	9/2	28043.749
5389.731	36	9/2	27384.059	11/2	8835.380
5390.511	32	9/2	11713.220	9/2	30259.211
5391.580	58	15/2	9745.391	15/2	28287.674
5394.051	91	9/2	8643.839	9/2	27177.628
5397.91	19	9/2	11549.619	11/2	30070.158
5405.006	46	7/2	6535.587	5/2	25031.771
5415.132	30	11/2	27195.110	13/2	8733.450
5415.839	nl 9	19/2	13626.687	19/2	32085.996
5416.123	nl 4	11/2	10841.417	13/2	29299.668
5423.186	30	15/2	8765.556	17/2	27199.779
5423.544	nl 10	15/2	10466.704	15/2	28899.719
5424.089	64	11/2	9268.741	11/2	27699.892
5425.204	nl 18	13/2	10423.669	13/2	28851.022
5433.716	nl 17	9/2	8320.255	9/2	26718.753
5435.134	55	5/2	9710.615	7/2	28104.309
5437.904	nl 6	15/2	10466.704	13/2	28851.022
5445.407	89	19/2	11151.448	19/2	29510.445
5446.326	35	13/2	10266.516	15/2	28622.414
5451.876	nl 23	15/2	11483.442	15/2	29820.657
5453.232	118	11/2	27066.095	13/2	8733.450
5453.533	22	9/2	9105.035	11/2	27436.682
5453.786	19	13/2	10423.669	15/2	28754.461
5456.397	69	9/2	8029.290	9/2	26351.314
5456.876	56	17/2	12736.636	19/2	31057.048
5458.007	41	5/2	9710.615	7/2	28027.233
5462.883	61	9/2	18300.341	9/2	0.000
5467.058	nl 7	11/2	4866.530	9/2	23152.820

[a] Previously unknown energy level

Table A.1 – Continued

		Even		Odd	
λ/Å	SNR	J-value	Level Energy/cm^{-1}	J-value	Level Energy/cm^{-1}
5467.974	nl 17	13/2	9464.455	15/2	27747.685
5469.027	nl 5	15/2	8765.556	15/2	27045.255
5471.965	79	15/2	8765.556	15/2	27035.451
5472.499	22	9/2	8320.255	11/2	26588.368
5498.743	nl 10	9/2	8643.839	11/2	26824.764
5506.379	nl 37	15/2	10466.704	15/2	28622.414
5513.962	nl 13	7/2	8013.104	7/2	26143.830
5514.855	nl 14	11/2	13872.290	9/2	32000.017
5517.615	nl 8	11/2	10841.417	13/2	28960.156
5529.822	37	9/2	30356.670	7/2	12277.947
5530.631	53	15/2	8765.556	15/2	26841.658
5532.249	nl 44	7/2	8013.104	7/2	26083.919
5534.181	55	7/2	8013.104	7/2	26077.608
5536.757	nl 10	11/2	10904.049	13/2	28960.156
5538.374	nl 240	11/2	26784.270	13/2	8733.450
5539.463	18	9/2	11549.619	11/2	29596.942
5542.481	nl 18	13/2	10266.516	13/2	28303.969
5553.752	nl 30	9/2	8320.255	7/2	26321.099
5556.142	nl 10	7/2	8013.104	9/2	26006.208
5561.672	nl 15	11/2	6714.199	9/2	24689.414
5568.074	nl 8	11/2	6714.199	13/2	24668.738
5575.709	nl 28	15/2	9745.391	15/2	27675.355
5576.243	nl 27	11/2	8829.078	11/2	26757.324
5580.634	46	17/2	14302.923	19/2	32217.025
5597.433	nl 10	5/2	9710.615	7/2	27570.943
5599.069	nl 14	11/2	6714.199	9/2	24569.356
5608.318	nl 14	7/2	28479.761	7/2	10654.110
5609.809	nl 7	15/2	10466.704	15/2	28287.674
5610.062	nl 38	11/2	6714.199	11/2	24534.366
5616.325	27	15/2	12804.483	17/2	30604.778
5617.018	nl 21	15/2	11483.442	17/2	29281.540
5617.656	54	17/2	11714.367	19/2	29510.445
5619.557	nl 16	7/2	11472.423	9/2	29262.534
5621.481	nl 15	15/2	10466.704	13/2	28250.672
5624.964	213	7/2	6535.587	9/2	24308.545
5627.906	nl 9	9/2	8320.255	7/2	26083.919
5628.833	nl 37	13/2	27444.925	13/2	9684.190
5630.257	nl 18	13/2	6603.606	11/2	24359.861
5631.009	nl 44	9/2	5822.905	9/2	23576.782
5637.642	nl 20	9/2	8320.255	11/2	26053.248

[a] Previously unknown energy level

Table A.1 – Continued

		Even		Odd	
λ/Å	SNR	J-value	Level Energy/cm^{-1}	J-value	Level Energy/cm^{-1}
5641.382	nl 23	7/2	29830.034	5/2	12108.819
5642.105	nl 23	13/2	7951.338	15/2	25670.302
5645.438	nl 10	15/2	10466.704	13/2	28175.209
5645.683	64	15/2	22088.820	15/2	4381.100
5648.399	nl 25	15/2	11483.442	15/2	29182.662
5648.941	nl 13	5/2	29806.252	5/2	12108.819
5649.278	56	11/2	9268.741	13/2	26965.207
5655.410	nl 20	11/2	11282.880	13/2	28960.156
5656.529	nl 11	15/2	28342.772	15/2	10668.960
5657.532	39	11/2	10904.049	13/2	28574.696
5659.018	29	9/2	8320.255	7/2	25986.288
5667.381	nl 12	11/2	9268.741	9/2	26908.682
5679.249	49	9/2	8029.290	11/2	25632.372
5680.337	nl 23	15/2	26333.170	13/2	8733.450
5681.381	nl 12	9/2	10920.378	11/2	28516.848
5685.419	nl 7	13/2	10266.516	13/2	27850.489
5688.309	nl 31	11/2	6313.239	9/2	23888.281
5691.836	nl 15	17/2	11714.367	15/2	29278.521
5697.225	nl 18	15/2	14780.939	17/2	32328.494
5697.712	nl 18	11/2	6313.239	11/2	23859.275
5703.627	37	9/2	8320.255	7/2	25848.090
5707.982	nl 18	13/2	10266.516	11/2	27780.979
5708.759	17	15/2	16650.620	13/2	34163.027
5709.143	nl 4	11/2	27195.110	13/2	9684.190
5712.192	22	13/2	12041.668	13/2	29543.224
5713.331	nl 9	13/2	13146.599	13/2	30644.667
5717.206	nl 12	7/2	11869.331	9/2	29355.515
5722.612	nl 17	11/2	27153.870	13/2	9684.190
5723.522	nl 25	11/2	6892.949	11/2	24359.861
5726.533	nl 11	7/2	11274.244	5/2	28731.850
5730.189	nl 5	9/2	10356.752	7/2	27803.341
5731.531	nl 5	11/2	11282.880	13/2	28725.383
5735.781	46	7/2	8013.104	9/2	25442.695
5740.167	nl 26	15/2	11483.442	15/2	28899.719
5745.760	30	9/2	8029.290	11/2	25428.607
5748.007	75	13/2	6603.606	15/2	23996.130
5752.234	nl 22	11/2	4866.530	11/2	22246.255
5753.327	61	11/2	9268.741	13/2	26645.170
5756.391	nl 81	11/2	8829.078	13/2	26196.253
5765.103	nl 10	11/2	12658.416	13/2	29999.348

[a] Previously unknown energy level

Table A.1 – Continued

		Even		Odd	
λ/Å	SNR	J-value	Level Energy/cm^{-1}	J-value	Level Energy/cm^{-1}
5766.634	15	9/2	8643.839	11/2	25980.167
5769.348	nl 13	7/2	28731.220	7/2	11403.067
5775.170	nl 7	15/2	15994.810	17/2	33305.651
5779.535	nl 13	9/2	10356.752	7/2	27654.383
5784.299	28	17/2	30848.875	15/2	13565.520
5787.119	nl 23	17/2	9770.288	15/2	27045.255
5788.603	nl 8	7/2	30189.694	7/2	12919.185
5790.406	nl 16	17/2	9770.288	15/2	27035.451
5796.352	nl 6	9/2	10356.752	9/2	27604.203
5817.908	nl 16	15/2	13439.023	15/2	30622.592
5818.866	nl 13	13/2	9464.455	13/2	26645.170
5820.126	nl 9	9/2	12519.718	11/2	29696.709
5825.121	nl 14	7/2	10194.780	7/2	27357.054
5827.462	nl 30	11/2	6892.949	11/2	24048.320
5837.561	nl 10	9/2	11549.619	9/2	28675.308
5843.479	53	9/2	8320.255	11/2	25428.607
5846.782	nl 10	13/2	10423.669	11/2	27522.363
5855.199	nl 12	7/2	15634.176	5/2	32708.095
5855.368	nl 19	11/2	19920.355	13/2	2846.744
5864.496	nl 8	13/2	12041.668	13/2	29088.699
5866.071	nl 24	7/2	17042.405	9/2	0.000
5875.487	28	11/2	10904.049	11/2	27919.207
5879.378	nl 8	7/2	9918.205	5/2	26922.093
5884.989	8	13/2	12041.668	11/2	29029.547
5893.492	234	11/2	6714.199	13/2	23677.365
5896.218	17	9/2	25205.463	9/2	8250.170
5897.409	nl 11	7/2	7617.455	9/2	24569.356
5904.524	nl 6	17/2	12736.636	17/2	29668.103
5906.519	14	13/2	9464.455	13/2	26390.208
5907.249	112	9/2	18300.341	11/2	1376.605
5924.633	25	13/2	10423.669	13/2	27297.680
5934.451	17	13/2	15772.560	13/2	32618.845
5936.246	nl 58	9/2	8029.290	11/2	24870.318
5938.827	24	11/2	6313.239	13/2	23146.917
5938.228	nl 11	11/2	16835.400	9/2	0.000
5940.178	34	13/2	29051.942	13/2	12222.100
5940.449	nl 22	13/2	28643.769	15/2	11814.660
5949.765	nl 171	17/2	27523.120	17/2	10720.400
5954.881	36	13/2	10423.669	15/2	27211.960
5957.238	11	13/2	12118.054	15/2	28899.719

[a] Previously unknown energy level

Table A.1 – Continued

		Even		Odd	
λ/Å	SNR	J-value	Level Energy/cm^{-1}	J-value	Level Energy/cm^{-1}
5970.186	17	15/2	10466.704	15/2	27211.960
5971.086	nl 18	7/2	11869.331	9/2	28612.095
5975.644	16	9/2	27384.059	7/2	10654.110
5977.377	nl 8	11/2	10904.049	13/2	27629.152
5985.748	nl 31	7/2	28104.689	7/2	11403.067
5987.819	nl 94	9/2	8320.255	11/2	25016.201
5993.095	16	7/2	28731.220	9/2	12049.950
5994.418	nl 82	9/2	18054.202	11/2	1376.605
6014.607	10	13/2	10423.669	15/2	27045.255
6023.642	68	15/2	27265.622	15/2	10668.960
6030.234	54	15/2	28342.772	17/2	11764.250
6035.413	21	11/2	6313.239	9/2	22877.542[a]
6061.992	70	9/2	27145.754	7/2	10654.110
6068.436	nl 8	13/2	11562.777	13/2	28036.928
6072.077	39	15/2	27133.216	15/2	10668.960
6074.285	18	17/2	10531.966	17/2	26990.251
6074.993	134	9/2	24706.499	9/2	8250.170
6076.144	nl 12	7/2	28731.220	7/2	12277.947
6083.735	78	11/2	6714.199	13/2	23146.917
6085.810	142	9/2	24677.280	9/2	8250.170
6094.119	31	13/2	25138.184	13/2	8733.450
6105.825	18	5/2	9710.615	7/2	26083.919
6107.014	90	9/2	25205.463	11/2	8835.380
6124.960	46	9/2	16322.152	9/2	0.000
6136.690	24	11/2	9675.044	13/2	25965.963
6138.092	9	15/2	30283.139	13/2	13996.091
6149.670	20	7/2	7617.455	5/2	23874.021
6161.073	34	9/2	8643.839	11/2	24870.318
6179.837	28	13/2	10470.344	15/2	26647.525
6222.780	9	13/2	10266.516	15/2	26332.055
6223.887	nl 6	9/2	28883.770	9/2	12821.083
6232.579	14	13/2	7630.147	11/2	23670.431
6239.883	nl 8	11/2	9268.741	9/2	25290.248
6242.330	nl 9	9/2	10356.752	7/2	26371.986
6246.546	nl 9	11/2	28054.356	9/2	12049.950
6251.682	10	11/2	30217.484	11/2	14226.248
6270.364	46	15/2	27689.962	13/2	11746.340
6280.999	54	11/2	27662.982	13/2	11746.340
6297.347	23	15/2	27689.962	15/2	11814.660
6298.408	nl 12	11/2	27195.110	11/2	11322.420

[a] Previously unknown energy level

Table A.1 – Continued

		Even		Odd	
λ/Å	SNR	J-value	Level Energy/cm^{-1}	J-value	Level Energy/cm^{-1}
6311.952	4	13/2	6603.606	15/2	22442.185^a
6312.170	nl 4	11/2	13250.690	13/2	29088.699
6337.797	17	7/2	26428.100	7/2	10654.110
6372.371	nl 16	5/2	9710.615	7/2	25399.020
6384.451	14	9/2	27936.663	7/2	12277.947
6389.825	10	11/2	12658.416	13/2	28303.969
6391.011	17	13/2	6603.606	11/2	22246.255
6416.572	15	15/2	27394.976	15/2	11814.660
6417.480	nl 15	11/2	11944.223	11/2	27522.363
6425.462	46	13/2	6603.606	15/2	22162.410
6438.160	nl 7	13/2	13659/247	15/2	29182.662
6440.364	53	13/2	13146.599	11/2	28669.174
6441.818	56	15/2	27265.622	13/2	11746.340
6442.859	14	13/2	7630.147	13/2	23146.917
6469.039	nl 10	13/2	25138.184	13/2	9684.190
6472.773	34	7/2	26586.550	5/2	11141.581
6479.760	nl 6	11/2	28764.269	13/2	13335.895
6485.370	nl 18	9/2	27145.754	9/2	11730.600
6486.560	650	17/2	25059.089	15/2	9646.850
6516.343	nl 9	9/2	19871.160	9/2	35213.021
6539.925	22	7/2	26428.100	5/2	11141.581
6559.597	10	13/2	27444.925	11/2	12204.304
6576.070	9	11/2	26524.890	11/2	11322.420
6577.508	nl 11	11/2	11282.880	9/2	26482.007
6581.885	7	5/2	9710.615	7/2	24899.636
6583.537	nl 6	11/2	9483.533	13/2	24668.738
6616.025	196	7/2	15110.661	9/2	0.000
6617.063	nl 4	17/2	12736.636	17/2	27844.904
6617.336	51	15/2	24759/250	15/2	9646.850
6630.181	15	9/2	9105.035	11/2	24183.415^a
6632.770	nl 4	15/2	29412.685	17/2	14340.210
6636.333	nl 5	13/2	9464.455	15/2	24528.854
6725.360	85	5/2	6451.823	7/2	21316.810
6765.297	12	15/2	28342.772	15/2	13565.520
6782.978	nl 21	3/2	9650.060	5/2	24388.702^a
6788.184	21	13/2	25138.184	13/2	10410.760
6797.865	34	13/2	25138.184	11/2	10431.720
6799.100	37	11/2	25135.518	11/2	10431.720
6833.879	nl 9	9/2	26032.009	7/2	11403.067
6847.480	27	13/2	10423.669	15/2	25023.550

[a] Previously unknown energy level

Table A.1 – Continued

		Even		Odd	
λ/Å	SNR	J-value	Level Energy/cm^{-1}	J-value	Level Energy/cm^{-1}
6855.001	nl 7	13/2	9464.455	11/2	24048.320
6893.023	36	7/2	27883.218	9/2	13379.780
6904.230	8	15/2	12250.534	13/2	26730.415
6930.502	nl 8	5/2	8737.448	7/2	23162.497
6941.753	45	13/2	17248.381	13/2	2846.744
6942.556	11	13/2	10470.344	11/2	24870.228
6944.485	nl 10	13/2	15772.560	11/2	1376.605
6954.744	nl 14	5/2	6451.823	5/2	20826.530^a
6995.508	52	7/2	6535.587	5/2	20826.530^a
6998.848	15	15/2	27620.060	13/2	13335.895
7004.906	nl 17	15/2	17118.558	13/2	2846.744
7008.332	6	11/2	22998.253	13/2	8733.450
7008.775	44	5/2	6451.823	3/2	20715.719
7026.094	nl 10	11/2	6714.199	11/2	20942.933^a
7037.560	nl 16	7/2	8013.104	9/2	22218.655
7038.110	6	9/2	9105.035	11/2	23309.476
7041.108	nl 4	13/2	10470.344	13/2	24668.738
7076.126	nl 4	11/2	9483.533	11/2	23611.664
7091.629	nl 7	5/2	8737.448	7/2	22834.790
7094.691	22	5/2	6451.823	7/2	20542.983
7101.187	nl 12	15/2	8363.910	15/2	22442.185^a
7117.560	24	11/2	16935.880	9/2	30981.669
7128.169	nl 24	13/2	7630.147	15/2	21655.124
7134.864	nl 8	13/2	7630.170	13/2	21641.950
7150.649	16	9/2	8320.255	7/2	22301.160^a
7163.745	15	17/2	12736.670	17/2	26692.000^a
7216.421	nl 4	13/2	27213.988	11/2	13360.529
7245.184	21	15/2	8363.916	15/2	22162.410
7255.175	380	13/2	15156.070	11/2	1376.605
7265.574	nl 5	13/2	10423.680	11/2	24183.415^a
7265.838	7	17/2	18380.340	17/2	32139.568
7281.341	nl 5	9/2	13974.730	7/2	27704.707
7302.256	nl 5	13/2	7951.350	13/2	21641.950
7309.733	nl 5	15/2	8765.570	15/2	22442.185^a
7319.268	23	7/2	14045.708	7/2	27704.707
7320.626	nl 7	7/2	7617.455	9/2	21273.728
7335.136	nl 2	13/2	24951.730	11/2	11322.420
7337.282	nl 4	11/2	6714.220	13/2	20339.470
7337.714	12	13/2	13897.891	11/2	27522.363
7346.172	nl 5	11/2	9268.741	9/2	22877.524^a

[a] Previously unknown energy level

Table A.1 – Continued

		Even		Odd	
λ/Å	SNR	J-value	Level Energy/cm^{-1}	J-value	Level Energy/cm^{-1}
7352.265	nl 5	15/2	11483.442	13/2	25080.951
7354.833	nl 3	13/2	10266.516	11/2	23859.275
7364.208	15	13/2	16422.207	13/2	2846.744
7379.937	nl 5	11/2	551.949	13/2	20439.490
7390.274	nl 2	15/2	12804.483	15/2	26332.055
7393.802	nl 6	9/2	14897.770	11/2	1376.620
7404.778	nl 2	11/2	23185.233	13/2	9684.190
7428.425	nl 3	11/2	13250.690	13/2	26708.776
7436.633	nl 12	13/2	7951.338	11/2	21399/281
7440.860	nl 4	13/2	10423.680	11/2	23859.280
7462.398	nl 4	15/2	8765.570	15/2	22162.410
7463.978	nl 9	11/2	9483.533	9/2	22877.524[a]
7479.184	nl 3	9/2	10356.752	7/2	23723.515
7498.888	nl 7	9/2	12746.082	7/2	26077.608
7509.508	nl 8	13/2	7630.147	11/2	20942.933[a]
7511.542	nl 15	17/2	11714.367	15/2	25023.550
7523.291	10	9/2	10920.378	9/2	24208.775
7536.197	nl 6	11/2	9483.540	11/2	22749.175[a]
7555.046	nl 8	13/2	24554.990	11/2	11322.420
7569.105	nl 6	13/2	16250.9	11/2	29458.91
7573.242	nl 3	5/2	8737.448	5/2	21938.328
7602.328	nl 2	9/2	8320.255	11/2	21470.498
7606.547	nl 1	15/2	11483.442	15/2	24626.392
7609.254	nl 17	19/2	11151.490	19/2	24289.760[a]
7651.767	36	19/2	13626.720	17/2	266920[a]
7684.518	18	11/2	8829.078	9/2	21838.677
7725.252	nl 12	13/2	10266.510	11/2	23207.530
7790.889	5	13/2	16626.890	11/2	29458.910
7806.808	nl 13	9/2	10356.752	7/2	23162.497
7817.033	nl 3	13/2	13897.891	11/2	26686.944
7842.577	nl 6	13/2	24951.730	11/2	12204.304
7866.150	nl 5	13/2	11462.912	15/2	24172.223
7873.840	nl 5	15/2	9745.391	15/2	22442.185[a]
7884.135	17	15/2	10466.704	13/2	23146.917
7889.311	60	17/2	9770.330	15/2	22442.185[a]
7910.501	nl 5	13/2	13146.599	11/2	25789/252
7929.466	nl 2	11/2	14760.320	9/2	27368.267
7940.172	29	5/2	15113.984	7/2	27704.707
7999.185	nl 3	13/2	10470.344	15/2	22968.185
8027.119	8	7/2	8013.108	5/2	20467.450[a]

[a] Previously unknown energy level

Table A.1 – Continued

		Even		Odd	
λ/Å	SNR	J-value	Level Energy/cm^{-1}	J-value	Level Energy/cm^{-1}
8062.49	6	15/2	16451.350	13/2	28851.022
8069.405	nl 5	17/2	14302.923	17/2	26692.000[a]
8086.784	nl 3	11/2	9268.741	9/2	21631.198
8111.028	20	13/2	10423.680	11/2	22749.175[a]
8139.924	nl 4	17/2	11714.367	15/2	23996.130
8174.676	11	13/2	11462.912	13/2	23692.444
8210.847	12	13/2	10266.510	15/2	22442.185[a]
8218.971	5	11/2	9675.044	9/2	21838.677
8222.482	nl 3	11/2	9483.533	13/2	21641.964
8233.786	10	13/2	12041.670	11/2	24183.415[a]
8301.271	12	7/2	8013.104	5/2	20056.146
8327.581	nl 4	11/2	9268.750	9/2	21273.710
8376.978	nl 35	15/2	14780.939	13/2	2846.744
8393.847	10	17/2	10532.001	15/2	22442.185[a]
8432.191	nl 2	15/2	15819.324	15/2	27675.355
8488.317	nl 3	3/2	14420.003	5/2	26197.8
8526.492	nl 3	9/2	13605.68	9/2	25330.615
8565.573	nl 3	9/2	8643.830	11/2	20315.280
8567.514	20	7/2	11668.787	9/2	0.000
8571.418	12	15/2	11483.442	13/2	23146.917
8592.744	nl 6	13/2	13146.599	13/2	24781.131
8614.061	nl 2	9/2	8643.839	11/2	20249.580
8624.877	nl 2	13/2	24951.730	11/2	13360.529
8644.635	10	15/2	13439.023	13/2	25003.715
8653.316	nl 15	17/2	12736.670	19/2	24289.760[a]
8724.067	nl 9	11/2	9483.540	11/2	20942.933[a]
8847.259	5	11/2	10904.070	11/2	22203.860
8859.101	13	17/2	15665.829	15/2	4381.120
8881.379	18	13/2	11462.858	13/2	22719.340
8918.421	nl 10	11/2	13376.992	11/2	24586.670
8962.403	20	3/2	11361.817	1/2	22516.490[a]
8993.509	67	9/2	19196.472	11/2	8080.440
9016.229	nl 6	3/2	12701.269	3/2	23789.203
9019.598	nl 3	5/2	12078.583	7/2	23162.497
9058.096	28	13/2	13146.600	11/2	24183.415[a]
9074.106	nl 2	11/2	23067.290	9/2	12049.950
9078.497	8	11/2	12658.416	11/2	23670.431
9132.968	25	9/2	19196.472	9/2	8250.170
9141.072	nl 7	17/2	22700.890	17/2	11764.250
9143.853	nl 10	11/2	11944.223	9/2	22877.524[a]

[a] Previously unknown energy level

Table A.1 – Continued

		Even		Odd	
λ/Å	SNR	J-value	Level Energy/cm^{-1}	J-value	Level Energy/cm^{-1}
9144.025	53	5/2	9710.615	3/2	20643.800
9174.839	nl 4	15/2	12250.534	13/2	23146.917
9176.122	27	7/2	13590.350	9/2	24485.187[a]
9183.414	nl 2	17/2	22700.890	15/2	11814.660
9189.156	6	13/2	11562.790	15/2	22442.185[a]
9208.296	nl 3	9/2	8029.29	9/2	18886.085
9216.883	nl 9	19/2	15845.359	17/2	26692.000[a]
9230.499	nl 21	13/2	10470.344	11/2	21301.023
9241.772	7	3/2	9650.06	5/2	20467.450[a]
9283.717	nl 10	7/2	10194.740	7/2	20963.330
9293.861	50	5/2	9710.640	5/2	20467.450[a]
9294.657	25	3/2	13033.479	3/2	23789.203
9307.186	11	13/2	12118.060	11/2	1376.620
9319.006	50	17/2	11714.367	15/2	22442.185[a]
9385.756	30	1/2	11865.001	1/2	22516.490[a]
9426.870	8	3/2	11911.437	1/2	22516.490[a]
9428.620	9	9/2	13605.68	9/2	24208.775
9553.105	nl 10	3/2	12051.530 2	1/2	22516.490[a]
9560.301	nl 24	9/2	10356.710	9/2	20813.780
9567.360	13	11/2	14760.320	11/2	25209.670
9586.286	14	5/2	12647.027	5/2	23075.728
9663.357	26	5/2	9710.640	5/2	20056.197
9684.477	6	15/2	20007.142	13/2	9684.19
9716.396	nl 3	9/2	11549.614	9/2	21838.683
9716.816	23	9/2	5822.905	7/2	16111.549
9751.899	45	1/2	12264.888	1/2	22516.490[a]
9768.643	12	9/2	13974.73	9/2	24208.775
9792.495	19	5/2	11107.705	7/2	21316.810
9864.788	18	5/2	10828.988	7/2	20963.372
9878.011	nl 3	13/2	12041.668	15/2	22162.41

[a] Previously unknown energy level

A.2 Spectral lines of Pr investigated by laser spectroscopy

In the table A.2 all investigated spectral lines of Pr by are listed. All of them have been investigated and/or classified by LIF spectroscopy. Column 1 gives the wavelength in Å of the investigated spectral line, columns 2 gives its relative intensity of the lines in the FT spectrum, where 1 is per definition the intensity of the noise in the FT spectrum and nl in front of the number means that this spectral line was investigated for the first time in this work. All other line have already been investigated in earlier works. The columns 3 to 5 give the level energy in cm^{-1}, the J-value and the parity of the upper level involved in the investigated line and the columns 6 to 8 the values of the lower level, respectively. All newly introduced levels are marked with an upper index ^{a}. Spectral lines which are marked with an asterisk are lines, which where excited by LIF spectroscopy and even LIF signals could be observed, but the spectral line could not be assigned as a transition between energy levels. The uncertainty of the level energies is ± 0.005 cm^{-1} and for the spectral lines it is ± 0.001 Å (no systematic error is taken into account).

Table A.2: Spectral lines of Pr which where investigated by LIF spectroscopy

		Upper Level			Lower Level		
λ/Å	SNR	Energy/cm^{-1}	J-value	parity	Energy/cm^{-1}	J-value	parity
3811.71	10	31094.014^{a}	6.5	o	4866.515	5.5	e
3820.153	nl 6	27546.13^{a}	5.5	e	1376.602	5.5	o
4095.875	nl 5	28840.138^{a}	4.5	o	4432.225	4.5	e
4349.96	nl 2	30599.76^{a}	2.5	o	7617.44	3.5	e
4359.646	nl 4	29466.768	2.5	o	6535.572	3.5	e
4363.157	nl 5	**					
4363.238	nl 10	**					
4422.278	nl 4	31343.998	1.5	o	8737.556	2.5	e
4422.44	nl 2	**					
4570.917	nl 1	28323.121^{a}	3.5	o	6451.808	2.5	e
4586.342	nl 7	28249.58^{a}	1.5	o	6451.808	2.5	e
4917.212	nl 1	30035.792	4.5	o	9704.744	3.5	e
4926.226	5	28323.121^{a}	3.5	o	8029.275	4.5	e
4962.215	23	29133.111	2.5	e	8986.421	1.5	o
5028.262	nl 1	29652.28^{a}	8.5	o	9770.273	8.5	e
5080.065	100	28323.121^{a}	3.5	o	8643.824	4.5	e
5155.182	nl 11	30543.982	10.5	o	11151.433	9.5	e
5314.696	nl 15	28457.348^{a}	6.5	e	9646.83	7.5	o
5319.36	nl 3	29750.67	1.5	o	10956.651	0.5	e
5331.018	nl 1	30035.792	4.5	o	11282.865	5.5	e
5370.562	40	28385.122	8.5	o	9770.273	8.5	e
5371.232	nl 3	28323.121^{a}	3.5	o	9710.6	2.5	e
5374.901	nl 16	28249.58^{a}	1.5	o	9649.970	1.5	e
5384.12	nl 1	30748.179	5.5	o	12180.207	5.5	e

^{a} Previously unknown energy level

** This optical transition was excited by laser light and a LIF signal could be detected, but it could not be assigned to an optical transition.

Table A.2 – Continued

		Upper level			Lower level		
λ/Å	SNR	Energy/cm^{-1}	J-value	parity	Energy/cm^{-1}	J-value	parity
5397.74	nl 10	30599.76[a]	2.5	o	12078.621	2.5	e
5403.647	75	29652.28[a]	8.5	o	11151.433	9.5	e
5431.817	18	28323.121[a]	3.5	o	9918.19	3.5	e
5450.756	294	23207.497	5.5	o	4866.515	5.5	e
5487.991	nl 9	29929.748	4.5	o	11713.236	4.5	e
5505.1	nl 15	**					
5505.28	nl 8	**					
5505.297	nl 7	25776.715	2.5	o	7617.44	3.5	e
5505.32	nl 10	**					
5505.349	nl 2	33579.22	6.5	o	15420.12	6.5	e
5505.55	nl 2	**					
5505.61	nl 9	**					
5505.62	nl 11	32384.45	6.5	e	14226.22	5.5	o
5505.797	nl 6	**					
5505.83	nl 4	**					
5506.49	nl 7	**					
5525.015	nl 15	29909.117	6.5	e	11814.647	7.5	o
5550.17	nl 6	**					
5582.391	nl 3	**					
5588.323	50	**					
5588.525	nl 9	**					
5591.16	nl 86	**					
5594.91	nl 46	**					
5595.98	nl 15	**					
5596.93	nl 7	**					
5597.283	nl 3	34545.57	5	e	16684.71	6	o
5598.149	26	31639.387	4.5	o	13781.374	3.5	e
5598.49	nl 3	**					
5598.596	nl 13	**					
5607.876	55	29541.472	9.5	o	11714.352	8.5	e
5610.216	23	27198.24	5	e	9378.54	5	o
5619.707	nl 32	28200.321	7.5	e	10410.745	6.5	o
5619.95	nl 52	**					
5620.26	nl 73	**					
5620.312	nl 11	29896.535	3.5	e	12108.867	2.5	o
5620.593	13	**					
5620.98	nl 32	**					
5621.311	nl 29	**					
5622.875	37	30781.578	7.5	e	13002.023	7.5	o

[a] Previously unknown energy level

** This optical transition was excited by laser light and a LIF signal could be detected, but it could not be assigned to an optical transition.

Table A.2 – Continued

		Upper level			Lower level		
λ/Å	SNR	Energy/cm^{-1}	J-value	parity	Energy/cm^{-1}	J-value	parity
5623.049	29	29820.642	7.5	o	12041.655	6.5	e
5623.052	14	28508.79	6	e	10729.72	6	o
5623.194	nl 21	33623.946	10.5	o	15845.28	9.5	e
5625.53	nl 1	29993.26	5.5	e	12222.091	6.5	o
5625.687	30	31668.549	7.5	o	13897.874	6.5	e
5626.03	nl 2	**					
5629	nl 9	**					
5629.21	nl 7	**					
5629.272	nl 18	**					
5629.29	nl 18	**					
5630.49	nl 10	**					
5630.651	nl 11	27500.414	6.5	o	9745.376	7.5	e
5630.97	nl 40	**					
5631.083	nl 34	**					
5632.48	nl 32	**					
5633.613	nl 12	**					
5633.857	nl 9	24058.128	4.5	o	6313.224	5.5	e
5634.46	nl 27	**					
5635.35	nl 6	**					
5635.399	nl 7	31562.535	5.5	o	13822.494	4.5	e
5635.42	nl 7	**					
5636.94	58	19111.8	6.5	e	1376.602	5.5	o
5637.41	nl 6	**					
5637.65	nl 13	**					
5638.333	nl 8	34473.61	9.5	e	16742.797	8.5	o
5639.35	nl 25	**					
5641.621	31	29123.494	4.5	e	11403.011	3.5	o
5641.7	nl 9	**					
5641.88	nl 10	**					
5642.02	nl 22	**					
5643.05	nl 8	**					
5643.162	77	28182.37	7.5	o	10466.689	7.5	e
5643.42	nl 12	**					
5643.753	13	**					
5647.713	nl 19	**					
5647.82	nl 3	**					
5647.886	nl 11	**					
5648.23	nl 10	**					
5650.053	nl 13	27340.868	6.5	e	9646.83	7.5	o

[a] Previously unknown energy level

** This optical transition was excited by laser light and a LIF signal could be detected, but it could not be assigned to an optical transition.

Table A.2 – Continued

		Upper level			Lower level		
λ/Å	SNR	Energy/cm^{-1}	J-value	parity	Energy/cm^{-1}	J-value	parity
5651.14	nl 17	**					
5651.429	nl 31	**					
5652.05	nl 8	**					
5652.29	nl 1	29909.117	6.5	e	12222.091	6.5	o
5652.56	nl 3	**					
5652.64	nl 4	**					
5652.91	nl 9	**					
5652.97	nl 301	**					
5653.13	nl 29	**					
5653.6	nl 5	**					
5653.665	nl 13	**					
5654.099	nl 8	31041.89	4.5	e	13360.511	5.5	o
5654.24	nl 17	**					
5656.15	nl 20	**					
5656.25	nl 9	**					
5656.64	nl 4	**					
5656.88	nl 42	**					
5656.954	nl 10	32472.296	8.5	e	14799.842	9.5	o
5656.98	nl 8	**					
5657.308	nl 6	**					
5658.274	nl 12	31664.262	5.5	e	13995.931	6.5	o
5659.66	nl 3	**					
5660.7	nl 106	**					
5660.77	nl 7	**					
5660.91	nl 4	**					
5664.96	nl 2	**					
5665.321	nl 12	**					
5665.6	nl 48	**					
5666.212	53	28054.356	5.5	e	10410.745	6.5	o
5666.624	nl 8	**					
5666.72	nl 8	**					
5666.82	nl 9	**					
5666.839	nl 18	**					
5668.63	nl 38	**					
5668.65	nl 51	**					
5668.68	nl 50	**					
5668.823	nl 22	**					
5669.32	nl 11	**					
5669.551	nl 12	34579.99	6	e	16946.8	7	o

[a] Previously unknown energy level

** This optical transition was excited by laser light and a LIF signal could be detected, but it could not be assigned to an optical transition.

Table A.2 – Continued

		Upper level			Lower level		
λ/Å	SNR	Energy/cm^{-1}	J-value	parity	Energy/cm^{-1}	J-value	parity
5669.65	nl 5	**					
5669.762	4	**					
5670.01	nl 13	**					
5670.992	nl 23	**					
5672.241	nl 37	**					
5672.34	nl 8	**					
5672.48	nl 1	29674.025	3.5	e	12049.942	4.5	o
5672.497	nl 21	**					
5672.62	nl 17	**					
5672.77	nl 3	**					
5672.945	78	**					
5677.47	nl 39	**					
5678.5	nl 8	**					
5678.76	nl 9	**					
5679.07	nl 9	**					
5679.13	nl 1	33808.497	7.5	e	16205.041	6.5	o
5680.01	nl 4	**					
5680.11	nl 3	**					
5680.51	nl 20	32672.439	7.5	o	15073.268	6.5	e
5680.609	nl 16	**					
5680.66	nl 10	**					
5681.07	nl 8	**					
5681.53	nl 2	33205.095	2.5	o	15609.1	2.5	e
5682.17	nl 1	32966.304	6.5	o	15372.271	6.5	e
5682.284	nl 9	29262.465	4.5	o	11668.794	3.5	e
5682.49	nl 12	**					
5682.737	nl 12	**					
5683.13	nl 3	**					
5683.463	nl 10	28731.614	2.5	e	11141.576	2.5	o
5683.533	nl 21	**					
5683.646	nl 17	29335.773	6.5	e	11746.328	6.5	o
5683.76	nl 6	**					
5688.13	nl 3	**					
5689.15	nl 23	**					
5689.891	nl 6	30626.056	1.5	o	13055.995	0.5	e
5689.902	31	29820.642	7.5	o	12250.519	7.5	e
5689.971	nl 10	**					
5690.049	nl 21	**					
5690.071	nl9	30447.257	4.5	e	12877.682	5.5	o

[a] Previously unknown energy level

** This optical transition was excited by laser light and a LIF signal could be detected, but it could not be assigned to an optical transition.

Table A.2 – Continued

		Upper level			Lower level		
λ/Å	SNR	Energy/cm^{-1}	J-value	parity	Energy/cm^{-1}	J-value	parity
5691.75	nl 15	**					
5692.491	27	**					
5692.975	nl 9	**					
5693.213	nl 13	**					
5694.74	nl 5	**					
5695.696	nl 10	32373.816	5.5	e	14821.565	5.5	o
5696.23	nl 10	**					
5696.25	nl 13	**					
5696.44	nl 6	**					
5696.678	nl 10	**					
5696.95	nl 3	**					
5696.98	nl 9	**					
5697.1	nl 31	**					
5697.16	nl 1	31887.92	7.5	e	14340.174	8.5	o
5697.53	nl 2	**					
5697.56	nl 3	**					
5697.712	nl 18	23859.26	5.5	o	6313.224	5.5	e
5698.6	nl 9	**					
5698.84	nl 1	32343.24	4.5	o	14800.68	5.5	e
5699.239	nl 17	26810.061	6.5	o	9268.726	5.5	e
5699.421	nl 10	31536.71	7.5	e	13995.931	6.5	o
5701.29	nl 1	33857.145	5.5	o	16322.122	4.5	e
5701.427	nl 11	**					
5701.46	nl 1	32772.68	6.5	o	15238.143	5.5	e
5703.21	nl 5	**					
5704.2	nl 9	**					
5704.28	nl 1	28800.063	2.5	o	11274.229	3.5	e
5704.441	32	**					
5704.49	13	26570.14	4	e	9044.98	3	o
5704.5	nl 10	**					
5704.66	nl 3	**					
5705.02	40	24237.76	5.5	o	6714.184	5.5	e
5705.116	nl 11	**					
5705.23	nl 2	**					
5705.28	nl 3	**					
5705.52	nl 50	**					
5705.7	nl 70	**					
5705.76	nl 55	**					
5705.893	53	**					

[a] Previously unknown energy level

** This optical transition was excited by laser light and a LIF signal could be detected, but it could not be assigned to an optical transition.

Table A.2 – Continued

		Upper level			Lower level		
λ/Å	SNR	Energy/cm^{-1}	J-value	parity	Energy/cm^{-1}	J-value	parity
5706.29	24	**					
5706.66	nl 7	**					
5706.831	37	29248.614	5.5	e	11730.668	4.5	o
5706.97	nl 5	**					
5707.619	250	28667.026	10.5	o	11151.433	9.5	e
5720.04	nl 13	32849.815	7.5	o	15372.271	6.5	e
5720.274	nl 9	30135.234	6.5	o	12658.401	5.5	e
5721.2	nl 8	30509.7	6.5	o	13035.697	5.5	e
5735.649	nl	31100.17[a]	2.5	o	13670.175	2.5	e
5739.564	nl 1	30035.792	4.5	o	12617.7	3.5	e
5747.18	nl 9	**					
5766.308	nl 5	31333.25	6.5	e	13995.931	6.5	o
5769.892	nl 7	26810.061	6.5	o	9483.518	5.5	e
5785.335	nl 10	36096.84	8.5	o	18816.311	8.5	e
5799.914	nl 5	29278.506	7.5	o	12041.655	6.5	e
5800.021	8	31324.042	7.5	o	14087.545	6.5	e
5800.036	nl 1	31462.756[a]	5.5	e	14226.22	5.5	o
5800.05	nl 1	29894.855	6.5	o	12658.401	5.5	e
5800.107	nl 5	32608.552	6.5	o	15372.271	6.5	e
5800.152	nl 2	27592.931	4.5	o	10356.737	4.5	e
5809.265	10	29444.05	6.5	o	12234.616	5.5	e
5809.285	nl 15	32608.119	6.5	e	15399.063	7.5	o
5809.44	6	27675.34	7.5	o	10466.689	7.5	e
5810.581	2	28816.267	9	e	11611.054	8	o
5810.571	nl 4	30859.797	5.5	o	13654.555	6.5	e
5810.609	nl 1	30932.614	4.5	o	13727.482	5.5	e
5811.414	8	27634.464	5.5	e	10431.716	5.5	o
5812.298	nl 34	29250.06	4.5	e	12049.942	4.5	o
5812.369	nl 35	28041.324	5.5	o	10841.407	5.5	e
5822.466	nl 16	27436.667	5.5	o	10266.501	6.5	e
5822.497	nl 55	33015.36[a]	10.5	o	15845.28	9.5	e
5822.635	nl 4	39442.19[a]	4.5	o	22272.466	3.5	e
5830.057	nl 4	30025.41[a]	5.5	e	12877.67	5.5	o
5832.008	16	28906.232	7.5	e	11764.216	8.5	o
5832.010	2	35978.22	5	o	18835.77	6	e
5832.049	nl 8	28249.58[a]	1.5	o	11107.696	2.5	e
5832.122	nl 4	30580.674	7.5	o	13439.009	7.5	e
5832.122	nl 4	30580.674	7.5	o	13439.009	7.5	e
5832.174	nl 2	36428.498	5.5	o	19286.646	4.5	e

[a] Previously unknown energy level

** This optical transition was excited by laser light and a LIF signal could be detected, but it could not be assigned to an optical transition.

Table A.2 – Continued

		Upper level			Lower level		
λ/Å	SNR	Energy/cm^{-1}	J-value	parity	Energy/cm^{-1}	J-value	parity
5832.213	2	25461.731	5.5	o	8320.24	4.5	e
5832.236	90	39102.27^a	3.5	o	21960.924	3.5	e
5832.236	225	25391.496	3.5	e	8250.141	4.5	o
5832.434	nl 15	30767.47^a	10.5	o	13626.672	9.5	e
5832.444	nl 14	25784.537	5.5	o	8643.824	4.5	e
5832.546	nl 17	35418.34	7.5	o	18277.874	7.5	e
5832.58	nl 1	29133.111	2.5	e	11992.788	1.5	o
5832.772	nl 7	28852.994	5.5	o	11713.236	4.5	e
5832.826	nl 4	28612.025	4.5	o	11472.41	3.5	e
5832.893	18	29188.81^a	4.5	o	12049.465	3.5	e
5832.93	nl 9	33248.24^a	5.5	o	16108.864	4.5	e
5832.971	nl 10	31226.83	6.5	o	14087.545	6.5	e
5833.003	nl 3	28622.399	7.5	o	11483.427	7.5	e
5833.131	nl 7	28323.121^a	3.5	o	11184.396	4.5	e
5833.215	nl 4	31140.75^a	5.5	e	14002.294	5.5	o
5833.239	nl 1	29942.851	7.5	o	12804.468	7.5	e
5833.38	nl 1	30284.567	6.5	o	13146.584	6.5	e
5833.395	nl 6	33432.297^a	7.5	o	16294.378	7.5	e
5833.47	nl 1	31343.998	1.5	o	14206.294	1.5	e
5833.985	20	33387.2^a	6.5	o	16250.9	6.5	e
5834.262	nl 25	31100.17 ^{a}	2.5	o	13964.855	2.5	e
5834.272	nl 13	27546.13^a	5.5	e	10410.745	6.5	o
5834.332	nl	25148.332	3.5	o	8013.089	3.5	e
5834.425	nl 16	28457.348^a	6.5	e	11322.443	5.5	o
5834.512	2	25498.544	7.5	o	8363.901	7.5	e
5834.659	nl 16	24751.633^a	3.5	o	7617.44	3.5	e
5841.28	nl 6	30896.17	4.5	o	13781.374	3.5	e
5867.744	nl 5	**					
5879.277	nl 14	31143.48^a	3.5	o	14139.306	4.5	e
5890.93	180	24921.451	5.5	o	7951.323	6.5	e
5901.072	14	27136.314	3.5	o	10194.768	3.5	e
5901.111	nl 6	29050.133^a	1.5	e	12108.867	2.5	o
5909.466	35	30543.982	10.5	o	13626.672	9.5	e
5909.700	20	35397.77	5.5	o	18481.131	5.5	e
5909.73	nl25	34164.92^a	6.5	o	17248.351	6.5	e
5909.794	nl 30	28965.9	4.5	o	12049.465	3.5	e
5909.812	nl 30	33694.83^a	5.5	o	16778.485	5.5	e
5910.033	70	29652.28^a	8.5	o	12736.621	8.5	e
5910.733	8	26831.753	2.5	o	9918.19	3.5	e

[a] Previously unknown energy level

** This optical transition was excited by laser light and a LIF signal could be detected, but it could not be assigned to an optical transition.

Table A.2 – Continued

		Upper level			Lower level		
λ/Å	SNR	Energy/cm^{-1}	J-value	parity	Energy/cm^{-1}	J-value	parity
5914.177	18	28088.172	4.5	o	11184.396	4.5	e
5914.561	nl 1	34164.92[a]	6.5	o	17262.144	7.5	e
5914.733	2	31919.024[a]	5.5	o	15016.789	4.5	e
5914.859	15	26170.465	4.5	o	9268.726	5.5	e
5914.927	nl 16	28385.122	8.5	o	11483.427	7.5	e
5915.139	5	**					
5915.7	nl 6	**					
5915.776	7	**					
5916.55	5	29929.748	4.5	o	13032.634	3.5	e
5916.75	nl 2	**					
5916.88	nl 5	**					
5916.928	6	28808.943	10.5	e	11913.115	9.5	o
5916.945	nl 1	28840.138[a]	4.5	o	11944.207	5.5	e
5917.091	18	28046.96	8.5	o	11151.433	9.5	e
5917.163	nl 6	32889.914	5.5	o	15994.584	4.5	e
5917.23	nl 1	21276.388	7.5	e	4381.072	7.5	o
5917.526	10	23207.497	5.5	o	6313.224	5.5	e
5917.59	2	31143.48[a]	3.5	o	14249.395	3.5	e
5917.611	2	29929.748	4.5	o	13035.697	5.5	e
5917.779	2	32425.14	5.5	o	15531.574	4.5	e
5917. 931	10	33098.154	7.5	e	16205.041	6.5	o
5918.088	10	30458.345	6.5	e	13565.49	7.5	o
5918.205	nl 4	28175.194	6.5	o	11282.865	5.5	e
5918.22	nl 4	33848.568	7.5	o	16956.282	7.5	e
5918.253	20	24921.451	5.5	o	8029.275	4.5	e
5918.27	nl 2	28889.285	5.5	e	11997.137	5.5	o
5918.583	2	31620.01[a]	4.5	e	14728.843	5.5	o
5923.399	nl 1	29698.58	4.5	e	12821.044	4.5	o
5923.456	10	26523.98	6	e	9646.62	6	o
5923.686	nl 4	29541.472	9.5	o	12664.765	10.5	e
5924.183	20	25608.736	6.5	e	8733.44	6.5	o
5924.633	14	27297.665	6.5	o	10423.654	6.5	e
5924.765	5	31408.016	5.5	e	14534.393	4.5	o
5925.080	nl 3	31094.014[a]	6.5	o	14221.272	7.5	e
6447.763	10	27449.229	5.5	o	11944.207	5.5	e
6447.860	nl 1	33997.515	8.5	e	18492.78	8.5	o
6448.763	nl 40	28323.602[a]	5.5	e	12821.044	4.5	o
6478.248	nl 7	25902.345	6.5	o	10470.329	6.5	e
6478.293	14	25350.082	3.5	o	9918.19	3.5	e

[a] Previously unknown energy level

** This optical transition was excited by laser light and a LIF signal could be detected, but it could not be assigned to an optical transition.

Table A.2 – Continued

		Upper level			Lower level		
λ/Å	SNR	Energy/cm^{-1}	J-value	parity	Energy/cm^{-1}	J-value	parity
6485.352	1	28613.753	9.5	e	13198.637	10.5	o
6485.370	nl 11	27145.714	4.5	e	11730.668	4.5	o
6545.400	nl 25	25191.854	2.5	o	9918.19	3.5	e
6563.932	nl 20	**					

[a] Previously unknown energy level

** This optical transition was excited by laser light and a LIF signal could be detected, but it could not be assigned to an optical transition.

A.3 Newly discovered energy levels of the Pr atom

Table A.3 lists all newly introduced energy levels of Pr. The first column gives the energy of the level in cm^{-1} and the second column its J-value. In column 3 the A-value with its uncertainty in brackets (in MHz) of the level of interest is given, while column 4 gives its parity. The given uncertainty of the A-value is the calculated standard deviation of the resulting A-values when fitting (usually) three different registrations of one spectral line. The last column gives the spectral lines (in Å), which can be explained with the new energy level. The uncertainty of the level energies is ± 0.005 cm^{-1} and for the spectral lines it is ± 0.001 Å (no systematic error is taken into account). If energies of certain levels are not known with such a high accuracy, they are given with two decimal places and have an uncertainty of ± 0.05 cm^{-1}.

Table A.3: New levels of Pr found by analysis of FT spectrum and by LIF spectroscopy.

energy/cm^{-1}	J-value	A [1]/MHz	parity	lines which can be explained (Å)
20467.450	2.5	792(16)	o	9293.848 9241.772 8027.119
20942.933	5.5	363(3)	o	9958.534, 9503.761, 8724.067, 8709.564, 7509.564, 7115.484, 7026.094
22442.185	7.5	959(9)	o	9319.011 9189.156 8393.847 8210.847 7889.311 7573.840 7309.733 7101.187 6311.952
22516.418	0.5	-994(5)	o	9751.899 9553.105 9420.870 9385.756 8962.403

[1] The value of the hyperfine constant B could not be determined with significance therefore it is not taken into account in this work. B was set to zero when determining A.

[a] The value of the hyperfine constant A of this energy level could not be determined with significance, because the recorded spectral line was eighter too noisy or a blend situation, the given value is only an estimated value.

[*] This newly introduced level seems to right, but could not be confirmed by a second laser excitation and there is no line in the FT spectrum which can be explained with it.

Table A.3 – Continued

energy/cm^{-1}	J-value	A [1]/MHz	parity	lines which can be explained (Å)
24183.415	5.5	969(3)	o	9058.096 8233.765 7265.574 6630.181
24289.708	9.5	990(3)	o	8653.316 7609.254
24751.780	3.5	1012(2)	o	5834.659 5281.501
26692.000	8.5	837(5)	o	9216.883 8069.405 7651.767 7163.745
28249.58	1.5	1467(19)	o	5832.049 5374.901 4586.342
28323.121	3.5	877(29)	o	6448.763 5833.131 5431.817 5371.232 5080.065 4926.226 4570.917
28840.138	4.5	889(5)	o	5916.93 5890.98 4095.875
29188.81	4.5	749.1(2)	o	5832.893 5797.36
29652.28	8.5	432(5)	o	5910.06 5403.647 5028.262
30099.668	5.5	398[a]	o	7475.908 7472.162 5896.846
30599.76	2.5	952(2)	o	8397.74 4349.95
30767.47	10.5	394(1)	o	5832.54 5069.449
31094.014	6.5	806(10)	o	5910.04 3811.71
31100.17	2.5	590(3)	o	5834.26 5734.262
31143.48	3.5	811(2)	o	5917.60 5880.89
31919.024	5.5	642[a]	o	5914.733 3695.463
32705.47	4.5	585[a]	o	5888.071 5800.18
33015.36	10.5	498(3)	o	5822.497 4912.490
33248.24	5.5	920(12)	o	5832.33 5121.23 5089.563
33250.18*	5.5	601(1)	o	5745.756
33387.20	6.5	410[a]	o	5833.985 4228.601
33432.297	7.5	620(1)	o	5833.395 3726.291
33694.83	5.5	1181(6)	o	5909.812 5006.780
34164.92	6.5	488(5)	o	5909.73 5914.56
35398.133	5.5	718(6)	o	5909.718 5025.14 4896.611
35802.062	2.5	800.2(1)	o	5810.940 5007.245
36027.68	4.5	524(1)	o	5833.54 4886.142
36056.56	6.5	344(8)	o	7508.8 6321.1
37413.76	4.5	587[a]	o	6469.46 6370.58 5258.26 4996.58
39102.27	3.5	661(16)	o	5832.236 3695.43
39442.19	4.5	546[a]	o	5822.635 3941.018
16059.886	0.5	2966(1)	e	7402.46 5816.30
18870.40	2.5	885(1)	e	6502.98 5865.24
26234.447*	3.5	239(15)	e	7508.18
27546.13	5.5	565[a]	e	5834.26 3820.153

[1] The value of the hyperfine constant B could not be determined with significance therefore it is not taken into account in this work. B was set to zero when determining A.

[a] The value of the hyperfine constant A of this energy level could not be determined with significance, because the recorded spectral line was eighter too noisy or a blend situation, the given value is only an estimated value.

* This newly introduced level seems to right, but could not be confirmed by a second laser excitation and there is no line in the FT spectrum which can be explained with it.

Table A.3 – Continued

energy/cm^{-1}	J-value	A ^{1}/MHz	parity	lines which can be explained (Å)
28457.348	6.5	658^a	e	5834.38 5314.696
29050.133	1.5	1209(2)	e	5901.114 5382.76
30025.41	5.5	666(11)	e	6535.609 5830.057
31140.75	5.5	488(12)	e	6091.452 6011.225 5833.215
31462.756	5.5	688^a	e	5800.036 5070.499
31620.01	4.5	532(8)	e	5918.64 5824.24
36973.918	7.5	835(1)	e	7462.915 6520.510 6350.375
39855.251	3.5	934(2)	e	78646.163 8137.475 493.03

[1] The value of the hyperfine constant B could not be determined with significance, therefore it is not taken into account in this work. B was set to zero when determining A.

[a] The value of the hyperfine constant A of this energy level could not be determined with significance, because the recorded the spectral line was eighter too noisy or a blend situation, the given value is only an estimated value.

[*] This newly introduced level seems to right, but could not be confirmed by a second laser excitation and there is no line in the FT spectrum which can be explained with it.

Appendix B

Lanthanum

B.1 Investigated spectral lines of La

In the table B.1 all investigated spectral lines of La are given. All them have been investigated and/or classified by OG and LIf spectroscopy. Column 1 gives the wavelength in Å of the investigated spectral line, columns 2 gives its relative intensity of the lines in the FT spectrum, where 1 is the intensity of the noise and nl in front of the number means that this spectral line was investigated for the first time in this work. The columns 3 to 5 give the energy in cm^{-1}, the J-value and the parity of the upper level involved in the investigated line and the columns 6 to 8 the values of the lower level, respectively. All newly introduced levels are marked with an upper index ^{a}. Spectral lines which are marked with an asterisk are lines, which where tried to excite by laser spectroscopy, but no signal could be detected, meaning that there is no spectral line. The uncertainty of the level energies is $\pm\,0.05\,\mathrm{cm}^{-1}$ and for the spectral lines it is $\pm\,0.01$ Å. If a wavelengths for certain spectral lines are given with three decimal places, then this lines are eighter visible in the FT spectrum or nearby a line visible in the FT spectrum and their uncertainty is $\pm\,0.001$ Å. For level energies with three given decimal places the uncertainty is $\pm\,0.005\,\mathrm{cm}^{-1}$. All uncertainties are given without any systematic error.

B. LANTHANUM

Table B.1: Spectral lines of La which where investigated eighter by LIF spectroscopy or by OG spectroscopy or by their appearance in the FT spectrum

		Upper Level			Lower Level		
λ/Å	SNR	Energy/cm^{-1}	J-value	parity	Energy/cm^{-1}	J-value	parity
3999.374	nl 8	39800.91[a]	3.5	e	14804.067	2.5	o
4018.893	nl 9	39679.496[a]	2.5	e	14804.067	2.5	o
4028.149	nl 4	39837.776[a]	4.5	e	15019.496	3.5	o
4056.255	nl 8	39355.233[a]	1.5	e	14708.913	1.5	o
4072.553	nl 5	39256.609[a]	1.5	e	14708.913	1.5	o
4114.526	nl 16	39800.91 [a]	3.5	e	15503.63	2.5	o
4182.698	nl 5	38705.343[a]	1.5	e	14804.067	2.5	o
4458.041	nl 4	38705.343[a]	1.5	e	16280.255	1.5	o
4549.095	nl 1	39543.751[a]	1.5	e	17567.517	0.5	o
4574.585	nl 3	39800.91[a]	3.5	e	17947.135	2.5	o
4618.934	nl 6	39800.91[a]	3.5	e	18156.96	2.5	o
4827.594	nl 7	39837.776 [a]	4.5	e	19129.307	4.5	o
5027.05	nl 5	41270.791 [a]	4.5	e	21383.994	4.5	o
5628.37	nl 1	39146.25	3.5	e	21383.994	4.5	o
5649.721	nl 1	39079.07	5.5	e	21383.994	4.5	o
5650.02	nl 1	*					
5650.16	nl 1	**					
5655.22	nl 1	36454.46	3.5	o	18776.615	2.5	e
5655.469	nl 1	39923.729	0.5	e	22246.635	0.5	o
5674.67	nl 1	40421.525	1.5	e	22804.25	2.5	o
5674.713	nl 3	35414.441	2.5	e	17797.301	1.5	o
5674.95	nl 1	36220.338	3.5	e	18603.922	3.5	o
5674.97	nl 1	41865.24[a]	4.5	e	24248.994	4.5	o
5682.72	nl 1	40813.42	3.5	e	23221.097	3.5	o
5700.8	nl 1	40797.43[a]	0.5	e	23260.912	0.5	o
5700.872	nl 1	123773.861	3	e	106237.552	2	o
5715.071	nl 1	*					
5717.02	nl 1	*					
5717.81	nl 1	39923.729	0.5	e	22439.347	1.5	o
5718.01	nl 1	39146.25	3.5	e	21662.504	3.5	o
5723.29	nl 1	**					
5723.39	nl 1	35414.441	2.5	e	17947.135	2.5	o
5723.48	nl 1	42229.665[a]	2.5	e	24762.602	1.5	o
5725.31	nl 1	41166.285	1.5	e	23704.816	1.5	o
5725.4	nl 1	37544.169	2.5	e	20082.982	1.5	o

[a] Previously unknown energy level

* This spectral line was tried to excite by laser light, but neighter an OG signal nor a LIF signal could be detected.

** This spectral was excited by laser light, but it was not possible to assign it to an optical transition, it is an unclassified structure.

Table B.1 – Continued

		Upper level			Lower level		
λ/Å	SNR	Energy/cm^{-1}	J-value	parity	Energy/cm^{-1}	J-value	parity
5725.52	nl 1	**					
5727.28	nl 1	22705.126	1	o	5249.679	0	e
5736.038	nl 1	**					
5746.20	nl 1	33678.22	2.5	e	16280.255	1.5	o
5746.27	nl 3	24409.684	3.5	o	7011.904	2.5	e
5746.334	nl 1	*					
5749.511	nl 6	35298.127	3.5	e	17910.164	3.5	o
5753.804	nl 27	*					
5757.10	nl 2	41453.91^a	2.5	e	24088.541	3.5	o
5757.166	nl 4	35537.177	0.5	e	18172.337	1.5	o
5759.46	nl 1	42576.098	3.5	e	25218.265	2.5	o
5761.21	nl 1	**					
5761.31	nl 1	39638.075	3.5	e	22285.766	4.5	o
5761.32	nl	**					
5765.62	nl 1	34906.899	1.5	e	17567.517	0.5	o
5774.60	nl 1	39751.77^a	2.5	e	22439.347	1.5	o
5774.64	nl 1	**					
5781.48	nl 1	124788.22	1	e	107496.417	1	o
5781.68	nl 1	39576.98	4.5	e	22285.766	4.5	o
5789.222	3300	20763.214	3.5	o	3494.525	3.5	e
5792.98	nl 1	35414.441	2.5	e	18156.96	2.5	o
5793.00	nl 1	40560.645^a	2.5	e	23303.257	3.5	o
5793.972	nl 1	42238.827^a	3.5	e	24984.294	2.5	o
5797.05	nl 1	42229.665^a	2.5	e	24984.294	2.5	o
5797.13	nl 1	35042.426	2.5	e	17797.301	1.5	o
5797.5715	132	19214.527	4	o	1970.705	4	e
5797.732	nl 5	*					
5798.287	nl 4	41490.658	4.5	e	24248.994	4.5	o
5801.854	nl 2	43004.9	6.5	e	25773.798	6.5	o
5813.75	nl 1	*					
5815.659	nl 1	34213.531	2.5	o	17023.342	3.5	e
5815.831	nl 2	42031.1	5.5	e	24841.41	5.5	o
5822.77	nl 3	40472.456	2.5	e	23303.257	3.5	o
5822.874	nl 8	36298.2	5.5	e	19129.307	4.5	o
5830.54	nl 1	*					
5839.783	135	18172.337	1.5	o	1053.161(3)	2.5	e
5848.88	nl 1	37855.757	2.5	e	20763.214	3.5	o

[a] Previously unknown energy level

* This spectral line was tried to excite by laser light, but neighter an OG signal nor a LIF signal could be detected.

** This spectral was excited by laser light, but it was not possible to assign it to an optical transition, it is an unclassified structure.

Table B.1 – Continued

		Upper level			Lower level		
λ/Å	SNR	Energy/cm^{-1}	J-value	parity	Energy/cm^{-1}	J-value	parity
5860.31	17	121161.314	1	e	104102.099	1	o
5860.525	nl 5	34968.76	3.5	e	17910.164	3.5	o
5866.80	nl 1	42123.7	4.5	e	25083.356	3.5	o
5867.901	nl 6	25089.316	4.5	o	8052.163	3.5	e
5869.952	21	25083.356	3.5	o	8052.163	3.5	e
5870.105	nl 1	40497.583	4.5	e	23466.834	4.5	o
5870.14	nl 3	36159.953	5.5	e	19129.307	4.5	o
5870.86	nl 1	**					
5871.09	nl 1	42408.25	3.5	e	25380.28	3.5	o
5871.76	nl 1	**					
5872.26	nl 1	41532.41	3.5	e	24507.871	2.5	o
5872.329	nl 1	34015.77	1.5	o	16991.47	0.5	e
5872.338	nl 1	38061.57	1.5	o	21037.296	1.5	e
5872.49	nl 1	41865.24^a	4.5	e	24841.41	5.5	o
5876.86	nl 1	42100.25	5.5	e	25089.316	4.5	o
5894.1575	nl 2	34758.552	1.5	e	17797.301	1.5	o
5894.33	nl 1	35117.7	2.5	e	18156.96	2.5	o
5894.561	nl 1	*					
5898.80	nl 1	**					
5898.91	nl 1	**					
5898.934	nl 1	*					
5899.50	nl 2	41453.91^a	2.5	e	24507.871	2.5	o
5920.33	nl 1	**					
5920.51	nl 1	35042.426	2.5	e	18156.96	2.5	o
5929.26	nl 1	37253.523	1.5	o	20392.631	0.5	e
5929.38	nl 1	40949.124	2.5	e	24088.541	3.5	o
5938.78	nl 1	39638.075	3.5	e	22804.25	2.5	o
5948.906	nl 1	*					
5955.301	nl 1	*					
5959.26	nl 1	41865.24^a	4.5	e	25089.316	4.5	o
5969.97	nl 1	39995.069	2.5	e	23221.097	3.5	o
5960.075	nl 4	32872.945	2.5	e	16099.276	3.5	o
5984.09	nl 1	**					
5984.145	nl 3	38991.953	3.5	e	22285.766	4.5	o
5984.47	nl 1	*					
5984.514	nl 1	*					
5989.31	nl 1	39995.069	2.5	e	23303.257	3.5	o

[a] Previously unknown energy level

* This spectral line was tried to excite by laser light, but neighter an OG signal nor a LIF signal could be detected.

** This spectral was excited by laser light, but it was not possible to assign it to an optical transition, it is an unclassified structure.

Table B.1 – Continued

		Upper level			Lower level		
λ/Å	SNR	Energy/cm^{-1}	J-value	parity	Energy/cm^{-1}	J-value	parity
5989.47	nl 1	41453.91[a]	2.5	e	24762.602	1.5	o
5989.62	nl 1	*					
5991.49	nl 1	*					
6003.62	nl 1	40180.44	0.5	e	23528.446	0.5	o
6013.90	nl 1	**					
6030.09	nl 1	*					
6062.533	nl 1	*					
6064.36	nl 1	40659.056	2.5	e	24173.83	1.5	o
6092.257	nl 15	25453.951	0.5	o	9044.212	0.5	e
6092.514	nl 1	*					
6155.238	7	122479.382	1	e	106237.552	2	o
6155.36	nl 1	42238.827[a]	3.5	e	25997.181	4.5	o
6155.473	nl 2	123372.925	2	e	107131.709	1	o
6160.58	nl 1	34400.079	2.5	e	18172.337	1.5	o
6160.70	nl 1	*					
6162.28	nl	*					
6163.05	nl 1	*					
6178.43	nl 1	43203.48[a]	2.5	e	27022.612	2.5	o
6178.443	nl 5	36298.2	5.5	e	20117.368	5.5	o
6181.413	nl 1	41014.465	4.5	e	24841.41	5.5	o
6182.09	nl 1	37833.795	3.5	e	21662.504	3.5	o
6182.11	nl 1	37833.795	3.5	e	21662.504	3.5	o
6187.11	nl 2	*					
6189.84	nl 1	39454.3	2.5	e	23303.257	3.5	o
6196.28	nl 1	*					
6196.46	nl 1	40896.48	1.5	e	24762.602	1.5	o
6196.60	nl	*					
6199.00	nl 1	*					
6202.99	nl 1	39377.729[a]	1.5	e	23260.912	0.5	o
6208.28	nl 1	*					
6211.31	nl 1	38341.85[a]	0.5	e	22246.635	0.5	o
6214.06	nl 1	39792.88	2.5	e	23704.816	1.5	o
6214.14	nl 1	*					
6217.23	nl 1	*					
6219.446	nl 16	30169.834	1.5	e	14095.677	0.5	o
6219.61	nl 1	**					
6219.74	nl 1	**					

[a] Previously unknown energy level

* This spectral line was tried to excite by laser light, but neighter an OG signal nor a LIF signal could be detected.

** This spectral was excited by laser light, but it was not possible to assign it to an optical transition, it is an unclassified structure.

Table B.1 – Continued

		Upper level			Lower level		
λ/Å	SNR	Energy/cm^{-1}	J-value	parity	Energy/cm^{-1}	J-value	parity
6220.00	nl 2	41453.91 [a]	2.5	e	25380.28	3.5	o
6220.35	nl 1	**					
6220.49	nl 1	**					
6220.63	nl 1	*					
6221.33	nl 1	42408.25	3.5	e	26338.934	2.5	o
6221.35	nl 1	40243.026	0.5	e	24173.83	1.5	o
6222.77	nl 1	124788.22	1	e	108722.619	0	o
6222.95	nl 1	39326.05	0.5	e	23260.912	0.5	o
6222.967	nl 1	34380.882	3.5	o	18315.822	4.5	e
6223.03	nl 1	41445.18	2.5	e	25380.28	3.5	o
6223.93	nl 1	*					
6224.753	nl 2	43515.76	2.5	e	27455.312	3.5	o
6224.79	nl 1	41044.63	3.5	e	24984.294	2.5	o
6224.877	nl 2	40148.67	3.5	e	24088.541	3.5	o
6224.898	nl 3	34663.997	3.5	e	18603.922	3.5	o
6225.82	nl 1	40231.52[a]	1.5	e	24173.83	1.5	o
6227.25	nl 1	41928.51	4.5	e	25874.5	5.5	o
6227.81	nl 1	**					
6227.95	nl 1	**					
6228.162	nl 1	44140.84	5.5	e	28089.18	4.5	o
6230.02	nl 1	36065.845	1.5	e	20018.977	1.5	o
6231.692	nl 2	36159.953	5.5	e	20117.368	5.5	o
6232.26	nl 1	*					
6232.61	nl 4	31059.702	3.5	e	15019.496	3.5	o
6234.67	nl 1	*					
6234.842	68	25218.265	2.5	o	9183.806	2.5	e
6235.09	nl 1	*					
6236.154	70	34635.015	4.5	e	18603.922	3.5	o
6236.63	nl 1	37692.38	3.5	e	21662.504	3.5	o
6236.774	70	23260.912	0.5	o	7231.416	0.5	e
6237.52	nl 1	41481.51	1.5	e	25453.951	0.5	o
6239.41	nl 1	40196.55[a]	2.5	e	24173.83	1.5	o
6240.96	nl 1	*					
6242.30	nl 1	39543.751[a]	1.5	e	23528.446	0.5	o
6242.46	nl 1	**					
6242.75	nl 1	42011.285[a]	3.5	e	25997.181	4.5	o
6242.81	nl 3	35393.395	2.5	e	19379.397	2.5	o

[a] Previously unknown energy level

* This spectral line was tried to excite by laser light, but neighter an OG signal nor a LIF signal could be detected.

** This spectral was excited by laser light, but it was not possible to assign it to an optical transition, it is an unclassified structure.

Table B.1 – Continued

		Upper level			Lower level		
λ/Å	SNR	Energy/cm^{-1}	J-value	parity	Energy/cm^{-1}	J-value	parity
6243.00	nl 1	37982.804	3.5	o	21969.299	2.5	e
6244.05	nl 1	*					
6244.66	nl 1	32108.512	3.5	e	16099.276	3.5	o
6244.974	nl 2	36027.422[a]	0.5	e	20018.977	1.5	o
6245.68	nl 2	40180.44	0.5	e	24173.83	1.5	o
6245.86	nl 1	*					
6247.445	nl 6	*					
6247.55	nl 1	39468.643	3.5	e	23466.834	4.5	o
6250.20	nl 1	*					
6250.24	nl 1	*					
6253.71	nl 1	40896.48	1.5	e	24910.375	1.5	o
6253.80	nl 1	*					
6253.88	nl 1	*					
6255.18	nl 1	39857.262[a]	3.5	e	23874.946	2.5	o
6256.81	nl 1	34015.77	1.5	o	18037.619	1.5	e
6258.174	nl 3	39679.496[a]	2.5	e	23704.816	1.5	o
6259.82	nl 1	**					
6259.93	nl 1	**					
6260.05	nl 1	41188.16[a]	2.5	e	25218.265	2.5	o
6260.24	nl 1	*					
6260.35	nl 1	42308.11[a]	3.5	e	26338.934	2.5	o
6260.55	nl 1	40014.725	3.5	e	24046.095	2.5	o
6260.92	nl 1	34124.647	2.5	e	18156.96	2.5	o
6260.95	nl 1	**					
6262.45	nl 1	42302.725[a]	2.5	e	26338.934	2.5	o
6262.96	nl 1	**					
6263.06	nl 1	39183.299	2.5	e	23221.097	3.5	o
6263.44	nl 1	41044.63	3.5	e	25083.356	3.5	o
6265.19	nl	*					
6265.75	nl 1	*					
6266.55	nl 1	*					
6267.87	nl 1	*					
6268.73	nl 9	29578.815	2.5	e	13631.032	2.5	o
6273.11	nl 1	*					
6273.97	nl 1	*					
6275.30	nl 1	41014.465	4.5	e	25083.356	3.5	o
6275.44	nl 1	*					

[a] Previously unknown energy level

* This spectral line was tried to excite by laser light, but neighter an OG signal nor a LIF signal could be detected.

** This spectral was excited by laser light, but it was not possible to assign it to an optical transition, it is an unclassified structure.

Table B.1 – Continued

		Upper level			Lower level		
λ/Å	SNR	Energy/cm^{-1}	J-value	parity	Energy/cm^{-1}	J-value	parity
6276.129	nl 3	35308.382	1.5	e	19379.397	2.5	o
6277.221	nl 2	40014.725	3.5	e	24088.541	3.5	o
6277.32	nl 1	39800.91^{a}	3.5	e	23874.946	2.5	o
6277.64	nl 1	39146.25	3.5	e	23221.097	3.5	o
6277.93	nl 1	39391.246	4.5	e	23466.834	4.5	o
6278.56	nl 1	34526.709	4.5	e	18603.922	3.5	o
6278.645	1	122160.15	3	e	106237.552	2	o
6279.15	nl 1	*					
6279.61	nl 1	*					
6285.97	nl 1	34060.977	1.5	e	18156.96	2.5	o
6286.11	nl 1	*					
6286.51	nl 1	40076.51^{a}	1.5	e	24173.83	1.5	o
6286.57	nl 1	38341.85^{a}	0.5	e	22439.347	1.5	o
6287.54	nl 1	*					
6287.61	nl 1	42238.827^{a}	3.5	e	26338.934	2.5	o
6287.74	nl 1	38185.34	3.5	e	22285.766	4.5	o
6287.746	7	25083.356	3.5	o	9183.806	2.5	e
6288.05	nl 1	39603.64^{a}	0.5	e	23704.816	1.5	o
6288.35	nl 1	*					
6288.554	6	25616.928	0.5	o	9719.429	1.5	e
6291.24	nl 1	40732.18	4.5	e	24841.41	5.5	o
6293.05	nl 1	*					
6293.12	nl 1	40525.211^{a}	1.5	e	24639.262	1.5	o
6295.12	nl 1	33678.22	2.5	e	17797.301	1.5	o
6295.14	nl 1	33678.22	2.5	e	17797.301	1.5	o
6295.46	nl 1	39183.299	2.5	e	23303.257	3.5	o
6296.59	nl 1	30908.886	2.5	e	15031.634	1.5	o
6298.36	nl 1	*					
6298.97	nl 1	*					
6300.05	nl 1	36065.845	1.5	e	20197.342	0.5	o
6301.15	nl 1	41740.23	4.5	e	25874.5	5.5	o
6303.81	nl 2	39080.13	4.5	e	23221.097	3.5	o
6304.17	nl 1	*					
6307.51	nl 1	30869.223	3.5	e	15019.496	3.5	o
6307.66	nl 1	122086.916	2	e	106237.552	2	o
6310.08	2	33753.424	4.5	e	17910.164	3.5	o
6310.19	nl 1	*					

^{a} Previously unknown energy level

* This spectral line was tried to excite by laser light, but neighter an OG signal nor a LIF signal could be detected.

** This spectral was excited by laser light, but it was not possible to assign it to an optical transition, it is an unclassified structure.

Table B.1 – Continued

		Upper level			Lower level		
λ/Å	SNR	Energy/cm^{-1}	J-value	parity	Energy/cm^{-1}	J-value	parity
6311.8	nl 1	40749.323	1.5	e	24910.375	1.5	o
6311.81	nl 1	39543.751^a	1.5	e	23704.816	1.5	o
6312.92	nl 1	32079.306	5.5	e	16243.165	4.5	o
6312.979	nl 1	38121.769^a	5.5	e	22285.766	4.5	o
6314.75	nl 1	*					
6314.75	nl 1	*					
6315.844	nl 1	39917.36	4.5	e	24088.541	3.5	o
6315.85	nl 1	38633.057	1.5	e	22804.25	2.5	o
6315.92	nl 1	42167.56	2.5	e	26338.934	2.5	o
6316.62	nl 1	39915.41	2.5	e	24088.541	3.5	o
6316.66	nl 1	39355.233^a	1.5	e	23528.446	0.5	o
6316.82	nl 1	41044.63	3.5	e	25218.265	2.5	o
6318.26	1	23874.946	2.5	o	8052.163	3.5	e
6318.38	nl 1	40663.892	6.5	e	24841.41	5.5	o
6318.71	nl 1	*					
6319.12	nl 1	43569.624^a	1.5	e	27748.969	0.5	o
6319.12	nl 1	**					
6319.33	nl	**					
6319.48	nl 1	*					
6320.76	nl 1	*					
6322.12	nl 1	51441.445	1.5	o	35628.354	1.5	e
6322.70	nl 1	*					
6322.96	nl 1	41453.91^a	2.5	e	25643.001	1.5	o
6323.14	nl 1	*					
6323.16	nl 1	*					
6323.37	nl 1	32348.346	2.5	e	16538.378	3.5	o
6324.21	nl 1	*					
6325.44	nl 1	41755.13	2.5	e	25950.323	1.5	o
6325.488	nl 1	41578.484	6.5	e	25773.798	6.5	o
6328.07	nl 1	*					
6328.32	nl 1	39326.05	0.5	e	23528.446	0.5	o
6329.04	nl 1	*					
6329.06	nl 1	*					
6329.73	nl 1	42849.03^a	4.5	e	27054.94	4.5	o
6332.262	nl 1	37731.59	2.5	o	21943.811	3.5	e
6332.308	nl 1	41241.615	1.5	e	25453.951	0.5	o
6332.63	nl 1	*					

[a] Previously unknown energy level

* This spectral line was tried to excite by laser light, but neighter an OG signal nor a LIF signal could be detected.

** This spectral was excited by laser light, but it was not possible to assign it to an optical transition, it is an unclassified structure.

Table B.1 – Continued

		Upper level			Lower level		
λ/Å	SNR	Energy/cm^{-1}	J-value	parity	Energy/cm^{-1}	J-value	parity
6333.20	nl 2	39006.544	4.5	e	23221.097	3.5	o
6333.798	nl 1	31287.605	3.5	e	15503.63	2.5	o
6334.32	nl 1	33820.31	0.5	o	18037.619	1.5	e
6334.47	nl 1	40421.525	1.5	e	24639.262	1.5	o
6334.65	nl 1	*					
6335.06	nl 1	*					
6336.64	nl 1	39080.13	4.5	e	23303.257	3.5	o
6338.34	nl 1	**					
6338.57	nl 1	41646.567^{a}	5.5	e	25874.5	5.5	o
6338.72	nl 1	39817.789^{a}	1.5	e	24046.095	2.5	o
6341.28	nl 1	*					
6342.50	nl 1	*					
6342.751	nl 1	33799.29	1.5	o	18037.619	1.5	e
6342.93	nl 1	*					
6344.36	nl 1	32492.762	2.5	o	16735.095	1.5	e
6345.16	nl 1	28543.068	3.5	o	12787.399	2.5	e
6345.51	nl 1	39800.91^{a}	3.5	e	24046.095	2.5	o
6347.5	nl 2	39923.729	0.5	e	24173.83	1.5	o
6347.66	nl 6	39454.3	2.5	e	23704.816	1.5	o
6347.76	nl 1	39837.776^{a}	4.5	e	24088.541	3.5	o
6347.98	nl 1	40659.056	2.5	e	24910.375	1.5	o
6348.25	nl 1	*					
6348.26	nl 4	*					
6348.75	nl 1	39792.88	2.5	e	24046.095	2.5	o
6348.86	nl 1	40835.832	4.5	e	25089.316	4.5	o
6349.20	nl 1	119847.77	1	e	104102.099	1	o
6349.97	nl 1	40827.059	3.5	e	25083.356	3.5	o
6350.251	nl 1	41740.23	4.5	e	25997.181	4.5	o
6351.44	nl 1	43489.08	1.5	e	27748.969	0.5	o
6351.88	nl 1	40148.67	3.5	e	24409.684	3.5	o
6352.01	nl 1	*					
6352.17	nl 1	35117.7	2.5	e	19379.397	2.5	o
6353.74	nl 1	25453.951	0.5	o	9719.429	1.5	e
6354.90	nl 1	*					
6355.08	nl 1	33678.22	2.5	e	17947.135	2.5	o
6355.93	nl 1	**					
6356.05	nl 1	*					

[a] Previously unknown energy level

* This spectral line was tried to excite by laser light, but neighter an OG signal nor a LIF signal could be detected.

** This spectral was excited by laser light, but it was not possible to assign it to an optical transition, it is an unclassified structure.

Table B.1 – Continued

		Upper level			Lower level		
λ/Å	SNR	Energy/cm^{-1}	J-value	parity	Energy/cm^{-1}	J-value	parity
6356.27	nl 1	39256.609^{a}	1.5	e	23528.446	0.5	o
6356.42	nl 1	24173.83	1.5	o	8446.039	1.5	e
6356.49	nl 1	36065.845	1.5	e	20338.25	2.5	o
6357.03	nl 1	24910.375	1.5	o	9183.806	2.5	e
6357.90	nl 1	40813.42	3.5	e	25089.316	4.5	o
6358.05	nl 1	*					
6358.10	nl 1	21441.69	1	o	5718.109	1	e
6359.13	nl 1	*					
6359.32	nl 1	**					
6359.58	nl 1	*					
6359.81	nl 1	29466.669	3.5	o	13747.276	4.5	e
6360.89	nl 1	35096.124	3.5	e	19379.397	2.5	o
6360.94	nl 1	42849.03^{a}	4.5	e	27132.434	3.5	o
6361.82	nl 1	39888.265^{a}	1.5	e	24173.83	1.5	o
6361.96	nl 1	*					
6362.64	nl 1	41166.285	1.5	e	25453.951	0.5	o
6362.78	nl 1	30908.886	2.5	e	15196.822	2.5	o
6362.80	nl 2	42050.93	3.5	e	26338.934	2.5	o
6363.64	nl 1	33657.057	1.5	e	17947.135	2.5	o
6363.83	nl 1	43102.49^{a}	3.5	e	27393.027	2.5	o
6364.60	nl 1	*					
6366.04	nl 1	41578.484	6.5	e	25874.5	5.5	o
6366.06	nl 1	*					
6366.73	nl 1	**					
6368.33	nl 1	*					
6369.065	nl 1	190106.3	1.5	o	174409.892	1.5	e
6369.57	nl 1	121932.848	1	e	106237.552	2	o
6370.42	nl 1	*					
6372.25	nl 1	38991.953	3.5	e	23303.257	3.5	o
6372.26	nl 1	40196.55^{a}	2.5	e	24507.871	2.5	o
6373.40	nl 1	*					
6373.45	nl 1	43141.05^{a}	2.5	e	27455.312	3.5	o
6374.08	nl 1	38221.49	2	e	22537.291	3	o
6374.38	nl 1	41300.4^{a}	0.5	e	25616.928	0.5	o
6375.05	nl 1	31924.993	3.5	e	16243.165	4.5	o
6375.46	nl 1	31923.96	4.5	e	16243.165	4.5	o
6376.02	nl 1	39146.25	3.5	e	23466.834	4.5	o

[a] Previously unknown energy level

* This spectral line was tried to excite by laser light, but neighter an OG signal nor a LIF signal could be detected.

** This spectral was excited by laser light, but it was not possible to assign it to an optical transition, it is an unclassified structure.

Table B.1 – Continued

		Upper level			Lower level		
λ/Å	SNR	Energy/cm^{-1}	J-value	parity	Energy/cm^{-1}	J-value	parity
6376.34	nl1	35875.976	1.5	e	20197.342	0.5	o
6376.51	nl 1	40896.48	1.5	e	25218.265	2.5	o
6377.92	nl 1	40659.056	2.5	e	24984.294	2.5	o
6378.056	nl 1	40084.08	4.5	e	24409.684	3.5	o
6378.62	nl 1	*					
6378.67	nl 1	39377.729[a]	1.5	e	23704.816	1.5	o
6378.69	nl 1	32290.16	0.5	o	16617.284	0.5	e
6378.9	nl 1	42011.285[a]	3.5	e	26338.934	2.5	o
6380.44	nl 1	34272.49	3.5	e	18603.922	3.5	o
6382.17	nl	41044.63	3.5	e	25380.28	3.5	o
6382.40	nl 1	*					
6382.62	nl 1	*					
6383.57	nl 1	*					
6384.95	nl 1	39362.32[a]	2.5	e	23704.816	1.5	o
6385.00	nl 1	41300.4[a]	0.5	e	25643.001	1.5	o
6386.00	nl 1	*					
6387.84	nl 1	39355.233[a]	1.5	e	23704.816	1.5	o
6387.90	nl 1	40560.645[a]	2.5	e	24910.375	1.5	o
6388.34	nl 1	*					
6389.15	nl 1	43102.49[a]	3.5	e	27455.312	3.5	o
6389.27	nl 1	40865.120[a]	2.5	e	25218.265	2.5	o
6390.05	nl 1	18895.375	2	o	3250.38	3	e
6390.44	nl 1	*					
6390.481	57	18235.558	3	o	2591.609	2	e
6390.83	nl 1	43036.114[a]	2.5	e	27393.027	2.5	o
6390.938	nl 2	40732.18	4.5	e	25089.316	4.5	o
6390.93	nl 1	40732.18	4.5	e	25089.316	4.5	o
6391.35	nl 1	41592.13	2	e		259	1
6391.77	nl 1	40148.67	3.5	e	24507.871	2.5	o
6391.81	nl 1	42695.63[a]	3.5	e	27054.94	4.5	o
6393.8	nl 1	211725.766	3.5	e	196089.939	2.5	o
6394.228	1536	19129.307	4.5	o	3494.525	3.5	e
6394.47	nl 4	41014.465	4.5	e	25380.28	3.5	o
6394.628	nl 1	41014.083	2.5	e	25380.28	3.5	o
6394.79	nl 1	39679.496[a]	2.5	e	24046.095	2.5	o
6399.93	nl 1	40260.13[a]	1.5	e	24639.262	1.5	o
6402.169	nl 5	31119.02	2.5	e	15503.63	2.5	o

[a] Previously unknown energy level

* This spectral line was tried to excite by laser light, but neighter an OG signal nor a LIF signal could be detected.

** This spectral was excited by laser light, but it was not possible to assign it to an optical transition, it is an unclassified structure.

Table B.1 – Continued

		Upper level			Lower level		
λ/Å	SNR	Energy/cm^{-1}	J-value	parity	Energy/cm^{-1}	J-value	parity
6402.301	nl 2	40599.361	3.5	e	24984.294	2.5	o
6402.396	nl 1	40525.211[a]	2.5	e	24910.375	1.5	o
6402.72	nl 1	*					
6404.98	nl 1	*					
6405.09	nl 1	39857.262[a]	3.5	e	24248.994	4.5	o
6405.17	nl 1	*					
6405.20	nl 1	*					
6406.26	nl 1	*					
6406.43	nl 1	40014.725	3.5	e	24409.684	3.5	o
6406.732	nl 1	34380.882	3.5	o	18776.615	2.5	e
6406.95	nl 1	40243.026	0.5	e	24639.262	1.5	o
6407.905	nl 2	40585.7	2.5	e	24984.294	2.5	o
6408.05	nl 1	*					
6408.70	nl 1	33756.46	3.5	e	18156.96	2.5	o
6409.00	nl 1	40106.64	3.5	e	24507.871	2.5	o
6409.07	nl 1	*					
6409.50	nl 1	42990.56[a]	2.5	e	27393.027	2.5	o
6410.50	nl 1	40813.42	3.5	e	25218.265	2.5	o
6410.54	nl 1	24639.262	1.5	o	9044.212	0.5	e
6410.982	4966	18603.922	3.5	o	3009.993	2.5	e
6411.66	nl 1	40231.52[a]	1.5	e	24639.262	1.5	o
6411.781	nl 3	39638.075	3.5	e	24046.095	2.5	o
6411.85	nl 1	**					
6412.00	nl 1	*					
6412.857	nl 4	34968.76	3.5	e	19379.397	2.5	o
6413.10	nl 1	39837.776[a]	4.5	e	24248.994	4.5	o
6414.59	nl 1	43204.7[a]	3.5	e	27619.548	4.5	o
6415.39	nl 1	16599.256	4	o	1016.087	3	e
6415.54	nl 1	**					
6416.282	nl 1	41578.224	5.5	e	25997.181	4.5	o
6416.50	nl 1	*					
6416.98	nl 1	39454.3	2.5	e	23874.946	2.5	o
6417.07	nl 1	40489.499	1.5	e	24910.375	1.5	o
6417.206	nl 13	24762.602	1.5	o	9183.806	2.5	e
6417.53	nl 1	39751.77[a]	2.5	e	24173.83	1.5	o
6418.21	nl 1	*					
6418.324	nl 4	33143.602	0.5	e	17567.517	0.5	o

[a] Previously unknown energy level

* This spectral line was tried to excite by laser light, but neighter an OG signal nor a LIF signal could be detected.

** This spectral was excited by laser light, but it was not possible to assign it to an optical transition, it is an unclassified structure.

Table B.1 – Continued

		Upper level			Lower level		
λ/Å	SNR	Energy/cm^{-1}	J-value	parity	Energy/cm^{-1}	J-value	parity
6418.48	nl 1	40659.056	2.5	e	25083.356	3.5	o
6419.40	nl 1	42628.42	3.5	e	27054.94	4.5	o
6419.481	nl 2	41447.78	5.5	e	25874.5	5.5	o
6421.01	nl 1	*					
6421.32	nl 1	35907.065	3.5	e	20338.25	2.5	o
6421.39	nl 1	40076.51^a	1.5	e	24507.871	2.5	o
6422.11	nl 1	*					
6423.21	nl 1	43233.58^a	3.5	e	27669.363	2.5	o
6423.64	nl 1	*					
6423.67	nl 1	*					
6423.80	nl 1	35581.783	0.5	e	20018.977	1.5	o
6426.08	nl 1	*					
6426.581	nl 20	31059.702	3.5	e	15503.63	2.5	o
6428.35	nl 1	39256.609^a	1.5	e	23704.816	1.5	o
6429.28	nl 1	39638.075	3.5	e	24088.541	3.5	o
6429.35	nl 1	*					
6429.495	nl 3	39077.463	1.5	e	23528.446	0.5	o
6430.24	nl 1	*					
6431.03	nl 1	43634.49^a	4.5	e	28089.18	4.5	o
6433.35	nl 1	39006.544	4.5	e	23466.834	4.5	o
6433.60	nl 1	43718.15	5.5	e	28179.043	5.5	o
6433.85	nl 1	41877.45	3.5	e	26338.934	2.5	o
6433.90	nl 1	*					
6434.086	nl 2	27968.534	1.5	o	12430.605	1.5	e
6434.12	nl 1	39242.66	2.5	e	23704.816	1.5	o
6434.17	nl 1	35875.976	1.5	e	20338.25	2.5	o
6435.00	nl 1	*					
6435.00	nl 1	*					
6435.16	nl 1	*					
6435.20	nl 1	41532.41	3.5	e	25997.181	4.5	o
6435.45	nl 1	38755.731	4.5	e	23221.097	3.5	o
6435.64	nl 1	*					
6435.68	nl 1	40518.374^a	3.5	e	24984.294	2.5	o
6436.30	nl 1						
6436.73	nl 1						
6440.91	nl 2	40505.755	2.5	e	24984.294	2.5	o
6440.994	nl 2	33678.22	2.5	e	18156.96	2.5	o

[a] Previously unknown energy level

* This spectral line was tried to excite by laser light, but neighter an OG signal nor a LIF signal could be detected.

** This spectral was excited by laser light, but it was not possible to assign it to an optical transition, it is an unclassified structure.

Table B.1 – Continued

		Upper level			Lower level		
λ/Å	SNR	Energy/cm^{-1}	J-value	parity	Energy/cm^{-1}	J-value	parity
6441.33	nl 1	*					
6441.44	nl 1	**					
6444.90	nl 1	*					
6445.85	nl 1	*					
6446.979	nl 6	40014.725	3.5	e	24507.871	2.5	o
6447.38	nl 7	33678.22	2.5	e	18172.337	1.5	o
6447.456	nl 3	34635.015	4.5	e	19129.307	4.5	o
6447.47	nl 3	39679.496[a]	2.5	e	24173.83	1.5	o
6448.32	nl 220	15503.63	2.5	o	0	1.5	e
6448.68	nl 1	*					
6448.86	nl 1	40585.7	2.5	e	25083.356	3.5	o
6448.96	nl 1	36265.3	4.5	e	20763.214	3.5	o
6449.20	nl 1	35839.845	3.5	e	20338.25	2.5	o
6449.31	nl 1	34880.63	2.5	e	19379.397	2.5	o
6449.31	nl 1	34880.63	2.5	e	19379.397	2.5	o
6449.82	nl 1	33657.057	1.5	e	18156.96	2.5	o
6449.97	nl 1	**					
6451.19	nl 1	*					
6452.08	nl 1	28754.915	2.5	e	13260.369	1.5	o
6453.34	nl 1	32348.346	2.5	e	16856.793	2.5	o
6454.501	2189	18156.96	2.5	o	2668.176	1.5	e
6455.11	nl 1	39362.32[a]	2.5	e	23874.946	2.5	o
6455.17	nl 1	39995.069	2.5	e	24507.871	2.5	o
6455.483	nl 103	34615.734	5.5	e	19129.307	4.5	o
6457.56	nl 1	39655.27[a]	0.5	e	24173.83	1.5	o
6458.00	nl 1	*					
6458.53	nl 1	40562.48[a]	4.5	e	25083.356	3.5	o
6459.29	nl 1	*					
6459.7	nl	43515.76	2.5	e	28039.448	3.5	o
6461.01	nl 1	*					
6461.05	nl 1	*					
6461.63	nl 1	43141.05[a]	2.5	e	27669.363	2.5	o
6462.79	nl 1	40231.52[a]	1.5	e	24762.602	1.5	o
6465.12	nl 1	*					
6466.552	7	122514.192	1	e	107054.272	0	o
6466.61	nl 1	*					
6469.02	nl 1	*					

[a] Previously unknown energy level

* This spectral line was tried to excite by laser light, but neighter an OG signal nor a LIF signal could be detected.

** This spectral was excited by laser light, but it was not possible to assign it to an optical transition, it is an unclassified structure.

Table B.1 – Continued

		Upper level			Lower level		
λ/Å	SNR	Energy/cm^{-1}	J-value	parity	Energy/cm^{-1}	J-value	parity
6470.38	nl 1	40361.19	2.5	e	24910.375	1.5	o
6470.453	nl 1	41447.78	5.5	e	25997.181	4.5	o
6470.69	nl 1	40434.372	2.5	e	24984.294	2.5	o
6471.30	nl 1	*					
6471.72	nl 1	39857.262[a]	3.5	e	24409.684	3.5	o
6472.03	nl 1	40827.059	4.5	e	25380.28	3.5	o
6472.24	nl 1	35784.667	2.5	e	20338.25	2.5	o
6472.79	nl 1	**					
6473.037	nl 1	38705.343[a]	1.5	e	23260.912	0.5	o
6473.36	nl 1	42576.098	3.5	e	27132.434	3.5	o
6473.77	nl 1	*					
6473.83	nl 1	40896.48	1.5	e	25453.951	0.5	o
6473.973	nl 1	*					
6474.12	nl 1	*					
6474.25	nl	**					
6474.29	nl 1	*					
6474.56	nl 1	40659.056	2.5	e	25218.265	2.5	o
6475.18	nl 2	42462	2.5	e	27022.612	2.5	o
6476.05	nl 1	40076.51	1.5	e	24639.262	1.5	o
6476.15	nl 1	**					
6476.19	nl 1	**					
6476.35	nl 1	*					
6476.83	nl 1	**					
6476.98	nl 1	40518.374[a]	3.5	e	25083.356	3.5	o
6477.01	nl 1	35552.325	4.5	e	20117.368	5.5	o
6477.25	nl 1	40073.62	2.5	e	24639.262	1.5	o
6477.329	nl 1	40073.62	2.5	e	24639.262	1.5	o
6477.43	nl 1	40196.55[a]	2.5	e	24762.602	1.5	o
6477.78	nl 1	40813.42	3.5	e	25380.28	3.5	o
6477.95	nl 1	42565.14[a]	2.5	e	27132.434	3.5	o
6478.11	nl	39307.26	3.5	e	23874.946	2.5	o
6479.16	nl 1	39603.64[a]	0.5	e	24173.83	1.5	o
6479.875	nl 1	39837.78 [a]	4.5	e	24409.684	3.5	o
6480.06	nl 1	**					
6480.166	nl 5	22439.347	1.5	o	7011.904	2.5	e
6480.24	nl 1	38730.52	3.5	e	23303.257	3.5	o
6481.145	2	122479.382	1	e	107054.272	0	o

[a] Previously unknown energy level

* This spectral line was tried to excite by laser light, but neighter an OG signal nor a LIF signal could be detected.

** This spectral was excited by laser light, but it was not possible to assign it to an optical transition, it is an unclassified structure.

Table B.1 – Continued

		Upper level			Lower level		
λ/Å	SNR	Energy/cm^{-1}	J-value	parity	Energy/cm^{-1}	J-value	parity
6481.85	nl 1	**					
6482.221	nl 1	39468.643	3.5	e	24046.095	2.5	o
6482.284	nl 1	40505.755	2.5	e	25083.356	3.5	o
6483.555	nl 3	25380.28	3.5	o	9960.904	3.5	e
6483.62	nl 1	*					
6483.65	nl 1	40329.5[a]	0.5	e	24910.375	1.5	o
6484.28	nl 1	40180.44	0.5	e	24762.602	1.5	o
6484.31	nl 1	40056.9[a]	0.5	e	24639.262	1.5	o
6484.49	nl 1	*					
6484.78	nl 1	**					
6485.536	217	23466.834	4.5	o	8052.163	3.5	e
6485.72	nl 1	*					
6487.05	nl 1	35494.062	1.5	e	20082.982	1.5	o
6487.48	nl 1	**					
6487.52	nl 1	36447.35	2.5	o	21037.296	1.5	e
6488.171	nl 1	31688.66	1.5	e	16280.255	1.5	o
6488.23	nl 2	40497.583	4.5	e	25089.316	4.5	o
6488.252	nl 5	39454.3	2.5	e	24046.095	2.5	o
6488.401	nl 4	34787.254	2.5	e	19379.397	2.5	o
6488.54	nl 1	39915.41	2.5	e	24507.871	2.5	o
6489.37	nl 1	39110.38	1.5	e	23704.816	1.5	o
6489.498	nl 5	30908.886	2.5	e	15503.63	2.5	o
6489.57	nl 1	38626.25[a]	4.5	e	23221.097	3.5	o
6490.85	nl 1	39276.99	2.5	e	23874.946	2.5	o
6491.03	nl 1	**					
6492.672	nl 1	44140.978	5.5	e	28743.254	5.5	o
6492.767	nl 1	41394.68	4.5	e	25997.181	4.5	o
6493.28	nl 1	41270.79[a]	4.5	e	25874.5	5.5	o
6493.90	nl 1	40379.1	3.5	e	24984.294	2.5	o
6493.969	3	121011.92	1	e	105617.27	2	o
6494.27	nl 1	*					
6494.36	nl 1	*					
6494.77	nl 1	38921.19	0.5	e	23528.446	0.5	o
6494.78	nl 1	38921.19	0.5	e	23528.446	0.5	o
6495.00	nl 1	*					
6495.41	nl 1	39800.91[a]	3.5	e	24409.684	3.5	o
6495.98	nl 1	30409.369	4.5	e	15019.496	3.5	o

[a] Previously unknown energy level

* This spectral line was tried to excite by laser light, but neighter an OG signal nor a LIF signal could be detected.

** This spectral was excited by laser light, but it was not possible to assign it to an optical transition, it is an unclassified structure.

Table B.1 – Continued

		Upper level			Lower level		
λ/Å	SNR	Energy/cm^{-1}	J-value	parity	Energy/cm^{-1}	J-value	parity
6496.50	nl 1	*					
6497.01	nl 1	*					
6497.01	nl 1	*					
6497.36	nl 5	31924.993	3.5	e	16538.378	3.5	o
6497.75	nl 1	*					
6497.795	nl 4	31923.96	4.5	e	16538.378	3.5	o
6497.89	nl 1	*					
6498.166	7	35787.523	2	e	20402.811	3	o
6498.8	nl 1	*					
6498.8	nl 1	*					
6499.45	nl 1	*					
6499.70	nl 1	40599.34	3.5	e	25218.265	2.5	o
6499.99	nl 1	*					
6502.01	nl 1	38904.078	1.5	e	23528.446	0.5	o
6502.30	nl 1	36822.775	4.5	e	21447.854	3.5	o
6502.78	nl 1	38178.025	3.5	e	22804.25	2.5	o
6503.28	nl 1	**					
6503.95	nl 1	*					
6504.04	nl 1	*					
6505.35	nl 1	39242.66	2.5	e	23874.946	2.5	o
6505.47	nl 1	40585.7	2.5	e	25218.265	2.5	o
6505.60	nl 1	**					
6505.66	nl 1	40129.64[a]	1.5	e	24762.602	1.5	o
6505.76	nl 1	43036.114[a]	2.5	e	27669.363	2.5	o
6506.177	110	30169.834	1.5	e	14804.067	2.5	o
6506.25	nl 1	*					
6511.75	nl 1	*					
6512.05	nl 1	40732.18	4.5	e	25380.28	3.5	o
6512.82	nl 1	41300.4[a]	1.5	e	25950.323	1.5	o
6512.96	nl 1	40260.13[a]	1.5	e	24910.375	1.5	o
6514.35	nl 1	36109.7	2.5	e	20763.214	3.5	o
6514.428	nl 1	33143.602	0.5	e	17797.301	1.5	o
6514.60	nl 2	*					
6514.89	nl	*					
6515.63	nl 1	*					
6515.63	nl 1	*					
6516.09	nl 1	40560.645[a]	2.5	e	25218.265	2.5	o

[a] Previously unknown energy level

* This spectral line was tried to excite by laser light, but neighter an OG signal nor a LIF signal could be detected.

** This spectral was excited by laser light, but it was not possible to assign it to an optical transition, it is an unclassified structure.

Table B.1 – Continued

		Upper level			Lower level		
λ/Å	SNR	Energy/cm^{-1}	J-value	parity	Energy/cm^{-1}	J-value	parity
6516.25	nl	*					
6517.18	nl 1	35537.177	0.5	e	20197.342	0.5	o
6519.24	nl 1	*					
6519.319	nl 46	30354.282	2.5	e	15019.496	3.5	o
6519.869	nl 17	41207.994^a	6.5	e	25874.5	5.5	o
6520.5	nl 1	*					
6520.644	nl 240	35449.041^a	6.5	e	20117.368	5.5	o
6521.104	nl 1	40172	5.5	e	24841.41	5.5	o
6521.57	nl 1	42462	2.5	e	27132.434	3.5	o
6521.79	nl 1	38857.4^a	1.5	e	23528.446	0.5	o
6521.94	nl 1	35446.006	4.5	e	20117.368	5.5	o
6522.27	nl 2	39576.98	4.5	e	24248.994	4.5	o
6522.313	nl 1	*					
6523.881	nl 22	24507.871	2.5	o	9183.806	2.5	e
6524.35	nl 1	38626.25^a	4.5	e	23303.257	3.5	o
6525.09	nl 1	42990.56^a	2.5	e	27669.363	2.5	o
6525.13	nl 1	40231.52^a	1.5	e	24910.375	1.5	o
6525.25	nl 1	36293.017	3.5	e	20972.166	2.5	o
6525.67	nl 1	*					
6526.24	nl 1	*					
6526.982	80	17211.918	2	o	1895.128	1	e
6527.22	nl 1	39362.32 ^{a}	2.5	e	24046.095	2.5	o
6528.18	nl 1	*					
6528.287	nl 11	22804.25	2.5	o	7490.521	1.5	e
6529.44	nl 1	40073.62	2.5	e	24762.602	1.5	o
6529.93	nl 1	*					
6530.28	nl 1	39355.233^a	1.5	e	24046.095	2.5	o
6531.18	nl 1	40525.211^a	2.5	e	25218.265	2.5	o
6531.55	nl 1	**					
6531.79	nl 1	**					
6533.01	nl 1	39391.246	4.5	e	24088.541	3.5	o
6533.92	nl 1	38767.361	3.5	e	23466.834	4.5	o
6534.09	nl 1	40518.374^a	3.5	e	25218.265	2.5	o
6534.12	nl 1	**					
6534.22	nl 1	**					
6535.00	nl 1	42753.29^a	4.5	e	27455.312	3.5	o
6536.59	nl 1	40056.9^a	0.5	e	24762.602	1.5	o

[a] Previously unknown energy level

* This spectral line was tried to excite by laser light, but neighter an OG signal nor a LIF signal could be detected.

** This spectral was excited by laser light, but it was not possible to assign it to an optical transition, it is an unclassified structure.

Table B.1 – Continued

		Upper level			Lower level		
λ/Å	SNR	Energy/cm^{-1}	J-value	parity	Energy/cm^{-1}	J-value	parity
6537.12	nl 1	39800.91[a]	3.5	e	24507.871	2.5	o
6537.60	nl 1	*					
6537.87	nl	*					
6540.22	nl 1	30305.597	2.5	e	15019.496	3.5	o
6540.26	nl 1	*					
6542.405	nl 1	*					
6542.49	nl 1	39454.3	2.5	e	24173.83	1.5	o
6542.65	nl 1	*					
6542.89	nl 1	*					
6543.1405	4300	17947.135	2.5	o	2668.176	1.5	e
6545.1	nl 1	123997.01	1	e	108722.619	0	o
6545.278	nl 5	30305.597	2.5	e	15031.634	1.5	o
6545.43	nl 1	41270.79[a]	4.5	e	25997.181	4.5	o
6545.53	nl 29	**					
6546.38	nl 1	36034.61	4.5	e	20763.214	3.5	o
6546.42	nl 1	40489.499	1.5	e	25218.265	2.5	o
6548.43	nl 1	*					
6549.43	nl 1	39673.95	4.5	e	24409.684	3.5	o
6549.70	nl 1	38730.52	3.5	e	23466.834	4.5	o
6549.88	nl 1	38566.48	3.5	e	23303.257	3.5	o
6550.42	nl 1	42881.51[a]	5.5	e	27619.548	4.5	o
6550.77	nl 1	39307.26	3.5	e	24046.095	2.5	o
6551.05	nl 1	*					
6554.19	nl 1	41592.13	2.5	e	26338.934	2.5	o
6554.21	nl 1	42308.11[a]	3.5	e	27054.94	4.5	o
6554.33	nl 3	42275.49[a]	2.5	e	27022.612	2.5	o
6554.567	nl 12	31351.6	2.5	e	16099.276	3.5	o
6555.75	nl 1	*					
6555.98	nl 1	39888.265[a]	1.5	e	24639.262	1.5	o
6556.35	nl1	36220.338	3.5	e	20972.166	2.5	o
6556.56	nl	*					
6556.76	nl 1	33419.552	0.5	e	18172.337	1.5	o
6558.18	nl 1	39751.771[a]	2.5	e	24507.871	2.5	o
6559.71	nl 1	42695.63[a]	3.5	e	27455.312	3.5	o
6559.76	nl 1	42695.63[a]	3.5	e	27455.312	3.5	o
6560.17	nl 1	36687.14	2.5	e	21447.854	3.5	o
6560.231	nl 1	34015.77	1.5	o	18776.615	2.5	e

[a] Previously unknown energy level

* This spectral line was tried to excite by laser light, but neighter an OG signal nor a LIF signal could be detected.

** This spectral was excited by laser light, but it was not possible to assign it to an optical transition, it is an unclassified structure.

Table B.1 – Continued

		Upper level			Lower level		
λ/Å	SNR	Energy/cm^{-1}	J-value	parity	Energy/cm^{-1}	J-value	parity
6560.80	nl 1	41188.16[a]	2.5	e	25950.323	1.5	o
6561.83	nl 1	39110.38	1.5	e	23874.946	2.5	o
6562.02	nl 1	*					
6563.12	nl 1	39995.069	2.5	e	24762.602	1.5	o
6563.21	nl 1	35570.492	3.5	e	20338.25	2.5	o
6564.40	nl 1	42849.03[a]	4.5	e	27619.548	4.5	o
6564.86	nl 1	39638.075	3.5	e	24409.684	3.5	o
6566.16	nl 1	35308.382	1.5	e	20082.982	1.5	o
6566.22	nl 1	*					
6566.26	nl 1	**					
6566.55	nl 1	122514.192	1	e	107289.7	2	o
6567.573	nl 1	40865.120[a]	2.5	e	25643.001	1.5	o
6567.81	nl 1	39470.565	5.5	e	24248.994	4.5	o
6568.06	nl 1	40601.36	4.5	e	25380.28	3.5	o
6568.43	nl 1	37659.49	0.5	e	22439.347	1.5	o
6568.535	23	15219.89	0.5	o	0	1.5	e
6568.66	nl 1	39468.643	3.5	e	24248.994	4.5	o
6568.90	nl 1	40599.361	3.5	e	25380.28	3.5	o
6569.04	nl 1	39307.26	3.5	e	24088.541	3.5	o
6569.23	nl 1	39306.747	4.5	e	24088.541	3.5	o
6569.35	nl 1	38478.915	1.5	e	23260.912	0.5	o
6569.47	nl 1	*					
6569.68	nl 1	**					
6570.05	nl 1	38921.19	0.5	e	23704.816	1.5	o
6570.10	nl 1	**					
6570.17	nl 1	40434.372	2.5	e	25218.265	2.5	o
6570.96	1	21441.69	1	o	6227.409	2	e
6571.79	nl 1	40196.55[a]	2.5	e	24984.294	2.5	o
6572.22	nl 1	*					
6572.58	nl 1	39256.609[a]	1.5	e	24046.095	2.5	o
6572.64	nl 1	*					
6572.87	nl 1	40852.85	2.5	e	25643.001	1.5	o
6574.07	nl 1	42229.665[a]	2.5	e	27022.612	2.5	o
6574.88	nl 1						
6575.50	nl 1	39377.729[a]	1.5	e	24173.83	1.5	o
6575.72	nl 1	40421.525	1.5	e	25218.265	2.5	o
6576.09	nl 1	*					

[a] Previously unknown energy level

* This spectral line was tried to excite by laser light, but neighter an OG signal nor a LIF signal could be detected.

** This spectral was excited by laser light, but it was not possible to assign it to an optical transition, it is an unclassified structure.

Table B.1 – Continued

		Upper level			Lower level		
λ/Å	SNR	Energy/cm^{-1}	J-value	parity	Energy/cm^{-1}	J-value	parity
6576.85	nl 1	36172.8	1.5	e	20972.166	2.5	o
6576.95	nl 1	*					
6577.31	nl 1	39707.46	3.5	e	24507.871	2.5	o
6577.34	nl 1	40109.889	2.5	e	24910.375	1.5	o
6577.45	nl 1	38904.078	1.5	e	23704.816	1.5	o
6577.53	nl 1	38903.885	2.5	e	23704.816	1.5	o
6577.64	nl 1	**					
6579.67	nl 1	43233.58[a]	3.5	e	28039.448	3.5	o
6579.95	nl 1	41532.41	3.5	e	26338.934	2.5	o
6580.133	nl 3	33350.009	2.5	e	18156.96	2.5	o
6581.60	nl 1	122479.382	1	e	107289.7	2	o
6581.98	nl 1	36851.325	2.5	e	21662.504	3.5	o
6582.42	nl 1	42320.21	4.5	e	27132.434	3.5	o
6584.11	nl 1	42238.827	3.5	e	27054.94	4.5	o
6584.47	nl	*					
6584.83	nl 1	32749.715	1.5	e	17567.517	0.5	o
6585.2	nl 1	39355.233[a]	1.5	e	24173.83	1.5	o
6585.57	nl 1	40797.432[a]	0.5	e	25616.928	0.5	o
6585.64	nl 1	**					
6586.40	nl 1	*					
6586.806	nl 17	33350.009	2.5	e	18172.337	1.5	o
6587.14	nl 1	38705.343[a]	1.5	e	23528.446	0.5	o
6587.67	nl 1	42308.11[a]	3.5	e	27132.434	3.5	o
6587.96	nl 1	*					
6588.49	nl 1	41124.115	2.5	e	25950.323	1.5	o
6588.58	nl 1	37612.922	1.5	e	22439.347	1.5	o
6588.94	nl 1	36556.744	4.5	e	21383.994	4.5	o
6589.04	nl 1	43141.05[a]	2.5	e	27968.534	1.5	o
6589.22	nl 1	42565.14[a]	2.5	e	27393.027	2.5	o
6589.43	nl 1	39679.496[a]	2.5	e	24507.871	2.5	o
6589.61	nl 1	**					
6589.85	nl 1	38391.75	3.5	e	23221.097	3.5	o
6590.01	nl 1	42302.725[a]	2.5	e	27132.434	3.5	o
6590.36	nl 7	25089.316	4.5	o	9919.826	4.5	e
6590.60	nl 21	23221.097	3.5	o	8052.163	3.5	e
6590.774	nl 2	35931.742	3.5	e	20763.214	3.5	o
6590.99	nl 1	*					

[a] Previously unknown energy level

* This spectral line was tried to excite by laser light, but neighter an OG signal nor a LIF signal could be detected.

** This spectral was excited by laser light, but it was not possible to assign it to an optical transition, it is an unclassified structure.

Table B.1 – Continued

		Upper level			Lower level		
λ/Å	SNR	Energy/cm^{-1}	J-value	parity	Energy/cm^{-1}	J-value	parity
6591.31	nl 1	39576.98	4.5	e	24409.684	3.5	o
6591.38	nl 1	*					
6591.38	nl 1	*					
6591.69	nl 1	34545.828	1.5	e	19379.397	2.5	o
6591.82	nl 1	40076.51	1.5	e	24910.375	1.5	o
6591.854	nl 11	29874.962	1.5	e	14708.913	1.5	o
6591.92	nl 1	43344.94	4.5	e	28179.043	5.5	o
6592.2	nl 1	43204.7^{a}	3.5	e	28039.448	3.5	o
6593.464		18172.337	1.5	o	3009.993	2.5	e
6593.97	nl 1	**					
6594.11	nl	*					
6594.14	nl 1	**					
6594.37	nl 29	36822.775	4.5	e	21662.504	3.5	o
6594.666	nl 1	123882.203	1	e	108722.619	0	o
6594.74	nl 1	38626.25^{a}	4.5	e	23466.834	4.5	o
6595.44	nl 1	38378.896	2.5	e	23221.097	3.5	o
6596.29	nl 1	*					
6596.30	nl 1	35494.062	1.5	e	20338.25	2.5	o
6596.84	nl 1	40797.43^{a}	2.5	e	25643.001	1.5	o
6596.91	nl 1	*					
6597.27	nl 1	39792.88	2.5	e	24639.262	1.5	o
6597.33	nl 1	*					
6597.61	nl 1	39915.41	2.5	e	24762.602	1.5	o
6597.728	nl 12	33756.46	3.5	e	18603.922	3.5	o
6597.89	nl 1	39326.05	0.5	e	24173.83	1.5	o
6598.28	nl 1	*					
6598.62	nl 1	34529.896	2.5	e	19379.397	2.5	o
6598.68	nl 1	122282.104	2	e	107131.709	1	o
6599.053	nl 18	33753.424	4.5	e	18603.922	3.5	o
6600.35	nl 1	40056.9^{a}	0.5	e	24910.375	1.5	o
6601.11	nl 1	*					
6601.33	nl 1	43233.58^{a}	3.5	e	28089.18	4.5	o
6601.51	nl 2	35907.065	3.5	e	20763.214	3.5	o
6601.804	nl 4	34272.49	3.5	e	19129.307	4.5	o
6601.93	nl 1	37086.731	2.5	o	21943.811	3.5	e
6601.95	nl 1	**					
6601.99	nl 1	*					

[a] Previously unknown energy level

* This spectral line was tried to excite by laser light, but neighter an OG signal nor a LIF signal could be detected.

** This spectral was excited by laser light, but it was not possible to assign it to an optical transition, it is an unclassified structure.

Table B.1 – Continued

		Upper level			Lower level		
λ/Å	SNR	Energy/cm^{-1}	*J*-value	parity	Energy/cm^{-1}	J-value	parity
6603.982	nl 3	30169.834	1.5	e	15031.634	1.5	o
6604.02	nl 1	40518.374[a]	3.5	e	25380.28	3.5	o
6604.26	nl 1	36109.7	2.5	e	20972.166	2.5	o
6604.43	nl 1	39183.299	2.5	e	24046.095	2.5	o
6605.74	nl 1	31751.484	1.5	o	16617.284	0.5	e
6605.92	nl 1	42753.29[a]	4.5	e	27619.548	4.5	o
6609.48	nl 1	40109.889	2.5	e	24984.294	2.5	o
6609.53	nl 2	40505.755	2.5	e	25380.28	3.5	o
6611.58	nl 1	42576.098		3.5	PG12 e	27455.312	3.5
6612.442	nl 23	35236.192	5.5	e	20117.368	5.5	o
6612.52	nl 1	**					
6612.75	nl 1	**					
6613.24	nl 1	38991.953	3.5	e	23874.946	2.5	o
6613.89	nl 1	*					
6614.1	nl 1	41453.91[a]	2.5	e	26338.934	2.5	o
6614.75	nl 2	40023.93	1.5	e	24910.375	1.5	o
6615.04	nl 1	*					
6615.19	nl 1	*					
6615.721	nl 1	28742.365	1.5	e	13631.032	2.5	o
6615.83	nl 1	35308.382	1.5	e	20197.342	0.5	o
6616.57	nl 1	18603.922	3.5	o	3494.525	3.5	e
6617.52	nl 1	41104.4	3.5	e	25997.181	4.5	o
6617.88	nl 1	42238.827	3.5	e	27132.434	3.5	o
6617.91	nl 1	40749.367	1.5	e	25643.001	1.5	o
6618.01	nl 1	43145.55	4.5	e	28039.448	3.5	o
6619.06	nl 1	*					
6619.3	nl 1	39276.99	2.5	e	24173.83	1.5	o
6620.62	nl 1	*					
6620.84	nl 1	38566.48	3.5	e	23466.834	4.5	o
6621.1	nl 1	37903.308	2.5	e	22804.25	2.5	o
6621.25	nl 1	35117.7	2.5	e	20018.977	1.5	o
6621.9	nl 1	*					
6622.32	nl 1	*					
6622.56	nl 1	*					
6622.56	nl 1	*					
6623.19	nl 1	*					
6624.47	nl 1	43634.49[a]	4.5	e	28543.068	3.5	o

[a] Previously unknown energy level

* This spectral line was tried to excite by laser light, but neighter an OG signal nor a LIF signal could be detected.

** This spectral was excited by laser light, but it was not possible to assign it to an optical transition, it is an unclassified structure.

Table B.1 – Continued

		Upper level			Lower level		
λ/Å	SNR	Energy/cm^{-1}	J-value	parity	Energy/cm^{-1}	J-value	parity
6625.369	nl 2	40073.62	2.5	e	24984.294	2.5	o
6625.67	nl 1	*					
6625.74	nl 1	38391.75	3.5	e	23303.257	3.5	o
6625.84	nl 1	*					
6626.20	nl 1	*					
6628.28	nl 1	39256.609[a]	1.5	e	24173.83	1.5	o
6628.31	nl 1	40172	5.5	e	25089.316	4.5	o
6628.412	nl 7	23528.446	0.5	o	8446.039	1.5	e
6629.09	nl 1	*					
6630.25	nl 1	35470.85	1.5	o	20392.631	0.5	e
6630.58	nl 1	*					
6632.72	nl 1	*					
6633.275	nl 6	31351.6	2.5	e	16280.255	1.5	o
6633.31	nl 1	*					
6633.475	nl 10	29874.962	1.5	e	14804.067	2.5	o
6634.93	nl 1	*					
6636.62	nl 1	*					
6636.87	nl 1	*					
6636.92	nl 1	43102.49[a]	3.5	e	28039.448	3.5	o
6639.28	nl 1	*					
6639.739	nl 22	158428.109	0.5	o	143371.436	1.5	e
6639.86	nl 1	43145.55	4.5	e	28089.18	4.5	o
6640.17	nl 1	*					
6640.41	nl 1	35393.395	2.5	e	20338.25	2.5	o
6642.56	nl 1	42275.49[a]	2.5	e	27225.243	1.5	o
6642.60	nl 1	**					
6642.776		35452.601	3	e	20402.811	3	o
6643.59	nl 1	42667.5	5.5	e	27619.548	4.5	o
6643.694	nl 18	157234.02	3.5	o	142186.315	4.5	e
6643.79	nl 1	41044.63	3.5	e	25997.181	4.5	o
6644.79	nl	42100.25	5.5	e	27054.94	4.5	o
6644.90	nl 1	**					
6646.28	nl 1	40260.13[a]	1.5	e	25218.265	2.5	o
6646.99	nl 1	39679.496[a]	2.5	e	24639.262	1.5	o
6647.261	nl 1	40023.93	1.5	e	24984.294	2.5	o
6649.75	nl 1	42088.98[a]	4.5	e	27054.94	4.5	o
6649.75	nl 1	42088.98[a]	4.5	e	27054.94	4.5	o

[a] Previously unknown energy level

* This spectral line was tried to excite by laser light, but neighter an OG signal nor a LIF signal could be detected.

** This spectral was excited by laser light, but it was not possible to assign it to an optical transition, it is an unclassified structure.

Table B.1 – Continued

		Upper level			Lower level		
λ/Å	SNR	Energy/cm^{-1}	J-value	parity	Energy/cm^{-1}	J-value	parity
6650.14	nl 1	*					
6650.80	4300	15031.634	1.5	o	0	1.5	e
6651.58	nl 1	42778.85	1.5	e	27748.969	0.5	o
6651.906	nl 1	38904.078	1.5	e	23874.946	2.5	o
6652.66	nl 1	*					
6653.17	nl	*					
6654.423	nl 1	35042.426	2.5	e	20018.977	1.5	o
6654.45	nl 3	24984.294	2.5	o	9960.904	3.5	e
6654.766	nl 1	33799.29	1.5	o		18776.615	2.5
6654.91	nl 1	**					
6655.05	nl 1	*					
6655.168	nl 2	*					
6656.062	nl 4	31119.02	2.5	e	16099.276	3.5	o
6657.148	nl 1	43056.8	2.5	e	28039.448	3.5	o
6657.19	nl 1	**					
6657.25	nl 2	**					
6657.33	nl 1	41014.083	3.5	e	25997.181	4.5	o
6657.40	nl 1	36400.733	4.5	e	21383.994	4.5	o
6657.40	nl 1	*					
6657.44	nl 1	**					
6657.55	nl 1	31751.484	1.5	o	16735.095	1.5	e
6657.7	nl 2	40659.056	2.5	e	25643.001	1.5	o
6658.9	nl 1	39923.729	0.5	e	24910.375	1.5	o
6658.95	nl 1	40231.52[a]	1.5	e	25218.265	2.5	o
6662.86	nl 1	*					
6664.592	nl 1	38705.343[a]	1.5	e	23704.816	1.5	o
6666.31	nl 1	*					
6666.358	nl 1	159706.534	0.5	o	144709.982	0.5	e
6666.44	nl 1	39837.776[a]	4.5	e	24841.41	5.5	o
6666.614	nl 1	28743.254	5.5	o	13747.276	4.5	e
6668.56	nl 1	39080.13	3.5	e	24088.541	3.5	o
6669.19	nl 1	40073.62	2.5	e	25083.356	3.5	o
6669.86	nl 1	*					
6669.99	nl 1	39076.918	2.5	e	24088.541	3.5	o
6672.52	nl 1	*					
6672.64	nl 1	38857.42[a]	1.5	e	23874.946	2.5	o
6674.49	nl 1	40196.55[a]	2.5	e	25218.265	2.5	o

[a] Previously unknown energy level

* This spectral line was tried to excite by laser light, but neighter an OG signal nor a LIF signal could be detected.

** This spectral was excited by laser light, but it was not possible to assign it to an optical transition, it is an unclassified structure.

Table B.1 – Continued

		Upper level			Lower level		
λ/Å	SNR	Energy/cm^{-1}	J-value	parity	Energy/cm^{-1}	J-value	parity
6674.67	nl 1	39888.265^a	1.5	e	24910.375	1.5	o
6674.80	nl 1	*					
6675.433	nl 6	42031.1	5.5	e	27054.94	4.5	o
6676.00	nl 1	43718.15	5.5	e	28743.254	5.5	o
6676.60	nl 1	*					
6676.83	nl 1	30169.834	1.5	e	15196.822	2.5	o
6679.72	nl 1	43145.55	4.5	e	28179.043	5.5	o
6680.57	nl 1	*					
6680.68	nl 1	39603.64^a	0.5	e	24639.262	1.5	o
6680.75	nl 1	38185.34	3.5	e	23221.097	3.5	o
6684.03	nl 1	38178.025	3.5	e	23221.097	3.5	o
6684.19	nl 1	*					
6684.29	nl 1	157673.413	2.5	o	142717.097	3.5	e
6685.82	nl 1	36400.733	4.5	e	21447.854	3.5	o
6685.95	nl 1	40827.059	4.5	e	25874.5	5.5	o
6686.04	nl 1	32749.715	1.5	e	17797.301	1.5	o
6686.359	nl 3	38172.793	4.5	e	23221.097	3.5	o
6686.55	nl 1	**					
6686.62	nl 1	*					
6686.92	nl 1	38478.915	1.5	e	23528.446	0.5	o
6688.96	nl 1	38991.953	3.5	e	24046.095	2.5	o
6689.16	nl 1	*					
6689.93	nl 21	*					
6689.96	nl 1	122440.067	2	e	107496.417	1	o
6691.85	nl 1	**					
6701.62	nl 1	*					
6702.45	nl 1	*					
6702.76	nl 1	42308.11^a	3.5	e	27393.027	2.5	o
6702.9	nl 1	*					
6703.38	nl 1	*					
6704.43	nl 1	40129.64^a	1.5	e	25218.265	2.5	o
6705.21	nl 1	42302.725^a	2.5	e	27393.027	2.5	o
6705.50	nl 1	36293.017	3.5	e	21383.994	4.5	o
6705.82	nl 1	*					
6706.2	nl 1	39817.789^a	1.5	e	24910.375	1.5	o
6706.53	nl 1	*					
6706.72	nl 1	*					

[a] Previously unknown energy level

* This spectral line was tried to excite by laser light, but neighter an OG signal nor a LIF signal could be detected.

** This spectral was excited by laser light, but it was not possible to assign it to an optical transition, it is an unclassified structure.

Table B.1 – Continued

		Upper level			Lower level		
λ/Å	SNR	Energy/cm^{-1}	J-value	parity	Energy/cm^{-1}	J-value	parity
6707.43	nl 1	24088.541	3.5	o	9183.806	2.5	e
6707.54	nl 1	39543.751[a]	1.5	e	24639.262	1.5	o
6707.92	nl 1	39077.463	1.5	e	24173.83	1.5	o
6708.02	nl 1	38991.953	3.5	e	24088.541	3.5	o
6708.15	nl 1	39076.918	2.5	e	24173.83	1.5	o
6708.55	nl 1	*					
6711.47	nl 1	42565.14[a]	2.5	e	27669.363	2.5	o
6712.03	nl 1	42119.75	1.5	e	27225.243	1.5	o
6712.15	nl 1	36556.744	4.5	e	21662.504	3.5	o
6712.485	nl 1	39532.768	2.5	e	24639.262	1.5	o
6712.67	nl 1	34272.49	3.5	e	19379.397	2.5	o
6712.86	nl 2	39655.27[a]	0.5	e	24762.602	1.5	o
6712.98	nl 1	38767.361	3.5	e	23874.946	2.5	o
6713.53	nl 1	*					
6713.69	nl 1	*					
6712.98	nl 1	38767.361	3.5	e	23874.946	2.5	o
6717.45	nl 1	39792.88	2.5	e	24910.375	1.5	o
6717.58	nl 1	40525.211[a]	2.5	e	25643.001	1.5	o
6717.63	nl 1	38185.34	3.5	e	23303.257	3.5	o
6719.08	nl 1	42011.285[a]	2.5	e	27132.434	3.5	o
6720.56	nl	*					
6720.92	nl 1	38178.025	3.5	e	23303.257	3.5	o
6721.48	nl 1	41928.51	4.5	e	27054.94	4.5	o
6728.424	nl 3	30055.037	3.5	e	15196.822	2.5	o
6728.54	nl 1	38904.078	1.5	e	24046.095	2.5	o
6728.63	nl 1	38903.885	2.5	e	24046.095	2.5	o
6728.67	nl 1	40732.18	4.5	e	25874.5	5.5	o
6729.62	nl 1	38730.52	3.5	e	23874.946	2.5	o
6729.72	nl 1	40073.62	2.5	e	25218.265	2.5	o
6729.96	nl	41877.45	3.5	e	27022.612	2.5	o
6730.13	nl 1	39362.32[a]	2.5	e	24507.871	2.5	o
6730.492	nl 4	*					
6732.5	nl 1	41188.16[a]	2.5	e	26338.934	2.5	o
6733.12	nl 1	41870.468[a]	2.5	e	27022.612	2.5	o
6733.35	nl 1	39355.233[a]	1.5	e	24507.871	2.5	o
6733.45	nl 1	40797.432[a]	0.5	e	25950.323	1.5	o
6733.74	nl 1	40489.499	1.5	e	25643.001	1.5	o

[a] Previously unknown energy level

* This spectral line was tried to excite by laser light, but neighter an OG signal nor a LIF signal could be detected.

** This spectral was excited by laser light, but it was not possible to assign it to an optical transition, it is an unclassified structure.

Table B.1 – Continued

		Upper level			Lower level		
λ/Å	SNR	Energy/cm^{-1}	J-value	parity	Energy/cm^{-1}	J-value	parity
6733.85	nl 1	*					
6734.06	nl 1	**					
6734.17	nl 1	37092.172	1.5	e	22246.635	0.5	o
6734.25	nl 1	*					
6736.02	nl 1	39751.77^a	1.5	e	24910.375	1.5	o
6736.26	nl 1	39603.64^a	0.5	e	24762.602	1.5	o
6738.21	nl 1	*					
6738.27	nl 1	*					
6738.35	nl 1	36220.338	3.5	e	21383.994	4.5	o
6739.38	nl 1	39917.36	4.5	e	25083.356	3.5	o
6739.64	nl 1	39817.789^a	1.5	e	24984.294	2.5	o
6739.88	nl 1	39242.66	2.5	e	24409.684	3.5	o
6740.07	nl 1	39673.95	4.5	e	24841.41	5.5	o
6740.38	nl 1	31688.66	1.5	e	16856.793	2.5	o
6740.71	nl 1	39080.13	4.5	e	24248.994	4.5	o
6741.05	nl 1	38705.343^a	1.5	e	23874.946	2.5	o
6741.194	nl 19	39079.07	5.5	e	24248.994	4.5	o
6743.107	nl 4	43004.9	6.5	e	28179.043	5.5	o
6745.69	nl 1	42275.49^a	2.5	e	27455.312	3.5	o
6747.355	nl 5	31059.702	3.5	e	16243.165	4.5	o
6747.49	nl 1	40813.42	3.5	e	25997.181	4.5	o
6747.89	nl 1	38903.885	2.5	e	24088.541	3.5	o
6748.03	nl 1	39454.3	2.5	e	24639.262	1.5	o
6748.112		23260.912	0.5	o	8446.039	1.5	e
6748.78	nl 1	38341.85^a	0.5	e	23528.446	0.5	o
6749.78	nl 1	42560.18^a	1.5	e	27748.969	0.5	o
6749.79	nl 1	36258.965	2.5	e	21447.854	3.5	o
6750.19	nl 1	42778.85	1.5	e	27968.534	1.5	o
6752.06	nl 1	*					
6756.508	nl 4	40014.725	3.5	e	25218.265	2.5	o
6756.69	nl 1	41928.51	4.5	e	27132.434	3.5	o
6756.81	nl 1	28543.068	3.5	o	13747.276	4.5	e
6757.26	nl 1	*					
6758.1	nl 1	*					
6758.29	nl 1	42462	2.5	e	27669.363	2.5	o
6758.39	nl 1	42881.51^a	5.5	e	28089.18	4.5	o
6758.67	nl 1	*					

^{a} Previously unknown energy level

* This spectral line was tried to excite by laser light, but neighter an OG signal nor a LIF signal could be detected.

** This spectral was excited by laser light, but it was not possible to assign it to an optical transition, it is an unclassified structure.

Table B.1 – Continued

		Upper level			Lower level		
λ/Å	SNR	Energy/cm^{-1}	J-value	parity	Energy/cm^{-1}	J-value	parity
6758.83	nl 1	40434.372	2.5	e	25643.001	1.5	o
6760.06	nl 1	*					
6760.171	nl 8	24507.871	2.5	o	9719.429	1.5	e
6761.27	nl 1	*					
6762.34	nl 1	*					
6762.42	nl	*					
6763.53	nl 1	*					
6765.15	nl 1	40231.52[a]	1.5	e	25453.951	0.5	o
6766.609	nl 17	121011.92	1	e	106237.552	2	o
6766.62	nl 1	42229.665[a]	2.5	e	27455.312	3.5	o
6766.98	nl 1	39183.299	2.5	e	24409.684	3.5	o
6768.6	nl 1	39532.768	2.5	e	24762.602	1.5	o
6769.01	nl 1	39276.99	2.5	e	24507.871	2.5	o
6769.01	nl 1	39679.496[a]	2.5	e	24910.375	1.5	o
6769.01	nl 1	39679.496[a]	2.5	e	24910.375	1.5	o
6769.80	nl 1	39751.77[a]	2.5	e	24984.294	2.5	o
6770.69	nl 1	41104.4	3.5	e	26338.934	2.5	o
6771.82	nl 1	42382.69	5.5	e	27619.548	4.5	o
6773.19	nl 1	31751.484	1.5	o	16991.47	0.5	e
6773.27	nl 1	42849.03[a]	4.5	e	28089.18	4.5	o
6774.371	nl 1	39006.544	4.5	e	24248.994	4.5	o
6774.323	nl 11	39006.544	4.5	e	24248.994	4.5	o
6775.76	nl 1	39837.776[a]	4.5	e	25083.356	3.5	o
6778.498	nl 1	39837.776[a]	4.5	e	25089.316	4.5	o
6779.93	nl 1	123467.973	1	e	108722.619	0	o
6780.08	nl 1	*					
6780.14	nl 1	39655.27[a]	0.5	e	24910.375	1.5	o
6783.094	nl 1	39377.729[a]	1.5	e	24639.262	1.5	o
6783.203	nl 1	36400.733	4.5	e	21662.504	3.5	o
6783.288	nl 1	41792.986	3.5	e	27054.94	4.5	o
6783.30	nl 1	41792.986	3.5	e	27054.94	4.5	o
6784.43	nl 1	**					
6788.30	nl 1	**					
6788.47	nl 1	40601.36	4.5	e	25874.5	5.5	o
6790.19	nl 1	39362.32[a]	2.5	e	24639.262	1.5	o
6794.45	nl 1	42753.29[a]	4.5	e	28039.448	3.5	o
6795.03	nl	*					

[a] Previously unknown energy level

* This spectral line was tried to excite by laser light, but neighter an OG signal nor a LIF signal could be detected.

** This spectral was excited by laser light, but it was not possible to assign it to an optical transition, it is an unclassified structure.

Table B.1 – Continued

		Upper level			Lower level		
λ/Å	SNR	Energy/cm^{-1}	J-value	parity	Energy/cm^{-1}	J-value	parity
6796.723	nl 1	14708.913	1.5	o	0	1.5	e
6798.093	nl 4	38172.793	4.5	e	23466.834	4.5	o
6798.21	nl 1	41044.63	3.5	e	26338.934	2.5	o
6798.32	nl 1	**					
6798.87	nl 1	34787.254	2.5	e	20082.982	1.5	o
6799.08	nl 1	40084.08	4.5	e	25380.28	3.5	o
6799.70	nl 1	42881.51[a]	5.5	e	28179.043	5.5	o
6800.03	nl 1	*					
6800.565	nl 4	32872.945	2.5	e	18172.337	1.5	o
6801.27	nl 1	39206.95	3.5	e	24507.871	2.5	o
6801.55	nl 1	*					
6802.16	nl 1	39915.41	2.5	e	25218.265	2.5	o
6803.06	nl 1	39679.496[a]	2.5	e	24984.294	2.5	o
6803.93	nl 1	40073.62	2.5	e	25380.28	3.5	o
6804.68	nl 1	39454.3	2.5	e	24762.602	1.5	o
6804.74	nl 1	30934.76	4.5	e	16243.165	4.5	o
6804.76	nl 1	38566.48	3.5	e	23874.946	2.5	o
6804.95	nl 1	23874.946	2.5	o	9183.806	2.5	e
6805.26	nl 1	**					
6806.40	nl 1	40562.48[a]	4.5	e	25874.5	5.5	o
6806.43	nl	*					
6806.56	nl 1	**					
6806.97	nl 1	39326.05	0.5	e	24639.262	1.5	o
6807.09	nl 1	40329.5[a]	0.5	e	25643.001	1.5	o
6807.60	nl 1	*					
6808.08	nl 1	38730.52	3.5	e	24046.095	2.5	o
6808.44	nl 1	38857.42[a]	1.5	e	24173.83	1.5	o
6808.531	nl 9	159393.385	1.5	o	144709.982	0.5	e
6808.814	nl 1	35446.006	4.5	e	20763.214	3.5	o
6808.86	nl 1	15698.781	4	o	1016.087	3	e
6809.08	nl 1	37903.308	2.5	e	23221.097	3.5	o
6809.38	nl 1	34060.977	1.5	e	19379.397	2.5	o
6810.65	nl 1	38767.361	3.5	e	24088.541	3.5	o
6810.93	nl 1	40452.035	5.5	e	25773.798	6.5	o
6810.97	nl 11	29874.962	1.5	e	15196.822	2.5	o
6811.68	nl 1	*					
6811.767	nl 1	42715.876[a]	3.5	e	28039.448	3.5	o

[a] Previously unknown energy level

* This spectral line was tried to excite by laser light, but neighter an OG signal nor a LIF signal could be detected.

** This spectral was excited by laser light, but it was not possible to assign it to an optical transition, it is an unclassified structure.

Table B.1 – Continued

		Upper level			Lower level		
λ/Å	SNR	Energy/cm^{-1}	J-value	parity	Energy/cm^{-1}	J-value	parity
6811.92	nl 1	43569.624 [a]	1.5	e	28893.526	0.5	o
6811.920	nl 1	43569.624[a]	1.5	e	28893.526	0.5	o
6812.11	nl 1	40129.64[a]	1.5	e	25453.951	0.5	o
6812.169	nl 2	34758.552	1.5	e	20082.982	1.5	o
6812.24	nl 1	39183.299	2.5	e	24507.871	2.5	o
6812.39	nl 1	41014.083	3.5	e	26338.934	2.5	o
6813.6155	nl 1	37209.732	3	e	22537.291	3	o
6813.95	nl 1	35009.99	1.5	e	20338.25	2.5	o
6814.54	nl 1	39080.13	3.5	e	24409.684	3.5	o
6814.75	nl 1	39888.265[a]	1.5	e	25218.265	2.5	o
6814.95	nl 1	34752.589	0.5	e	20082.982	1.5	o
6815.22	nl 1	*					
6815.48	nl 1	*					
6815.72	nl 1	27455.312	3.5	o	12787.399	2.5	e
6817.48	nl 1	42753.29[a]	4.5	e	28089.18	4.5	o
6817.70	nl 1	34861.01	0.5	e	20197.342	0.5	o
6818.53	nl 1	36109.7	2.5	e	21447.854	3.5	o
6818.63	nl 1	43204.7[a]	3.5	e	28543.068	3.5	o
6821.17	nl 1	35628.354	1.5	e	20972.166	2.5	o
6821.63	nl 1	**					
6821.759	nl 10	38121.769[a]	5.5	e	23466.834	4.5	o
6822.5	nl 1	34032.734	3.5	e	19379.397	2.5	o
6823.48	nl 1	35414.441	2.5	e	20763.214	3.5	o
6826.28	nl 1	*					
6827.792	nl 5	38730.52	3.5	e	24088.541	3.5	o
6828.00	nl 1	**					
6828.27	nl 1	**					
6828.80	nl 1	**					
6829.18	nl 1	39857.262[a]	3.5	e	25218.265	2.5	o
6829.47	nl 1	*					
6829.70	nl 1	43381.1	5.5	e	28743.254	5.5	o
6830.03	nl 1	**					
6830.10	nl 1	*					
6830.82	nl 1	37172.79	4	e	22537.291	3	o
6830.86	nl 1	40585.7	2.5	e	25950.323	1.5	o
6830.95	nl 1	*					
6831.21	nl 1	37855.757	2.5	e	23221.097	3.5	o

[a] Previously unknown energy level

* This spectral line was tried to excite by laser light, but neighter an OG signal nor a LIF signal could be detected.

** This spectral was excited by laser light, but it was not possible to assign it to an optical transition, it is an unclassified structure.

Table B.1 – Continued

		Upper level			Lower level		
λ/Å	SNR	Energy/cm^{-1}	J-value	parity	Energy/cm^{-1}	J-value	parity
6831.22	nl 1	43141.05[a]	2.5	e	28506.411	2.5	o
6831.66	nl 1	42088.98[a]	4.5	e	27455.312	3.5	o
6831.81	nl 1	39543.751[a]	1.5	e	24910.375	1.5	o
6832.08	nl 1	**					
6833.15	nl 1	34968.76	3.5	e	20338.25	2.5	o
6833.31	nl 1	35393.395	2.5	e	20763.214	3.5	o
6833.78	nl 4	39470.565	5.5	e	24841.41	5.5	o
6834.95	nl 1	*					
6836.13	nl 1	44978.6	1.5	o	30354.282	2.5	e
6836.131	nl 1	**					
6837.914	nl 1	17211.918	2	o	2591.609	2	e
6838.21	nl 1	*					
6838.39	nl 1	42238.827	3.5	e	27619.548	4.5	o
6838.87	nl 1	*					
6838.93	nl 1	39707.46	3.5	e	25089.316	4.5	o
6839.402	nl 3	40260.13[a]	1.5	e	25643.001	1.5	o
6840.50	nl 1	39995.069	2.5	e	25380.28	3.5	o
6840.59	nl 1	40231.52[a]	1.5	e	25616.928	0.5	o
6841.85	nl 1	41837.14	2.5	e	27225.243	1.5	o
6842.66	nl 1	40949.124	2.5	e	26338.934	2.5	o
6843.88	nl 1	**					
6843.98	nl 1	**					
6844.05	nl 1	**					
6844.17	nl 1	36853.596	1.5	e	22246.635	0.5	o
6844.24	nl 1	*					
6844.50	nl 1	*					
6844.58	nl 1	**					
6845.67	nl 1	**					
6845.83	nl 1	39242.66	2.5	e	24639.262	1.5	o
6845.884	nl 3	**					
6846.01	nl 1	40056.9[a]	0.5	e	25453.951	0.5	o
6846.12	nl 1	36265.3	4.5	e	21662.504	3.5	o
6846.25	nl 1	39110.38	1.5	e	24507.871	2.5	o
6846.40	nl 1	40599.361	3.5	e	25997.181	4.5	o
6846.61	nl 1	43344.94	4.5	e	28743.254	5.5	o
6846.91	nl 1	**					
6847.40	nl 1	37903.308	2.5	e	23303.257	3.5	o

[a] Previously unknown energy level

* This spectral line was tried to excite by laser light, but neighter an OG signal nor a LIF signal could be detected.

** This spectral was excited by laser light, but it was not possible to assign it to an optical transition, it is an unclassified structure.

Table B.1 – Continued

		Upper level			Lower level		
λ/Å	SNR	Energy/cm^{-1}	J-value	parity	Energy/cm^{-1}	J-value	parity
6847.42	nl 1	40243.026	0.5	e	25643.001	1.5	o
6847.56	nl 1	39362.32^a	2.5	e	24762.602	1.5	o
6847.65	nl 1	39817.789^a	1.5	e	25218.265	2.5	o
6847.84	nl 1	43570.94^a	2.5	e	28971.829	1.5	o
6848.47	nl 1	*					
6848.90	nl 1	39006.544	4.5	e	24409.684	3.5	o
6849.26	nl 1	43102.49 ^{a}	3.5	e	28506.411	2.5	o
6849.51	nl 1	*					
6850.13	nl 1	36840.808	0.5	e	22246.635	0.5	o
6850.82	nl 1	32749.715	1.5	e	18156.96	2.5	o
6850.92	nl 1	**					
6851.167	nl 4	27022.612	2.5	o	12430.605	1.5	e
6851.36	nl 1	42560.18^a	1.5	e	27968.534	1.5	o
6851.36	nl 1	*					
6852.07	nl 1	*					
6852.6	nl 1	42628.42	3.5	e	28039.448	3.5	o
6852.81	nl 1	40231.52 ^{a}	1.5	e	25643.001	1.5	o
6860.61	nl 1	*					
6862.61	nl 1	*					
6863.47	nl 1	*					
6863.53	nl 1	157673.413	2.5	o	143107.68	2.5	e
6863.74	nl 1	*					
6866.493	nl 6	39543.751^a	1.5	e	24984.294	2.5	o
6868.13	nl 1	*					
6872.288	nl 1	29578.815	2.5	e	15031.634	1.5	o
6872.38	nl 29	**					
6872.57	nl 1	**					
6872.94	nl 1	*					
6886.88	nl 1	*					
6897.407	nl 5	38903.885	2.5	e	24409.684	3.5	o
6901.5	nl 1	*					
6913.133	nl 3	39679.496^a	2.5	e	25218.265	2.5	o
6914.919	nl 13	39837.776^a	4.5	e	25380.28	3.5	o
8531.538	nl 5	29874.962	1.5	e	18156.96	2.5	o
8727.064	nl 14	32492.762	2.5	o	21037.296	1.5	e

^{a} Previously unknown energy level

* This spectral line was tried to excite by laser light, but neighter an OG signal nor a LIF signal could be detected.

** This spectral was excited by laser light, but it was not possible to assign it to an optical transition, it is an unclassified structure.

B.2 Newly discovered energy levels of the La atom

Table B.2 lists all newly introduced energy levels of La. All energy levels where found by the different techniques of laser spectroscopy. The first column gives the energy of the level in cm^{-1} and the second column its J-value. In column 3 the A-value with its uncertainty in brackets (in MHz) of the level of interest is given, while column 4 gives its parity. The given uncertainty of the A-value is the calculated standard deviation of the resulting A-values when fitting (usually) three different registrations of one spectral line. The last column gives the spectral lines (in Å), which where excited in order to excite the newly introduced energy level. The uncertainty of the level energies is $\pm\,0.05\,\mathrm{cm}^{-1}$ and for the spectral lines it is ± 0.01 Å. If wavelengths for certain spectral lines are given with three decimal places, then this lines are eighter visible in the FT spectrum or nearby a line visible in the FT spectrum and their uncertainty is ± 0.001 Å. For level with well known energies with three given decimal places the uncertainty is $\pm\,0.005\,\mathrm{cm}^{-1}$. All uncertainties are given without any systematic error.

Table B.2: New La levels found by LIF spectroscopy and by OG spectroscopy.

energy/cm^{-1}	J-value	A [1]/MHz	parity	excited spectral lines (Å)
35449.04[*]	6.5	-8.0(5)	e	6520.20
38121.769	5.5	168(2)	e	6821.761 6313 6312.98 6821.76
38341.85	0.5	-917(2)	e	6286.57 6211.31
38626.25	4.5	163 [a]	e	6594.80 6524.35 6489.57
38705.343	1.5	-175(15)	e	6473.04 6587.156664.12
38857.42	1.5	241(5)	e	6521.79 6672.64 OG
39256.609	1.5	-13.6(4)	e	6428.35 6572.586628.25
39355.233	1.5	46(2)	e	6530.28 6585.20 6387.86
39362.32	2.5	82.4(4)	e	6847.56 6455.11 6527.22 6730.13 6790.19
39377.729	1.5	189(2)	e	6783.12 6575.45 6378.70 6202.99
39543.751	1.5	168.6(7)	e	6866.49 6831.81 6707.54
39603.64	0.5	-203(7)	e	6680.68 6479.16 6736.26 6288.05
39655.27	0.5	160(5)	e	6712.86 6457.563 6780.14
39679.496	2.5	69(1)	e	6913.13 6769.015 6646.99 6394.79 6589.43 6803.06
39751.77	2.5	13(1)	e	6736.02 6769.80 6558.18 6417.53

[1] The value of the hyperfine constant B could not be determined with significance therefore it is not taken into account in this work. B was set to zero when determining A.

[a] The value of the hyperfine constant A of this energy level could not be determined with significance, because the recorded spectral lines was eighter too noisy or a blend situation, the given value is only an estimated value.

[*] This newly introduced level could not yet be confirmed by a second laser excitation, it seems right though.

Table B.2 – Continued

energy/cm^{-1}	J-value	A [1]/MHz	parity	excited spectral lines(Å)
39800.91	3.5	304(1)	e	6245.51 6537.12 6495.41
39817.789	1.5	109.5(4)	e	6338.72 6706.20 6739.64
39837.776	4.5	224(4)	e	6914.93 6778.50 6775.76 6347.76 6769.01 6646.99 6666.44 6413.09
39857.262	3.5	442(4)	e	6471.67 6405.90 6339.915 6721.75 6829.18 6255.18
39888.265	1.5	93(2)	e	6361.82 6674.67 6814.75
40056.9	0.5	-766(1)	e	6600.35 6536.60 6484.31
40076.51	1.5	276(2)	e	6591.79 6421.39 6476.05 6286.51
40129.64	1.5	163(6)	e	6704.43 6505.66 6812.11
40196.55	2.5	666.4(7)	e	6477.43 6239.41
40231.52	1.5	-78(22)	e	6840.59 6225.82 6411.66 6462.79 6525.13 6658.95 6852.81
40260.13	1.5	120(1)	e	6839.42 6646.29 6512.96 6399.93
40329.5	0.5	-472(10)	e	6483.65 6807.09
40432.076	4.5	118(2)	e	6239.54 6515.93 6513.40 6412.32
40518.374	3.5	683.6(7)	e	6435.68 6476.99 OG6604.02
40525.211	1.5	63(9)	e	6402.396 6531.18 6717.58
40560.645	2.5	-15(6)	e	6387.90 6516.27
40562.48	4.5	69(6)	e	6806.40 6458.53
40797.43	0.5	450(12)	e	6733.47 6585.57
40865.120	2.5	67(4)	e	6567.573 6389.27
41188.16	2.5	97(3)	e	6560.80 6732.50
41207.994	6.5	91.6(5)	e	6519.87 6108.319
41270.79	4.5	152(14)	e	a6493.27 6545.50
41300.40	0.5	228(3)	e	6385.01 6512.82 6374.38
41453.91	2.5	316(8)	e	6322.96 6614.10
41646.567*	5.5	76(5)	e	6338.57
41865.24	4.5	87(2)	e	5872.49 5959.26
41870.468	2.5	-13(10)	e	6733.12 6783.30
42011.285	3.5	222(16)	e	6378.90 6719.08 6242.75
42088.98	4.5	242(29)	e	6831 6649.75
42229.665	2.5	302(1)	e	6574.07 6766.62
42238.827	3.5	137(9)	e	6584.11 6838.39 6617.88 6155.36 6287.61
42275.49	2.5	337(25)	e	6554.33 6745.69
42302.725	2.5	121(5)	e	6590.01 6705.21
42308.11	3.5	302.0(9)	e	6587.67 6260.35 6702.76

[1] The value of the hyperfine constant B could not be determined with significance therefore it is not taken into account in this work. B was set to zero when determining A.

[a] The value of the hyperfine constant A of this energy level could not be determined with significance, because the recorded spectral lines was eighter too noisy or a blend situation, the given value is only an estimated value.

* This newly introduced level could not yet be confirmed by a second laser excitation, it seems right though.

Table B.2 – Continued

energy/cm^{-1}	J-value	A [1]/MHz	parity	excited spectral lines(Å)
42560.18*	1.5	74(9)	e	6749.79
42565.14	2.5	137(6)	e	6589.22 6477.95
42695.63*	3.5	120 [a]	e	6559.76
42715.876*	3.5	157(2)	e	6811.767
42753.29	4.5	50(11)	e	6817.50 6794.45 6605.92 6535.00
42849.03	4.5	72(12)	e	6564.40 6773.27 6360.94 6329.73
42881.51	5.5	28.3(2)	e	6799.70 6550.42 6578.39
42990.56	2.5	150 [a]	e	6525.10 6409.50
43036.114	2.5	220(16)	e	6505.75 6505 6390.83
43102.49	3.5	189.1(9)	e	6636.92 6363.83
43141.05	2.5	225 [a]	e	6831.21 6373.45 6461.63
43203.48*	2.5	280 [a]	e	6178.41
43204.70	3.5	124(5)	e	6818.63 6414.59 6592.20
43233.58	3.5	160(12)	e	6579.67 6423.21
43569.624	1.5	240(20)	e	6811.920 6319.12
43570.94*	2.5	-73(6)	e	6847.84
43634.49	4.5	43(8)	e	6431.03 6624.47

[1] The value of the hyperfine constant B could not be determined with significance therefore it is not taken into account in this work. B was set to zero when determining A.

[a] The value of the hyperfine constant A of this energy level could not be determined with significance, because the recorded spectral line was eighter too noisy or a blend situation, the given value is only an estimated value.

* This newly introduced level could not yet be confirmed by a second laser excitation, it seems right though.

References

[1] Arnold Sommerfeld. *Atombau und Spektrallinien Band II.* Nachdruck der 4. Auflage. Verlag Harri Deutsch, 1987.

[2] Joseph Fraunhofer. **Bestimmung des Brechungs- und des Farbenzerstreungs-Vermögens verschiedener Glasarten, in Bezug auf die Vervollkommung achromatischer Fernröhre**. *Annalen der Physik*, **56**:7, 1817.

[3] Wolfgang Demtröder. *Experimentalphysik 3.* 4., überarb. Aufl. Springer-Verlag, 2010.

[4] Ludwig Bergmann Clemens Schäfer Wilhelm Raith. *Bergmann Schäfer Lehrbuch der Experimentalphysik Band 4 BESTANDTEILE DER MATERIE Atome, Moleküle, Atomkerne, Elementarteilchen.* 2. Auflage. Walter de Gruyter & Co.KG, 2003.

[5] Charles Schwartz. **Theory of hyperfine structure**. *Physical Review*, **97**:380, 1955.

[6] I I Sobelman. *An Introduction to the Theory of Atomic Spectra.* Oxford: Pergamon, 1972.

[7] O Laporte and W F Meggers. **Some rules of spectral structure**. *Journal of the Optical Society of America*, **11**:459, 1925.

[8] Franz Schwabl. *Quantenmechanik.* 6. Auflage. Springer-Verlag, 2002.

[9] Wolfgang Nolting. *Grundkurs Theoretische Physik 5/1.* 5. Auflage. Springer-Verlag, 2004.

[10] R B Firestone V S Shirley C M Baglin S Y F Chu J Zipkin. *Table of Isotopes*. Wiley, 1996.

[11] R M Macfarlane D P Burum and R M Shelby. **New Determation of the Nuclear Magnetic Moment of ^{141}Pr**. *Physical Review Letters*, **49**:636, 1982.

[12] K D Böklen T Bossert W Foerster H H Fuchs and G Nachtsheim. **Hyperfine structure measurements in the ^{4}I9/2 ground state of ^{141}Pr**. *Zeitschrift für Physik A*, **274**:195, 1975.

[13] Robert L Kurucz. **Atomic data for interpreting stellar spectra: isotopic and hyperfine data**. *Physica Scripta*, **T47**:110, 1993.

[14] A . King and Arthur. **Temperature Classification of the Stronger Lines of Cerium and Praseodymium**. *Astrophysical Journal*, **68**:194, 1928.

[15] A Ginibre. **Fine and Hyperfine Structures of Single Ionized Praseodymium: I. Energy Levels, Hyperfine Structures and Zeeman Effect, Classified Lines**. *Physica Scripta*, **39**:710, 1989.

[16] A Ginibre. **Fine and Hyperfine Structures of Single Ionized Praseodymium: II. Parametric Interpretation of Fine and Hyperfine Structures for the Even Levels of Single Ionised Praseodymium**. *Physica Scripta*, **39**:710, 1989.

[17] J Ruczkowski E Stachowska M Elantkowska G H Guthöhrlein and J Dembczyñski. **Interpretation of the Hyperfine Structure. of the Even Configuration System of Pr I**. *Physica Scripta*, **68**:133, 2003.

[18] B Furmann A Krzykowski D Stefañska and J Dembczyñski. **New Levels and Hyperfine Structure Evaluation in Neutral Praseodymium**. *Physica Scripta*, **74**:658, 2006.

[19] B Furmann A Krzykowski D Stefañska and J Dembczyñski. **New Levels and Hyperfine Structure Evaluation in Singly Ionized Praseodymium**. *Physica Scripta*, **72**:300, 2006.

[20] A Krzykowski B Furmann D Stefańska A.Jarosz and A Kajoch. **Hyperfine structures in the configuration $4f^3 5d6s$ of the praseodymium atom**. *Optics Communications*, **140**:216, 1997.

[21] B Gamper Z Uddin M Jahangir O Allard H Knöckel E Tiemann and L Windholz. **Investigation of the hyperfine structure of Pr I and Pr II lines based on highly resolved Fourier transform spectra**. *Journal of Physics B: Atomic, Molecular and Optical Physics*, **44**:045003, 2011.

[22] K Shamim I Siddiqui and L Windholz. **Experimental investigation of the hyperfine spectra of Pr I-lines; discovery of new fine structure levels with low angular momentum**. *The European Physical Journal D*, **64**:209, 2011.

[23] T I Syed I Siddiqui K Shamim Z Uddin G H Guthöhrlein and L Windholz. **New even and odd parity levels of neutral praseodymium**. *Physica Scripta*, **84**:065303, 2011.

[24] H Krüger O Lutz and H Oehler. **Nuclear magnetic moments and ratios of quadrupole moments ^{135}Ba, ^{137}Ba, ^{138}La, ^{139}La by NMR spectroscopy**. *Physical Letters A*, **62**:131, 1977.

[25] J Bauche J-F Wyart Z Ben Achmed and K Guidara. **Interpretation of the hyperfine structures in the low even configurations of lanthanum II**. *Zeitschrift für Physik A*, **304**:285, 1982.

[26] O Anderson. **The Nuclear Mechanical Moment of Lanthanum from Hyperfine Structure**. *Physical Review*, **45**:685, 1934.

[27] G Luhrs. **Das Kernquadrupolmoment des 57 La^{139}**. *Zeitschrift für Physik A*, **141**:486, 1955.

[28] Y Tring. *Physical Review*, **108**:295, 1975.

[29] W J Childs and L S Goodman. **Hyperfine and Zeeman Studies of Low–Lying Atomic Levels of La^{139} and the Nuclear Electric-Quadrupole Moment**. *Physical Review A*, **3**:25, 1971.

[30] W J Childs and L S Goodman. **Complete resolution of hyperfine structure in the close doublet λ 5930.6 of ^{139}La by laser-atomic-beam spectroscopy**. *Journal of the Optical Society of America*, **67**:1230, 1977.

[31] W J Childs and L S Goodman. **Hyperfine structure of excited, odd–parity levels in ^{139}La by laser-atomic-beam fluorescence**. *Journal of the Optical Society of America*, **68**:1348, 1978.

[32] W J Childs and U Nielsen. **Hyperfine structure of the (5d+6s)^3 configuration of 139 : New measurements and ab initio multiconfigurational Dirac-Fock calculations**. *Physical Review A*, **37**:6, 1988.

[33] W J Childs and L S Goodman. **^{138,139}La nuclear electric-quadrupole–moment ratio by laser-rf double resonance**. *Physical Review A*, **20**:1922, 1979.

[34] H O Behrens and G H Guthöhrlein. **High Resolution Optogalvanic Spectroscopy as a useful Tool in the Determination of Atomic Hyperfine Parameters and Isotopic Shifts**. *Journal de Physique Colloques*, **44**:C7–149, 1983.

[35] C Luo J Qu L Zhu and F Lin. **Studies on the hyperfine structure of La I in a hollow-cathode discharge tube**. *Journal of Physics D: Applied Physics*, **23**:1327, 1990.

[36] G Basar G Basar and S Kröger. **High Resolution measurements of the hyperfine structure of the Lanthanum atom for energetically low lying levels of odd parity**. *Optics Communications*, **282**:562, 2009.

[37] B Furmann J Ruczkowski D Stefańska M Elantkowska and J Dembczyñski. **Hyperfine structure in La II odd configuration levels**. *Journal of Physics B: Atomic, Molecular and Optical Physics*, **41**:215004, 2008.

[38] Y Nighat M Raith M Hussain and L Windholz. **Investigation of the hyperfine structure of lanthanum lines by a laser-induced fluorescence technique**. *Journal of Physics B: Atomic, Molecular and Optical Physics*, **43**:125001, 2010.

[39] F Güzelimen I Siddiqui G Basar S Kröger and L Windholz. **New energy levels and hyperfine structure measurements of neutral lanthanum by laser-induced fluorescence spectroscopy**. *Journal of Physics B: Atomic, Molecular and Optical Physics*, **45**:135005, 2012.

[40] B Furmann M Elantkowska D Stefañska J Ruczkowski and J Dembczyñski. **Hyperfine structure in La II even configuration levels**. *Journal of Physics B: Atomic, Molecular and Optical Physics*, **41**:235002, 2008.

[41] B Furmann D Stefañska and J Dembczyñski. **Experimental investigations of the hyperfine structure in neutral La: II. Even parity levels**. *Journal of Physics B: Atomic, Molecular and Optical Physics*, **43**:015001, 2010.

[42] B Furmann D Stefañska and J Dembczyñski. **Experimental investigations of the hyperfine structure in neutral La: I. Odd parity levels**. *Journal of Physics B: Atomic, Molecular and Optical Physics*, **42**:175005, 2009.

[43] I Siddiqui S Khan B Gamper J Dembczyñski and L Windholz. **Optogalvanic spectroscopy of the hyperfine structure of weak La I lines: discovery of new even parity fine structure levels**. *Journal of Physics B: Atomic, Molecular and Optical Physics*, **46**:065002, 2013.

[44] T H Maiman. **Stimulated Optical Radiation in Ruby**. *Nature*, **187**:493, 1960.

[45] Wolfgang Demtröder. *Laserspektroskopie: Grundlagen und Techniken*. 5. Auflage. Springer-Verlag, 2007.

[46] H Schüler. **Über eine neue Lichtquelle und ihre Anwendungsmöglichkeiten**. *Zeitschrift für Physik*, **35**:323, 1926.

[47] H Schüler. **Über die Anregung von Spektren zur Untersuchung von Hyperfeinstrukturen**. *Zeitschrift für Physik*, **59**:149, 1930.

[48] J E Lawler A I Ferguson J E M Goldsmith D J Jackson and A L Schawlow. **Doppler-free Intermodulated Optogalvanic Spectroscopy**. *Physical Review Letters*, **42**:1046, 1979.

[49] F M Penning. **Demonstration of the new optogalvanic effect**. *Physica*, **8**:137, 1928.

[50] Randy D May. **Spatial charcteristics of the optogalvanic effect in striated rare-gas discharges**. *Journal of Applied Physics*, **58**:1169, 1985.

[51] A Siegel J E Lawler B Couillaud and T W Hänsch. **Doppler-free spectroscopy in a hollow-cathode discharge: Isotope-shift measurements in molybdenum**. *Physical Review A*, **23**:2457, 1981.

[52] B Gamper. *Aufnahme von Fourier-Transformations-Spektren und laserspektroskopische Untersuchung der Hyperfeinstruktur von Praseodym*. Master's thesis, Graz University of Technology, 2007.

[53] L Windholz and G H Guthöhrlein. **Classification of Spectral Lines by Means of their Hyperfine Structure. Application to Ta I and Ta II Levels**. *Physica Scripta*, **2003**:55, 2003.

[54] Z Uddin. PhD thesis, Graz University of Technology, 2006.

[55] A Ginibre. PhD thesis, Université de Paris-sud, 1988.

[56] G H Guthöhrlein. **Program package Fitter**. Universität der Bundeswehr Hamburg, 1998.

[57] B Gamper S Khan I Siddiqui and L Windholz. **Modelling of emission spectra of Pr I by summarizing hyperfine patterns of overlapping spectral lines**. *European Physical Journal D: Atomic, Molecular and Optical Physics*, **in press**, 2013.

[58] B Furmann D Stefanska and J Dembczynski. **Hyperfine structure analysis odd configurations levels in neutral lanthanum: I. Experimental**. *Physica Scripta*, **76**:264, 2007.